



HAL
open science

GEMINI SURFACTANTS AND SURFACTANT OLIGOMERS

Martin In

► **To cite this version:**

Martin In. GEMINI SURFACTANTS AND SURFACTANT OLIGOMERS. John Texter. Reactions and Synthesis in Surfactant Systems, CRC Press, 2001, 978-0824702557. 10.1201/9780203908662-8 . hal-03767782

HAL Id: hal-03767782

<https://hal.archives-ouvertes.fr/hal-03767782>

Submitted on 2 Sep 2022

HAL is a multi-disciplinary open access archive for the deposit and dissemination of scientific research documents, whether they are published or not. The documents may come from teaching and research institutions in France or abroad, or from public or private research centers.

L'archive ouverte pluridisciplinaire **HAL**, est destinée au dépôt et à la diffusion de documents scientifiques de niveau recherche, publiés ou non, émanant des établissements d'enseignement et de recherche français ou étrangers, des laboratoires publics ou privés.

GEMINI SURFACTANTS AND SURFACTANT OLIGOMERS

Martin In

Complex Fluids Laboratory

CNRS-Rhodia, Prospect Plains Road

Cranbury, NJ 08512

I. INTRODUCTION

Covalent linking of several amphiphilic moieties at the headgroup level yields a “surfactant oligomer“ (Figure 1a). The surfactant oligomers we are going to deal with are higher homologues of the gemini surfactants (surfactant dimers) (Figure 1c) [1]. They are distinguished from “oligomeric surfactants” (macrosurfactants) which consist of amphiphilic diblock copolymers (Figure 1b), and are also currently the subject of active research [2]. In surfactant oligomers, the structural repeating unit is amphiphilic by itself. The chemical group that connects the amphiphilic moieties is of variable nature and length.

Gemini surfactants have been synthesized and patented for more than fifty years [3], especially cationic ones. They have become topical again in the last two decades and their properties have been the subject of several reviews [1, 4-13]. They are of industrial and academic interest for diverse reasons. Cationic geminis were first described [14-16] and claimed as good textile softeners whose action resists laundering and dry cleaning operations [17, 18] or as efficient bactericidal and fungicidal agents with good diffusion properties and skin compatibility [19, 20]. More recently Devinsky, aiming to establish the relationship between biological activity and surfactant structure, synthesized and studied a large variety of cationic gemini surfactants [21]. Okahara and Ikeda have developed a new and easy synthetic route to oligo(ethylene glycol)

diglycidyl ethers and described various types of derivatives including anionic gemini surfactants [6]. Zana and Talmon pointed out the importance of the length of the connecting chain between the headgroups, the “spacer”, in controlling the microstructure of the self-assemblies [22]. Menger raised the question of the micellar structure of surfactants, which could not aggregate without exposing hydrocarbon moieties to water [23].

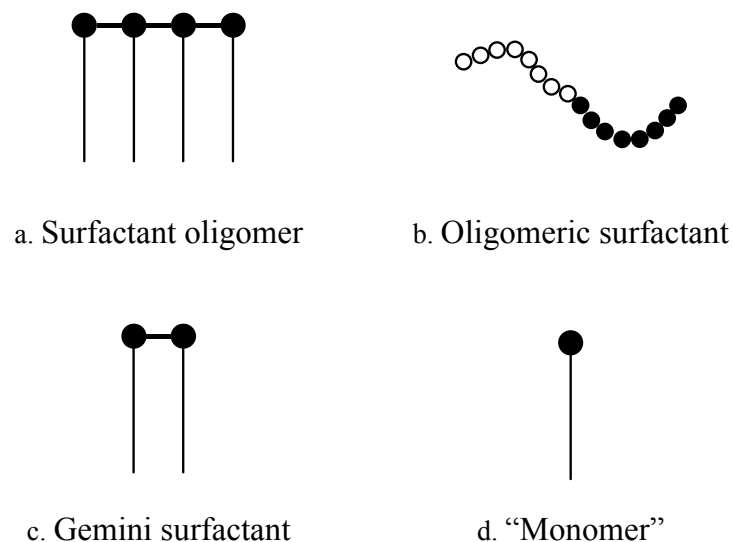


Figure 1 Surfactant oligomers (a), are distinguished from oligomeric surfactants (b) by the fact that the structural repeating unit is amphiphilic by itself. Surfactant oligomers are higher homologues of gemini surfactants (c). The structural repeating unit (d) corresponds to a conventional surfactant, which will be referred to as the “monomer”.

Finally, Rosen pointed out the unexpected effectiveness of these surfactants in lowering surface tension and their enhanced synergistic effect in

mixtures. He analyzed the consequences on performance properties [4], which could make gemini the “new generation of surfactants”. The number of patents, (which concern predominantly anionic and non-ionic geminis), filed since then attests that this was rather convincing [24]. Gemini surfactants were considered the starting point for surfactant oligomers. Synthesis and physicochemical studies of surfactant trimers were reported [1, 5]. Some surfactant oligomers have been synthesized and studied in other contexts. For instance, cationic lipids are mostly studied as carriers in the intracellular delivery of bioactive agents [25, 26], and more specifically as non-viral transfecting agents [27]. Lipophilic di- and triamides have been used as ionophores for alkaline earth metal cations [28] and lipophilic cyclopolymers are potential liquid membrane sensors for nucleosides [29]. The synthesis of higher homologues also provides an alternative path to the study of the transition from surfactant to polysoap behavior [30].

Gemini surfactants have shown many “unexpected properties”, which are *a posteriori* rather well understood, and concepts long known [31, 32] explain at least qualitatively these observations. Surfactant self-assembly results from two opposing forces. Attraction between the hydrophobic tails induces the aggregation, while repulsion between the hydrophilic headgroups ensures the existence of a large interfacial area. Classical ways to modify the micellization, the shape of the micelles or the lyotropic behavior consist of tuning these opposing forces by varying the length of the hydrophobic tail and the nature of the headgroup. The concept of surfactant oligomers provides new parameters to tune this balance of opposing forces.

The degree of oligomerization x , i.e. the number of amphiphilic moieties in the surfactant, is a new variable parameter. The length of the linker s can vary along with its hydrophobicity and rigidity. This allows achieving a more direct and more efficient control of the optimal interfacial area per

headgroup. As in conventional surfactants, the length of the tail, m , and the chemical nature of the headgroup are possible chemical variables. These two variables are not specific to surfactant oligomers, but the study of their influence brings insight to the properties of surfactant oligomers. Gemini surfactants can also be non-symmetric, i.e. both amphiphilic moieties can be different in terms of chain length and in headgroup nature.

A large variety of surfactant oligomers will be discussed in the next section where their synthesis is reviewed. Following Zana, the cationic surfactant dimers with simple structure are referred to as m-s-m, 2X, when the spacer consists of $-(CH_2)_s-$ chain, and m-s/3-m, 2X when the spacer consists of $s/3$ ethylene oxide units. In the same logic, trimers are referred to as m-s-m-s-m, 3X. Some anionic surfactants with simple structure are designated the same way but the head group nature is precised.

The new parameters s and x , have a strong influence on the surface activity and the packing at interface of surfactant oligomers, as well as on their self-assembling properties in the bulk. This is described in section III and IV. Like conventional surfactants, oligomers have been used in analytical and synthesis chemistry, as selective receptors, as hosting or templating agents but also as reactants. This will be the subject of the last section.

II. SYNTHESIS. STRUCTURE DIVERSITY.

A. Surfactant Dimers (Gemini).

1. Cationic Geminis

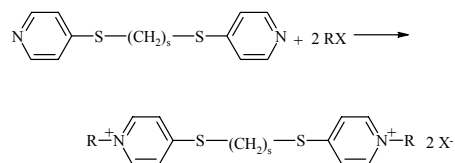
Cationic surfactants are among the first gemini reported in the literature [3, 14-20]. First claimed as good fabric softeners, or developed for their biological activity, they have also been studied for micellar catalysis. Easier to synthesize, they have been the materials of choice for fundamental studies. The

influence of various parameters such as the length of the hydrophobic chains, their dissymmetry, as well as the nature (hydrophilic or hydrophobic) and the length of the spacer, have been studied. Some examples of cationic gemini surfactants are shown in Figure 2.

Synthetic methods for preparing diquatery ammonium (Figure 2a) [14, 21, 33-42] and dipyridinium [19, 43] gemini rely on the same reactions (quaternization of a tertiary amine with bromoalkane) as those used for their corresponding monomer, except for the use of difunctional reagents.

Two routes can be distinguished. The first one proceeds by quaternization of a tertiary diamine (route 1) [14, 21, 33, 38, 42] as exemplified in Scheme 1 [14, 20]. The second one couples two tertiary fatty amines with dibromoalkane (route 2) [36-39, 41] as shown in Scheme 2 [38]. Two tertiary diamines can also be coupled with epichlorhydrin giving a hydroxypropylene spacer [44, 45].

Quaternary ammonium gemini with hydrophilic spacer (Figure 2b) have been synthesized using route 2, by reacting tertiary amines with α,ω -dibromo-alcohols [46], or an α,ω -dibromo oligo(oxyethylene) [47-49] (the latter being synthesized via bromination of oligo(oxyethylene)glycol with phosphorus tribromide). Other methods have been reported to produce diquatery ammonium surfactants with oxyalkylene [50].



Scheme 1

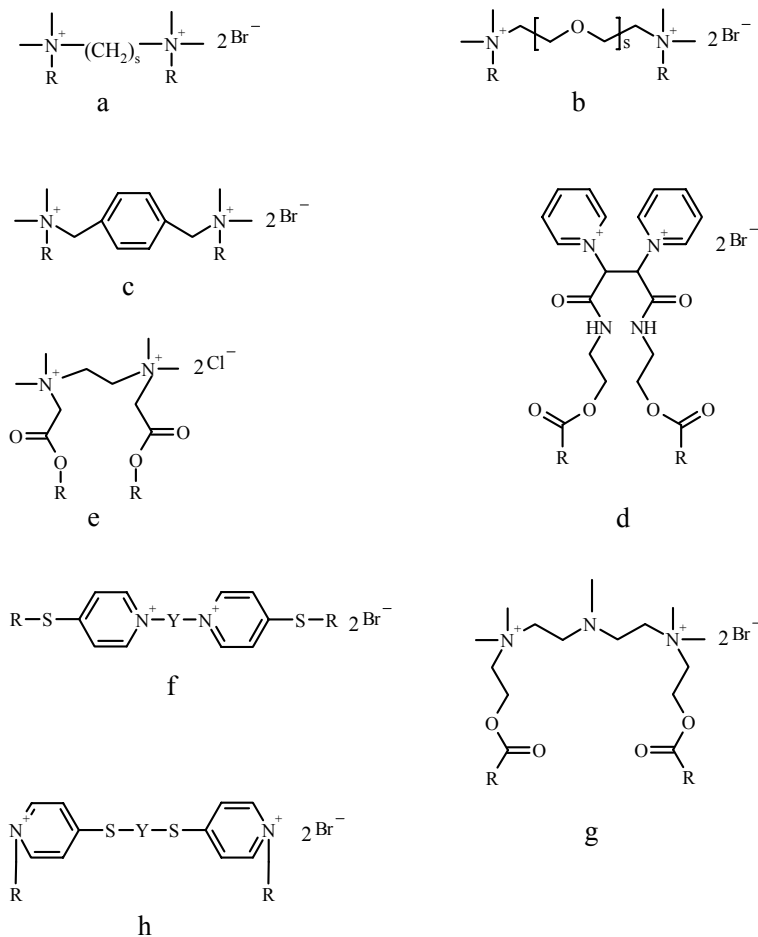
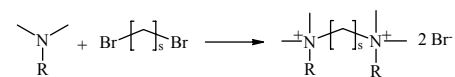


Figure 2: Examples of cationic gemini surfactants.



Scheme 2

2. Anionic Gemini

A large variety of anionic gemini surfactants (cf. Figure 3: sulfonate 3a, sulfate 3b, phosphate 3c, carboxylate 3d) with hydrophilic spacer have been prepared from the corresponding fatty diols, according to the conventional procedure used for classical surfactants [51-59] (Scheme 3, second step). Intermediate fatty diols have been prepared by the reaction of diglycidyl ethers (prepared according to [60]) with the appropriate fatty alcohol, leading to gemini surfactants with hydrophilic spacer (Scheme 3, first step). The intermediate fatty diols are nonionic gemini surfactants. They are not soluble in water, but their emulsifying properties [57] and insoluble monolayers at the air/water interface have been studied [61].

Sulfation of the diols proceeds with chlorosulfonic acid in the presence of glacial acetic acid in dichloromethane at room temperature [51] or chloroform at 0 °C [52], followed by neutralization with aqueous sodium carbonate or alcoholic sodium hydroxide (see Scheme 3).

Phosphatation is carried out with polyphosphoric acid in dry benzene at 50 °C. Use of phosphorus pentoxide leads to some undesirable dehydration of the secondary alcohol, and phosphorus oxychloride leads to a complex reaction mixture [53].

Disodium sulfonates (Figure 3a) are prepared from 1,3-propanesultone in the presence of NaOH [51] or NaH in dry THF at 60 °C [51, 54, 55]. In all cases, pure products are obtained after extraction and separation by silica gel column chromatography or by HPLC.

The synthesis of dicarboxylate gemini (Figure 3d) proceeds first by reacting the diols with bromoacetic acid in t-BuOH under basic condition, followed by esterification with methanol under acid conditions. This ester is purified on a silica gel column and finally hydrolyzed by NaOH in methanol [59].

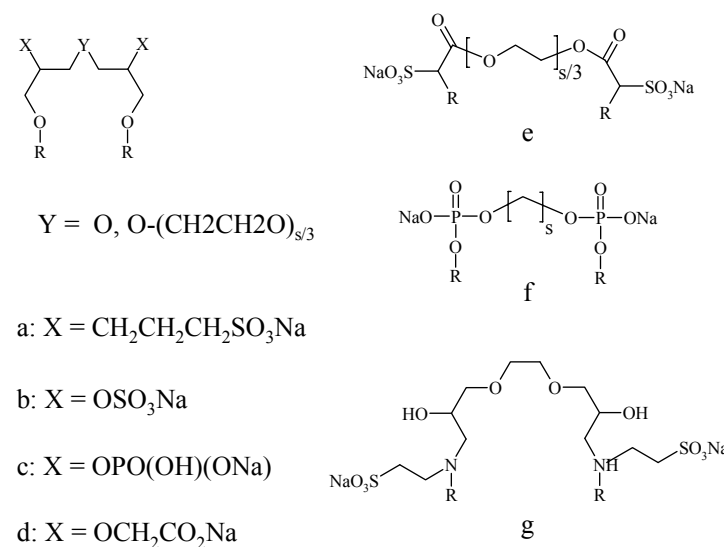
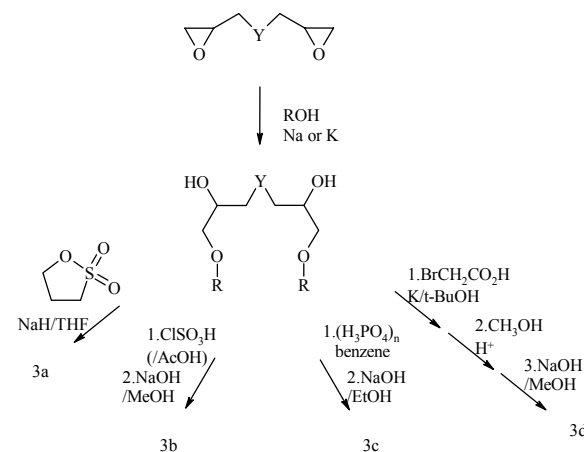


Figure 3: Examples of anionic gemini surfactants.



Scheme 3

Taurine gemini surfactants (Figure 3g) were synthesized by reaction of ethylene glycol diglycidyl ether with *N*-(alkyl)taurine in the presence of sodium carbonate in ethanol [56]. *N*-(alkyl)taurines are prepared by reaction of the corresponding fatty amines with sodium 2-bromoethane-1-sulfonate. Anionic gemini surfactants with hydrophilic spacer (Figure 3e) were also synthesized by diesterification of polyethylene glycol with α -sulfonated fatty acids in carbon tetrachloride under reflux [62]. Esterification of polyethylene glycol with α -sulfonated acid (prepared as described in [63]) yield monoester (about 50%), diester (about 25%) and unreacted PEG (25%); separation and purification of the components were carried out by reversed-phase chromatography [62]. The same type of sulfonate surfactants with a hydrophobic spacer, have been synthesized by disulphonation of fatty diesters of adipic acid [64]. Another possible route to these compounds, coupling 2-hydroxy-1-alkanesulfonates with diacids, has proven unsuccessful [64]. The synthesis of other anionic gemini surfactants with hydrophilic spacer of different lengths has been reported [65]. Dihydroxyl precursors such as tartaric acid have been used to prepare asymmetric anionic gemini surfactants [66].

Alkylphosphate gemini with hydrophobic spacer (Figure 3f) have been obtained by coupling alkyl phosphate tetramethylammonium salts with dibromoalkanes [67] or α,α' -dibromoparaxylene [39] according to Bauman's method [68]. This route relies on the fact that monoalkyl phosphates $[\text{ROP}(\text{O})\text{O}_2]^{2-}$ are better nucleophiles than dialkyl phosphates $[(\text{RO})_2\text{P}(\text{O})\text{O}_2]$. Alternatively, Eibl's method [69] (phosphorylation of the diol using POCl_3 in the presence of triethylamine) has been used to synthesize phosphate gemini with $-(\text{CH}_2)_s-$ spacer (Figure 3.d) [70] or rigid hydrophobic spacer [39]. Gemini glycerophosphates with long flexible hydrophobic spacer have also been synthesized as models for Archaeobacterial membrane lipids [71].

Sarcosine type surfactant dimers have been synthesized from fatty acid and ethylene diamine diacetic acid via the mixed anhydride method [72]. Their efficiency as flotation agent is improved as compared to its monomer and strong synergistic effects have been observed when mixed with fatty amines.

3. Amino Acids Derivatives

The use of amino acids to prepare gemini surfactants offers a large variety of headgroup structures. Moreover, it facilitates the synthesis of enantiomerically pure surfactants. Amino acid-based gemini surfactants have better biocompatibility. Some of them have been shown to be less hemolytic and less irritating. They also have proven to be good immuno-adjuvants for the formulation of vaccines. Some examples are presented in Figure 4.

Nonionic geminis (Figure 4a) have been prepared by condensation of N^α, N^ϵ -diacyl lysine with *N,N*-bis(methylpolyoxyethylene) amine [73]. Their structure is close to the structure of natural lecithin, and they do not rigorously correspond to surfactant dimers as defined in the introduction. Recently the same type of compounds with alkyl chains of different length has been synthesized [74].

Gemini cationic surfactants with variable spacer length have been synthesized from arginine [75-78] (Figure 4b). The synthesis proceeds in three steps: 1) protection of the guanido group of arginine with a nitro group ; 2) coupling of two protected arginines via condensation of the α -carboxyl group to both primary amino groups of the α,ω -alkane-diamine using benzotriole-1-yl-oxy-tris-(dimethylamino)-phosphonium hexafluoro-phosphate (BOP) in presence of an activating base (DABCO); and 3) catalytic hydrogenation to unprotect the guanido group.

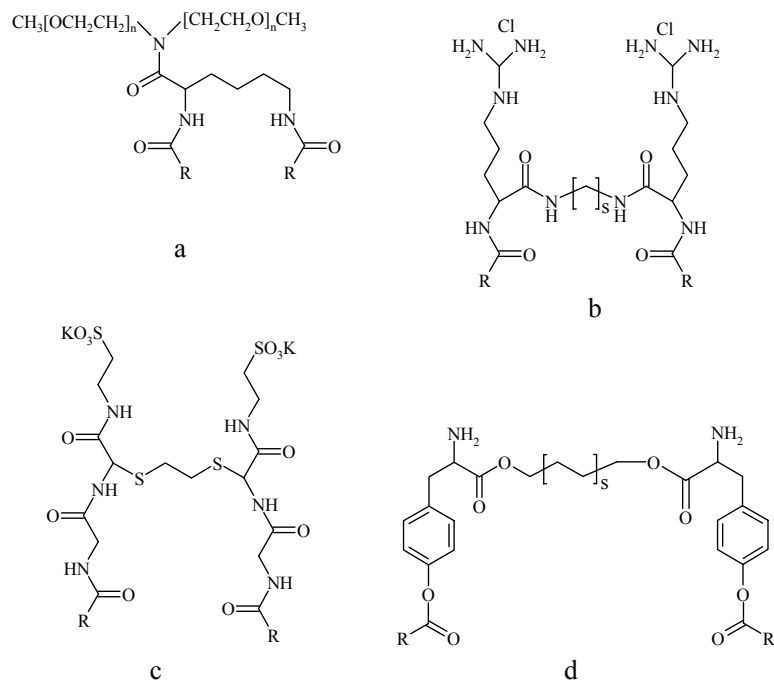


Figure 4: Examples of amino acid-based gemini surfactants.

Anionic gemini surfactants have also been synthesized from L-cysteine (Figure 4c) [79]. A chemoenzymatic route for the preparation of a variety of amino acid-based gemini surfactants has been developed [80]. Immobilized lipases efficiently catalyze the formation of diester (respectively diamide) from *N*-protected amino acids and α,ω -alkane-diols (respectively α,ω -alkane-diamine), with hydrocarbon spacers of different lengths. Tyrosine (Figure 4d) and serine-based geminis were then obtained by acylation with acyl chloride followed by removal of the carbobenzyloxy-protecting group by catalytic

hydrogenation under standard conditions. For glutamic acid-based geminis, the carboxyl group of the residue was esterified prior to lipase action. For lysine-based geminis, the *N*-protected acylated amino acid turned out to be a better substrate for the lipase than the *N*-protected amino acid itself [80].

4. Sugar derivatives

Carbohydrates based-gemini surfactants present the advantage of being derived from renewable source. The presence of two sugar headgroups is expected to enhance intra and intermolecular hydrogen bonding but it was also hoped that the gemini structure could lower the Kraft temperature (a point which often limits the practical use of polyalkylglucosides) [81]. Examples are given in Figure 5.

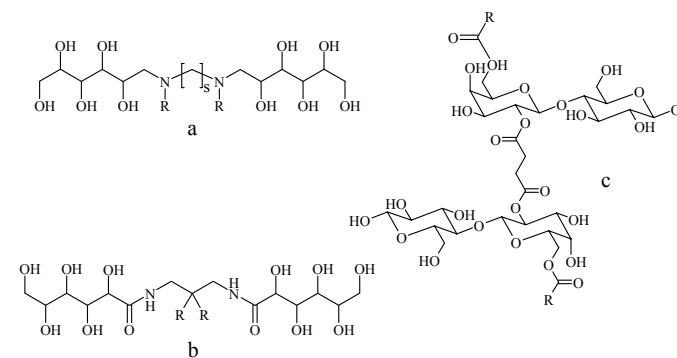


Figure 5: Examples of sugar-based gemini surfactants.

The synthesis of the compound of Figure 5b, proceeds by reaction of carbohydrate lactone with a 2,2-dialkylpropane-1, 3-diamine in methanol [82, 83]. The diamine was obtained by dialkylation of malonitrile with bromoalkane in DMSO, followed by a reduction of the nitrile groups into primary amine

groups by LiAlH_4 in dry ether or with lithium in liquid ammonia-ethanol mixture.

Sugar-based surfactants with variable spacer length (Figure 5a) have been prepared by catalytic hydrogenation of D-glucose and the appropriate α,ω -alkanediamine [84]. At that step, a bola-amphiphile is obtained; it is acylated with fatty acid anhydride to get a gemini surfactant.

Nonionic glucoside gemini surfactants with the two amphiphilic moieties linked at C-6 have been synthesized [85]. A large variety of xylose, glucose, galactose and lactose (Figure 5c) derived gemini surfactants, with different chain and spacer lengths, have been prepared from partially protected sugars (isopropylidene derivatives), using enzymes to regioselectively introduce fatty acids into carbohydrate moieties [86]. Both amphiphilic moieties were connected via different hydroxyl groups in the sugar molecule and a heterodimer xylose-lactose (Figure 6d) gemini was prepared [86].

5. Surfactant heterodimers

Gemini surfactants can be non-symmetric, it means that the two amphiphilic moieties can differ either in the length of the hydrophobic tail [87], or in the nature of the headgroup [88, 89]. Some examples of surfactant heterodimers are presented in Figure 6.

Cationic gemini surfactants with two hydrophobic chains of different lengths (Figure 6a) were obtained in two steps from the permethylated diamine as described above [87]. The intermediate alkyl dimethyl [1-(2-dimethylamino)ethyl] ammonium bromide is recrystallized in ether. Hybrid hydrocarbon-fluorocarbon cationic gemini surfactant have also been synthesized the same way [90].

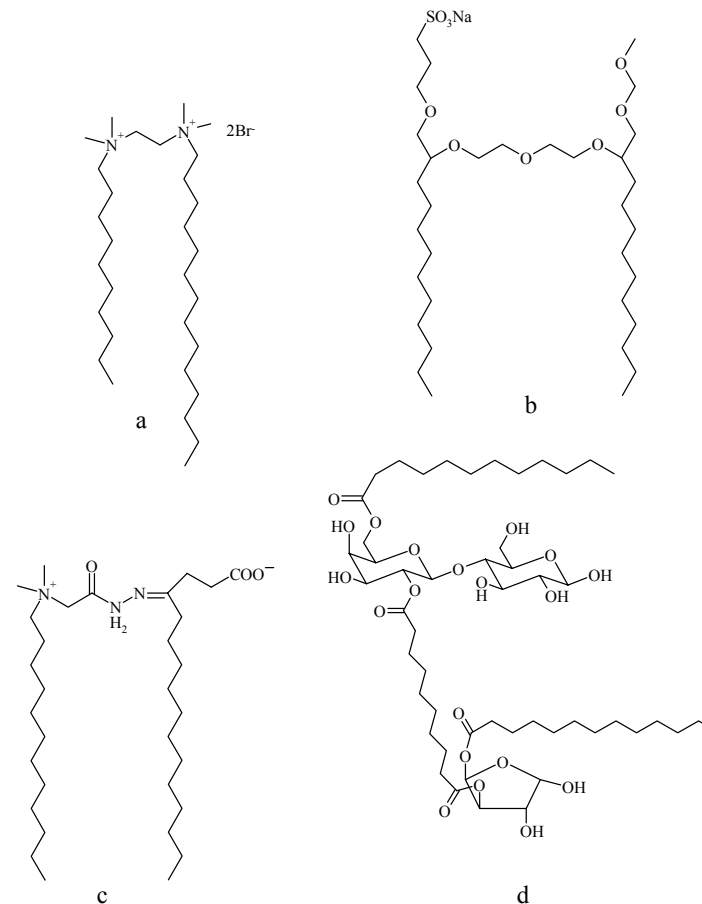


Figure 6: Examples of surfactant heterodimers.

The synthesis of gemini surfactants with two different hydrophilic headgroups (cationic-anionic, nonionic-nonionic, anionic-nonionic) (Figure 6b-d) involves more steps. For example, the compound of Figure 6c was synthesized in three steps: An alkyl dimethyl amine reacts first with ethylbromoacetate, then with hydrazine to give the surfactant

$\text{RMe}_2\text{N}^+\text{CH}_2\text{CONHNH}_2\text{Br}^-$. The latter reacts with fatty keto acids resulting in the surfactant of Figure 6c. A ^{13}C NMR study revealed that it was obtained as the E isomer with respect to the carbon-nitrogen double bond [88]. This study also provided an example of a cleavable spacer gemini surfactant (see Section II.7). The chemoenzymatic route to sugar based surfactant described above allows the synthesis of nonionic surfactant heterodimers (Figure 6d) [86].

6. Chiral Gemini Surfactants

Enantiomerically pure gemini surfactants derived from aminoacids have already been mentioned above. Other types of chiral surfactants have been synthesized from tartaric acid, with anionic hydrophilic groups such as phosphates (Figure 7a) [91], carboxylates and sulfates [66], as well as cationic headgroup [66]. More recently chiral cationic gemini surfactants have been synthesized from chiral biphenyl (Figure 7b) [92].

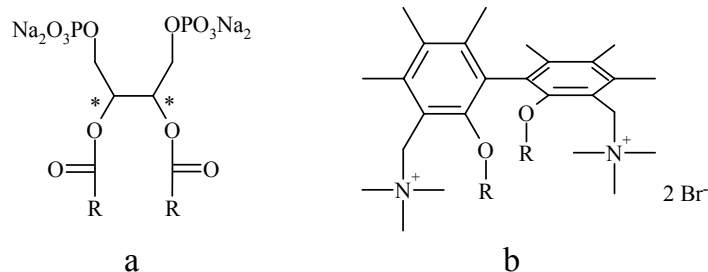


Figure 7: Examples of asymmetric gemini surfactants.

7. Functional Gemini Surfactants

a) Cleavable Surfactants.

Several types of cleavable gemini surfactants have been synthesized based on disulfide [93], hydrazine [88], acetal [94-96], or ozone cleavable double bonds [97].

The synthesis of cationic surfactants containing a disulfide bond in the spacer has been achieved by condensation of an alkyldimethylamino betaine with cystine or cystamine via the mixed anhydride method [93]. The betaine is first converted to a mixed anhydride by reaction with isobutyl chloroformate. The second step is an aminolysis of the anhydride by the amino group of cystine dimethyl ester or cystamine. In aqueous solutions the disulfide surfactants obtained decompose at room temperature at $\text{pH} > 8.0$, but are stable even at higher temperature (50°C) at lower pH . These surfactants have potential applications in the textile and cosmetic field, since the disulfide bond can also react with thiol groups (of reduced keratin for instance) (thiol/disulfide interchange) [93]. Disulfide-based phospholipid dimers have been synthesized from functionalized monomer surfactant in the micellar state. This was done to study nearest neighbor recognition in membranes [98].

The simplest synthesis of gemini surfactants with acetal (1,3-dioxalane) based spacer proceeds by acid catalyzed condensation of diethyl tartrate with fatty ketones followed by alkaline hydrolysis [94]. The synthesis presented in reference [95] is more involved and does not strictly give a gemini surfactant, because the linkage between the two amphiphilic moieties is not located at the headgroup but in the middle of the fatty chains. In that respect these surfactants provide interesting intermediate structures between gemini and bolaform surfactants [7].

Anionic gemini surfactants with an ozone cleavable spacer (bearing carbon-carbon double bond) [97] have been synthesized with unsaturated

diglycidyl ether by the same method as in [54]. Their ozonolysis has been studied by proton NMR [97].

b) *Miscellaneous.*

Ferrocenyl cationic gemini have been synthesized by the same procedure as the simple diquaternary ammonium gemini using bromooctylferrocene to quaternize permethylated propane diamine [99]. It was known that a variation of the oxidation state of the ferrocene moiety allowed to control bulk as well as surface properties of ferrocenyl surfactant solutions (see Table 26) [100]. With gemini ferrocenyl surfactants the range of concentration for which this control is efficient is greatly extended [99] (see chapter by Abott in this volume). Finally, anionic gemini surfactant with azo groups in the spacer have been synthesized and used as initiator for radical polymerization (inisurfs) [101]. As any inisurfs they suffer from poor radical yield.

B. Oligomers

A large variety of surfactant oligomers, mostly trimers, has been reported in the literature. Their structures are presented in Figure 8. Some of them are obtained pure; others consist of mixtures of surfactant oligomers with different oligomerization degree.

Triazine derived trialkyltri-quaternary ammonium surfactants have been synthesized by quaternization of trialkyl triazine with dimethylsulfate and claimed as efficient antibacterial, antifungal and antiviral agents with weaker toxicity [102].

Trimer of DTAB with $s=3$, 12-3-12-3-12, 3Br, was first synthesized in a multiple steps procedure described in Scheme 4 [103]. More recently its synthesis has been improved starting with bis(aminopropylamine) as shown in Scheme 5 [104]. The first step (permethylation) is carried out in acidic aqueous

solution with formaldehyde and sodium borohydride as reducing agent, as described in [105]. The second step consists of the quaternization with bromododecane in acetonitrile at 80°C. The purification proceeds by recrystallization [104].

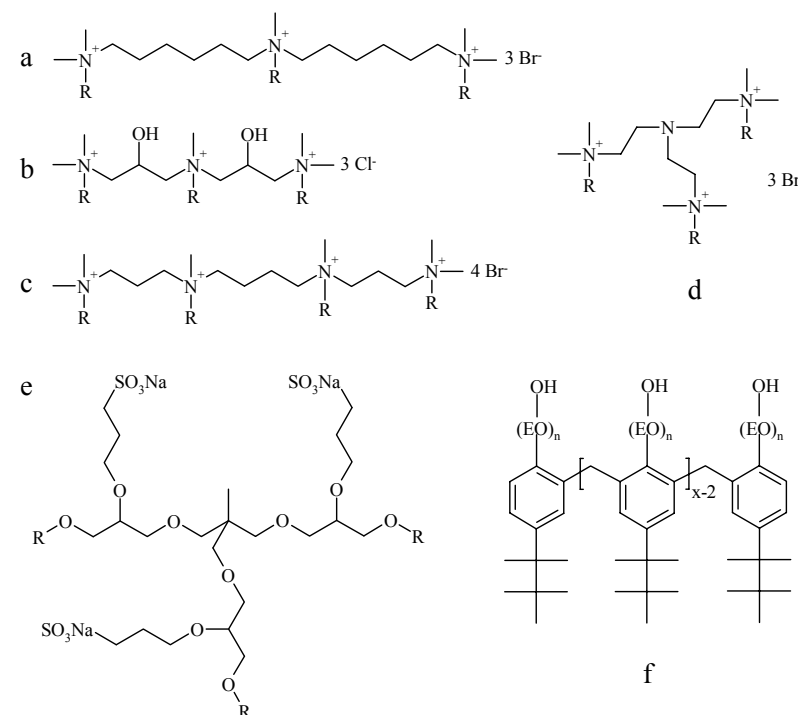
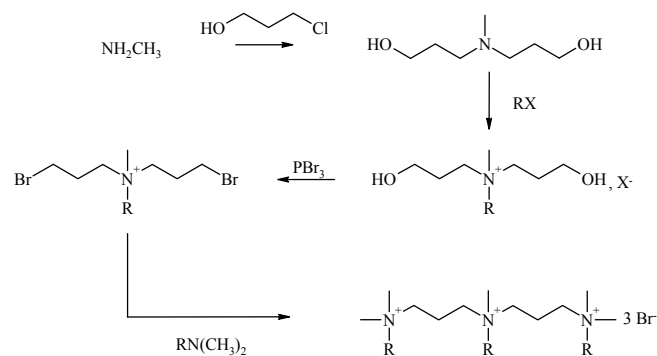


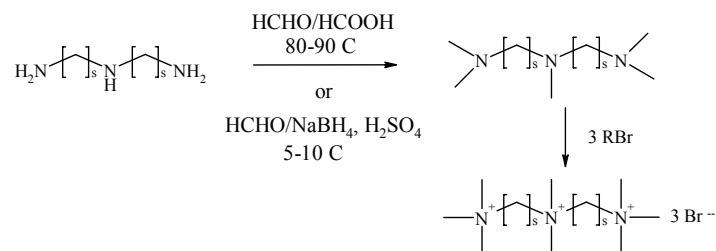
Figure 8: Examples of surfactant oligomers.

8-3-8-3-8, 3 Br, 16-3-16-3-16, 3 Br [106] and the tetramer 12-3-12-4-12-3-12, 4 Br (Figure 8c) [104] have been synthesized the same way. The above two-step procedure has been used to prepare m-6-m-6-m, 3Br (Figure 8a) as well as triquaternary ammonium with a three armed star shaped spacer (Figure 8d)

[106]. For these surfactants with $s \neq 3$, permethylation could be performed via the Eschweiler-Clarke reaction (with a C_3 spacer this reductive alkylation induces fragmentation of the triamine and yields the permethylated diamine [107]). The synthesis of 12-2-12-2-12, 3 Br by the same route has been reported, but after the quaternization reaction, the trimer had to be purified from a mixture of dimer and trimer [108].

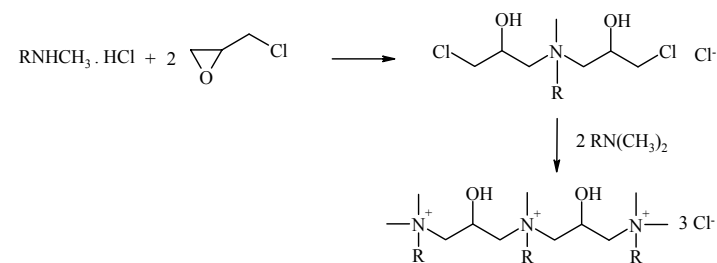


Scheme 4



Scheme 5

Another procedure to synthesize cationic surfactant trimers uses epichlorohydrin (Scheme 6) to produce cationic trimers with hydrophilic spacers (Figure 8b) [109]. This route allows interesting variations in the structure. One can also obtain triquaternary ammonium surfactants with two fatty chains or diquaternary ammonium ones with three hydrophobic chains, depending on the nature of the amine which reacts with epichlorohydrin at the first step.



Scheme 6

The synthesis of diglycidyl ether from diol has been generalized to polyglycidyl ether from polyols [110] and opened the path to the synthesis of sulfonate surfactant trimers with hydrophilic star shaped spacer (Figure 8e) [111, 112]. Other surfactants with unequal numbers of ionic groups and hydrophobic chains, triple chain/double ionic groups, were synthesized from alkylglyceroldiglycidyl ether [113]. Triple chain surfactants with hydrophobic chains of different lengths were also obtained [113].

Nonionic surfactants with three hydrophilic heads and two lipophilic tails have been patented [114]. As Tiloxapol (Figure 8g) [115], they probably consist of a mixture of different oligomerization degree. The chemoenzymatic route to sugar-based gemini surfactant described above, was also used to prepare nonionic surfactant trimers [86].

III. SURFACE ACTIVITY AND STRUCTURE AT INTERFACE.

A. Air-water interface

The surface activity of soluble surfactant oligomers in aqueous solution has been extensively studied by tensiometry to determine their critical micelle concentration (cmc), to address their packing at the air-water interface, and to determine their performance properties (see appendix section VII, Tables 5, 9, 10, 13, 15-22, 24-27, 29, 31-34, 36-46). The results of are often summarized by four parameters : C_{20} , γ_{cmc} , Γ_m and the cmc. C_{20} , which is the concentration needed to decrease the surface tension by 20 mN/m, characterizes the *efficiency* of a surfactant to lower surface tension. (The efficiency of the surfactant is actually often reported by $pC_{20} = -\text{Log}C_{20}$). The C_{20} value reflects the partitioning of the surfactant between the bulk and the interface and is related to the standard free energy of adsorption at the air-water interface [116]. The surface tension at the cmc, γ_{cmc} , characterizes the *effectiveness* of a surfactant to lower surface tension. It relates to the maximum film pressure a surfactant can build up at the air-water interface, Π_{cmc} , before self-assembling in the bulk is thermodynamically favorable. Γ_m is the maximum excess surface concentration and is obtained from a γ -c plot through the Gibbs equation:

$$d\gamma = nRT\Gamma d\ln c. \quad (\text{Equation 1}).$$

These four parameters are related by the following equation [116]:

$$\Pi_{cmc} = 20 + k\Gamma_m \text{Log}(cmc/C_{20}) \quad (\text{Equation 2}).$$

From Γ_m the minimum surface area per molecule of surfactant A_m , or per amphiphilic moiety a_m , have been determined.

Nonionic and long hydrophobic chain ionic surfactant oligomers are insoluble in water. The diagram of state of the insoluble monolayers they form at the air-water interface has been established with the Langmuir film balance. The Π -A isotherms obtained are characterized by the lift off area A_L , the limiting surface area A_∞ , and the collapse pressure Π_c . A_L corresponds to the highest surface area per molecule where a monolayer shows detectable resistance to compression. It is the inverse of the minimum surface concentration, at which a surfactant builds up sensible pressure. A_∞ approximates the surface area per molecule at maximum compression and is obtained from the following relation :

$$A_\infty = A_c - \Pi_c(dA/d\Pi)_{\Pi_c}, \quad (\text{Equation 3})$$

where A_c is the area per molecule at Π_c .

1. Efficiency to Lower Surface Tension.

The efficiency of surfactant oligomers to lower surface tension is greater than that of conventional surfactants (see appendix section VII, Tables 16, 17, 20, 21, 25, 32-34, 39, 40, 42-46). Typical C_{20} values for $m = 12$ conventional surfactants lie in the millimolar range, while for $m = 12$ gemini surfactants C_{20} values are currently close to 10^{-4} M. This is of course correlated to the lower cmc. The lower C_{20} of gemini surfactants as compared to conventional ones means that the standard free energy of adsorption is more negative. This can result *a priori* from either an increase in the standard chemical potential of the surfactant in the bulk or a decrease in the standard chemical potential at the interface. The observation that C_{20} decreases exponentially with the length of the alkyl chain in most of the gemini surfactants and with the same rate as it does for conventional surfactants, suggests that the first hypothesis is the dominant factor. This is because the unfavorable contact between water and hydrocarbon for a gemini surfactant is twice that of the corresponding monomer.

When the length of the alkyl chains m exceeds a certain value, which is about 16 but varies with physicochemical conditions, the m -dependence of C_{20} is weaker than expected and can reverse (see Tables 17, 21, 44) [39, 23, 46, 117, 118]. In a few cases, C_{20} has been observed to increase with m . For anionic surfactant trimers (the spacer being star shaped), the C_{20} increases with m from $m = 10$ to 14 (see, Tables 44) [111, 112]. These rather surprising results have been observed with surfactant oligomers whose spacer contains heteroatoms or aromatic rings, but not with $-(CH_2)_s-$ spacers. They have been interpreted in terms of pre-micellization [39, 46, 117, 118]. An alternative explanation could be that intramolecular association occurs between the long alkyl chains. Such intramolecular interactions have been suggested on the basis of volumetric measurements [119]. If the surfactant molecule limits the contact between hydrocarbon chain and water, by intramolecular hydrophobic association, without losing too much conformational entropy, its chemical potential in water will be reduced and so will be its tendency to adsorb at air-water interface.

2. Effectiveness and Packing at the Air-Water Interface.

The effectiveness of surfactant oligomers to lower surface tension is not very different from conventional surfactants. γ_{cmc} values for most surfactant oligomers lie between 30 and 40 mN/m. The dependence of γ_{cmc} on the alkyl chain length has been extensively studied for cationic gemini [39, 45, 46, 120,], and appears to vary with the composition of the spacer. For $-(CH_2)_s-$ spacers (hydrophobic and flexible) γ_{cmc} decreases slightly when m increases (see Table 13), as observed in conventional surfactant. However when a heteroatom is present in the spacer (either, S, O or N), the m -dependence of γ_{cmc} is non-monotonic (see Tables 18-22), and long alkyl chain gemini surfactants are significantly less effective in reducing surface tension [120].

Short spacer gemini surfactants ($s < 5$) are more effective than their corresponding conventional surfactant. However, increasing s decreases significantly the effectiveness (increase in γ_{cmc}) [40, 46, 52-56, 120-124] as illustrated in Figure 9. This s -dependence of γ_{cmc} is confirmed with trimers. Short spacer cationic trimers are more effective than short spacer cationic dimers [104, 108], while long spacer cationic trimers are less effective than long spacer cationic dimers (Table 43) [104].

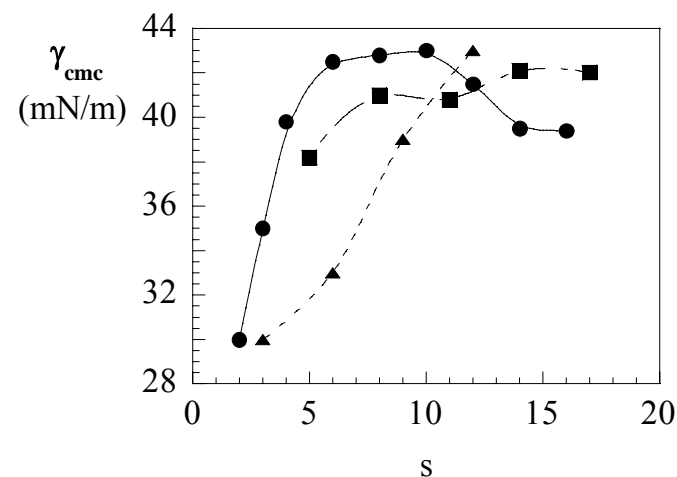


Figure 9: γ_{cmc} vs Spacer length, s , for 12- $(CH_2)_s$ -12, 2Br (λ) [122], 12- $CH_2(EO)_{s/3}CH_2$ -12, 2Br (ν) [123], and the compound of Figure 3d, $m = 10$, $Y = O$ (EO) $_{s/3-1}$ [59] (σ). For comparison, γ_{cmc} of DTAB is 39 mN/m.

The surface area occupied by a surfactant molecule at the air-water interface A_m has been determined from the concentration dependence of the surface tension using Gibbs equation. As already discussed this is rigorously correct only when the surfactant are dissolved in brine because the prefactor n in

the Gibbs equation is known ($n = 1$). In the absence of additional electrolyte, comparison were made between analogous surfactants, taking $n = x+1$. A recent neutron reflectivity study suggested that for the cationic gemini surfactant 12-s-12, 2Br, the correct value for n in the Gibbs equation is 2 instead of 3 [125]. Figure 10 shows that diquaternary ammonium geminis with a hydrophilic spacer $-(EO)_{s/3}-$ are more densely packed at the air-water interface than their homologues with hydrophobic $-(CH_2)_s-$ spacers. Note that in Figure 10 presents the surface area per amphiphilic moiety a_m , not per surfactant molecule. a_m goes through a maximum between $s = 10$ and $s = 12$ in the case of hydrophobic spacers [122], whereas it increases monotonically for oxyethylene spacers [123].

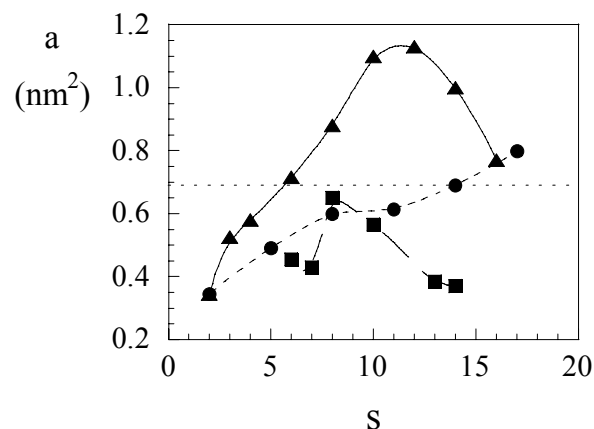


Figure 10: Minimum Surface area per amphiphilic moiety as a function of the spacer length for cationic dimers: 12- $(CH_2)_s$ -12, 2Br- (σ) [122]; 12- $(EO)_{s/3}$ -12, 2Br- (λ) [123]; arginine based surfactant (ν) [77]. DTAB and the arginine monomer have the same the specific surface area, which is represented by the dotted line.

The non-monotonic behavior in the case of hydrophobic spacers was also observed with arginine based cationic geminis (Figure 4b) [77]. For the anionic gemini of Figure 3d, the minimum surface area per molecule increases monotonically in the range of length studied (from 1 to 4 EO groups) (see Table 39) [59].

The non-monotonic dependence of A_m , and the position of the maximum has been accounted for theoretically [126, 127] by considering the competition between the spacer geometrical characteristics (length and flexibility) and the interactions between the amphiphilic moieties. Monte Carlo simulations [128] have reproduced the experimental observation that hydrophilic spacer gemini have a smaller specific surface area than hydrophobic spacer gemini. The possibility for hydrophilic spacers to buckle into water, where half of the space is forbidden for hydrophobic ones explains these results. These simulations [128] however did not reproduce the non-monotonic dependence of A_m upon s , for hydrophobic spacer.

The packing of a $m=18$ cationic surfactant with rigid phenyl spacer at the air-water interface has also been studied using the Langmuir film balance [39]. The high surface activity of gemini was readily observed in pressure vs area curve : $A_L = 2.40 \text{ nm}^2/\text{molecule}$, a value which is close to the square of the molecule dimension in its all-anti conformation. Upon compression, the monolayer collapsed at about $0.76 \text{ nm}^2/\text{molecule}$. The same type of measurements done with succinimide surfactant monomers, dimers and trimers [129] showed that A_L increases as the degree of oligomerization increases : 0.7, 1.3, $1.7 \text{ nm}^2/\text{molecule}$ for the C_{18} monomer, dimer and trimer, respectively; A_∞ is 0.56, 0.96, $1.22 \text{ nm}^2/\text{molecule}$, respectively. For the dimers and the trimers the surface area was less sensitive to the alkyl chain length (comparison between $m = 8, 12$ and 18) than for the monomer and was determined by the structure of the headgroup. The Π -A curve has been established for glycerophosphate gemini

with $m = s/2$ [71] and amphiphilic phthalocyanines, which can be considered as surfactant oligomers with a cyclic headgroup structure [130].

Neutrons reflectivity studies on nonionic sugar derivative gemini [131] and on cationic gemini [125] have been reported.

3. Foaming Ability and Foam Stability.

Gemini surfactants have good foaming properties. Cationic gemini surfactants with short spacers have shown good foamability (with foam volume ten times that obtained with DTAC) associated with a good stability of the foam after 30 minutes, for $m = 12$ and 14 [45]. The structure of the spacer does not influence the foamability to large extent, but seems to be an important parameter for the stability [45]. The same trends have been observed with anionic gemini surfactants studied in Okahara's group. With sulfate geminis (Figure 3b), foamability and foam stability decrease as the spacer length increases [51, 52]. Phosphate geminis (Figure 3c) have shown very good foam stability for $Y = (EO)_1$ or $(EO)_2$ [53]. Sulfonate gemini (Figure 3a) with $m = 12$ and short spacers produce about 30% more foam than the corresponding surfactant monomers. They still show a good foamability for all spacer length, but foam stability is lost when the spacer contains more than 2 EO groups [54]. The foam stability can be improved by varying the composition of the spacer. For instance, sulfonate gemini with a sulfone group (see the structure in Table 32) in the spacer form very stable foams [57]. With carboxylate geminis (Figure 3d), larger (35%) volumes of foam can be obtained as compared to the conventional carboxylate surfactant, but its stability is not greatly improved [59]. α -Sulfonated fatty acid oligoethylene glycol diester (Figure 3e) showed some improvement in foam stability but not in foamability (Figure 11) [62]. The foaming properties of surfactants containing an unequal number of hydrophobic chains and headgroups have also been studied [55, 109, 113].

The stability of soap films produced from dilute and semi-dilute cationic gemini surfactant 12-2-12, 2Br solutions have been studied with a thin film balance [132]. Stable common black films can be produced from 12-2-12, 2Br solutions at the cmc, while it is impossible to form stable films with the corresponding monomer (DTAB). Only longer chain cationic surfactants can produce stable films by themselves, and the formation of stable film from DTAB solutions requires addition of co-surfactant or salt [132, 133].

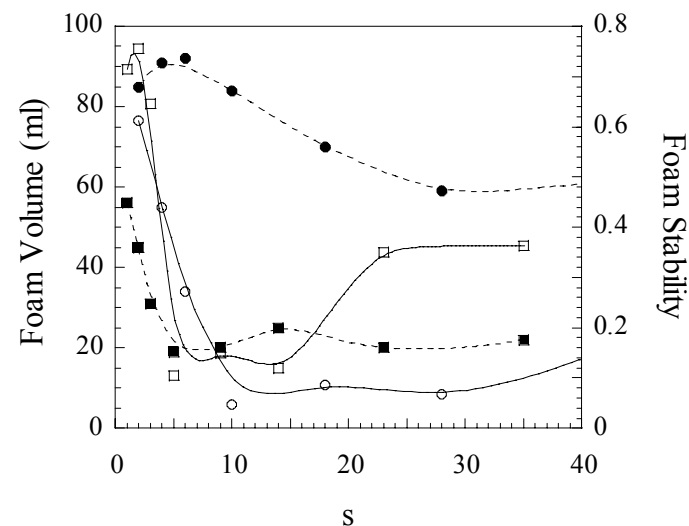


Figure 11: Foaming properties of the gemini surfactants of Figure 3e (squares) and of their corresponding monomers (circles). Filled symbols: volume of foam obtained right after shaking (foam ability). Empty symbols: the fraction of foam volume remaining after 30 minutes standing (foam stability) [62].

Moreover, upon addition of salt, the 12-2-12 soap films undergo a sharp thickness transition from common black films to Newton black films 5-6 nm thick. DLVO theory accounts well for the thickness dependence of the disjoining pressure. It also suggests that the apparent charge density on 12-2-12 films is one order of magnitude lower than on DTAB films, (0.0047 C/m^2 instead of 0.046 C/m^2 for DTAB). This low charge density, in conjunction with a decrease in the hydration due to the spacer between the headgroups, explains the possible transition to Newton black films with 12-2-12. However, it does not explain the difference in film stability, which may be related to the high viscosity of 12-2-12 semi-dilute solutions. Correlation between foam stability and bulk viscosity has also been pointed out in [57].

B. Solid-Water Interface

1. Adsorption Isotherms

Multi-step adsorption processes have been seen with several cationic gemini surfactants adsorbing onto silica (40 μm , washed several times with hydrochloric acid, specific surface area $29 \text{ m}^2/\text{g}$) [134]. The amount of surfactant adsorbed, sodium, bromide, and proton concentration in the supernatant along the binding isotherm, and the electrophoretic mobility were measured. The first step consists of a rapid but small increase of the surfactant amount adsorbed, followed by a plateau which starts at the point of zero charge. It corresponds essentially to an exchange of the residual sodium ions bound to the silica. After the first adsorption plateau, whose broadness decreases as s increases, a second rapid increase in the amount adsorbed corresponds to the formation of surfactant aggregates at the interface. These aggregates (admicelles) bind bromide ions less than the corresponding bulk micelles (contrary to what has been observed with DTAB). Their positive charges induce a reduction of the pK_a of the silanol groups of the silica surface, as evidenced by the sharp drop of the pH

(particularly with the short spacer gemini 12-2-12, 2Br) associated with this second step. At saturation, the amount of adsorbed surfactant is inversely proportional to the spacer length, s . It was suggested that for short spacer gemini surfactants, the first step may involve charge redistribution at the silica interface. In a more recent study the same authors compared the adsorption isotherms of DTAB and 12-2-12, 2Br onto the same silica particles treated differently (with and without HCl-wash) [135]. The adsorption mechanism of the monomer and the dimer on the unwashed and on the washed silica is qualitatively the same. However, the variation in the state of the surface induces quantitative differences: the amount of surfactant adsorbed at the point of zero charge and at saturation is larger with the unwashed silica. This makes the multi-step mechanism difficult to observe with unwashed silica and may explain the results of other studies [104, 137]. The adsorption of 12-2-12, 2Br starts at much lower concentration than for the corresponding monomer DTAB, and the point of zero charge (PZC) of the particles is reached at much lower concentration for 12-2-12, 2Br. However, the maximum amount differs only a little. Both surfactants keep on adsorbing at the silica surface even after their micellization in the supernatant, the saturation being reached at an equilibrium concentration of about 1.5 times the cmc.

Those results have been confirmed recently by force balance measurements and direct imaging with atomic force microscopy (AFM) [136]. The charges of the mica surface are neutralized (suppression of the repulsive double-layer force) at a bulk concentration of 1 to 5 μM of surfactant. As the concentration of surfactant increases, hydrophobicity of the surfaces increases (high pull-off force) and discrete surfactant monolayer patches grow and eventually merge. A further increase in concentration (5 μM to 0.01 mM) decreases the pull-off force, steadily increases the electrostatic repulsive force and increases the compressed layer thickness, suggesting the formation of a

bilayer. This step was observed directly by AFM to occur also by growth of patches. At a concentration of 2mM, a full bilayer is formed. The force profile at 0.8 mM presents an extra repulsive force attributed to further adsorption on top of the bilayer. This interpretation is supported by AFM measurement of the surface roughness. The authors pointed out the time dependence of the force profiles obtained and concluded on a slow process of adsorption [133].

Adsorption isotherms of DTAB, 12-2-12, 2Br, and 12-2-12-2-12, 3Br on silica (0.3 μ m and specific surface area 16.7m²/g) in 10⁻² M NaBr have been established [137]. Electrophoretic mobility along the isotherm suggests that bilayers are formed with all surfactants, but a two-step adsorption process was observed only for the DTAB. The amount of surfactant adsorbed at saturation decreases from 57 μ mol/g to 48 μ mol/g from the monomer to the dimer, and down to 30 μ mol/g for the trimer. Higher concentration of salt increases the amount of surfactant adsorbed at saturation and no addition of salt reveals the two-step adsorption process for 12-2-12, 2Br [138]. The same studies have been carried out on laponite [139], and on titanium dioxide (bare or hydrophobically modified) [140]. The adsorption of cationic trimers of the same type with longer spacers ($s = 3$ and 6) onto silica has also been published [104].

2. Interfacial Packing and Aggregate Geometry.

From the amount of surfactant adsorbed at saturation, and knowing the specific surface area of the solid substrate, an average limiting surface area per surfactant molecule is readily obtained. For comparison, since the maximum amount of adsorbed surfactant depends on the state of the substrate surface, the surface area per amphiphilic moiety in gemini surfactants A_2 , is normalized by the surface area of the corresponding monomer A_1 , measured in the same series of experiments. For the cationic surfactant 12-s-12, 2Br, the normalized surface area increases linearly with the spacer length (Figure 12) [134].

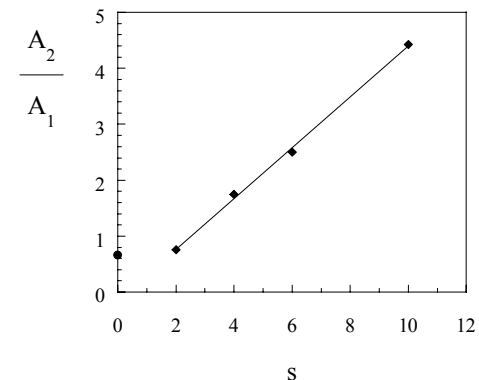


Figure 12: Normalized limiting surface area per amphiphilic moiety in 12-s-12, 2Br gemini surfactants, as a function of the spacer chain length, s [134]. Normalization is done with respect to the limiting surface area of DTAB, A_1 , measured in the same series of experiments; “ $s = 0$ ” corresponds to DDAB [141].

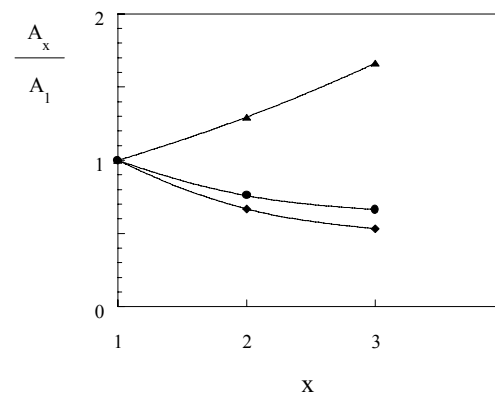


Figure 13: Normalized limiting surface area per amphiphilic moiety as a function of the degree of oligomerization x [104]: $s = 3$ (λ); $s = 6$ (σ); surfactant tetramer of Figure 8c (v). multiple chain surfactants, “ $s=0$ ”, (v) [141].

The average surface area occupied by an amphiphilic moiety is larger than the one for DTAB for except for $s = 2$. This spacer dependence is amplified with higher degrees of oligomerization (Figure 13). For short spacers ($s = 2$ [137] and $s = 3$ [104]) the per amphiphilic moiety slightly decreases with the degree of oligomerization. This means that each amphiphilic moiety is more densely packed in layers of surfactant oligomers with short spacers. However, for long spacers ($s = 6$), the surface area increases almost linearly with the degree of oligomerization [104]. For comparison, results obtained for C_{12} multiple chain surfactants with one cationic headgroup [141] have also been reported in Figure 13. This illustrates the fine-tuning of the packing that can be achieved with surfactant oligomers by playing with the spacer length and the degree of oligomerization.

By atomic force microscopy (AFM), using the precontact repulsive force (within the electrical double layer) [142] [143], Manne *et al.* observed directly the aggregates formed by the cationic gemini surfactants 12-s-12, 2Br on the cleavage plane of mica [144]. The gemini surfactant with the shortest spacer, $s = 2$, which gives worm-like micelle in bulk solution, form bilayers on mica surfaces. Bilayers were also observed with the double chain surfactant DDAB, known to form vesicles in dilute solutions. Parallel cylinders are obtained when adsorbing the 12-4-12, 2Br surfactant and DTAB. These surfactants form spherical micelles in dilute solutions, which can slightly elongate at high enough concentration for the surfactant dimer. With the single chain divalent surfactant, referred to as 12-2-1, 2Br, spherical admicelles form. From these observations, the authors conclude that the dimensionless packing parameter as defined in [32] to explain the morphology of micelles in the bulk, determines the shape of interfacial aggregate as well. However, the mica surface playing the role of a huge “counter-ion”, the curvature of the aggregate at interface can be (and most often is) lower than the curvature of the aggregate in the bulk.

IV. STRUCTURE AND PROPERTIES OF SURFACTANT OLIGOMERS SELF-ASSEMBLIES

A. Critical Micelle Concentration

The cmc of surfactant oligomers has been measured by tensiometry, by conductimetry, dye solubilization and dye fluorescence measurements. Gemini surfactants are characterized by a cmc which is ten to a hundred times lower than the corresponding conventional surfactant (monomer), the reduction factor being essentially determined by the cmc of the monomer.

Cmc values are reported in the tables of the appendix. It can be seen that different methods can yield very different values. Some difficulties in determining cmc have indeed been reported rather often for geminis and surfactant oligomers. In conductivity measurements, ion pairing can sometime interfere with micellization, especially with short chain surfactants [145]. Slow adsorption at the interface may sometime mask the cmc in surface tension measurements. This has already been discussed [1].

1. Alkyl Chain Length Dependence of the Cmc - Comparison with Monomers

The hydrophobic chain length m is not a variable specific to surfactant oligomers. However, The study of its influence on the cmc brings good insight into the micellization properties of surfactant oligomers. In most cases, the m -dependence of the cmc is classical, meaning that the cmc decreases exponentially as the alkyl chain length increases (see tables 14-24) [146, 147]:

$$\ln \text{cmc} = A - B_m m. \quad (\text{Equation 4})$$

Figure 14 shows that the B_m factor is nearly independent of the spacer length and rather close (but not equal) to the one obtained for conventional surfactants. The same has been observed for the compounds of Figure 2e when compared to their monomer (see Table 23) [119] and for anionic gemini of Figure 3e (see Table 30) [62]. This means that the free energy of transfer of one CH_2 from water into the micelle core $\Delta G_{\text{tr}}(\text{CH}_2)$ is close in both types of surfactants [38, 42, 63]. This provides an important clue to understand the low cmc values of surfactant oligomers. Gemini surfactants have lower cmc than conventional ones because each molecule contains more methylene groups which water does not like to solvate. The slope B_m is actually not equal for both types of surfactant and the two straight lines in Figure 14 go further apart when m increases. (B_m is 1 for geminis and 0.7 for monomers, but for a correct comparison the B_m value of 1 should be divided by 2, since m corresponds only to half the number of methylene groups in geminis).

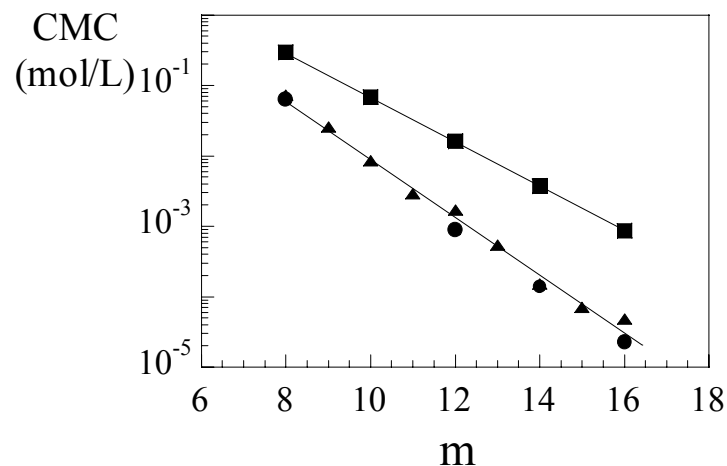


Figure 14: Cmc vs alkyl chain length, m , in gemini and monomeric homologues: m -2- m , 2Br (\blacktriangledown) [147]; m -5- m , 2Br (\bullet) [146]; m -6- m , 2Br (\blacksquare) [146]; monomer (σ) [155].

This means that the ratio $\text{cmc}(\text{monomer})/\text{cmc}(\text{dimer})$ increases with m . Thus, when going from the monomer to the dimer the cmc is decreased by a factor, which is essentially determined by the cmc of the monomer. This suggests that the free energy of micellization *per amphiphilic moiety* $\Delta G_{\text{M}}^{\circ}$ is equal in both types of surfactants (rather than the $\Delta G_{\text{tr}}(\text{CH}_2)$). This has been shown by calculating $\Delta G_{\text{M}}^{\circ}$ from the cmc value and the ionization degree of the micelles at the cmc. Zana established the following relation for ionic surfactant oligomers [148]:

$$\Delta G_{\text{M}}^{\circ} = RT(1/x+\beta)\ln \text{cmc} - RT \ln x/x, \quad (\text{Equation 5})$$

where $\beta = 1-\alpha$ is the degree of association of the counter-ions to the micelles, and where the cmc is expressed in mole of amphiphilic moiety per liter. Applying equation 5 to various $m = 12$ surfactant oligomers shows that ΔG° is about -20kJ per mol of amphiphilic moiety [104, 148], almost independent of the degree of oligomerization. (There are small differences that are going to be discussed in section II.A.3.).

In Figure 15, the cmc is plotted against $x \cdot m$, the total number of methylene groups belonging to the hydrophobic tails. It can be seen that, to get the same cmc with a dimer as with an $m=16$ conventional surfactant, the surfactant dimer must contain 24 methylene groups in its hydrophobic chains. This may sound like a waste and is due to the fact that the additional methylene groups in gemini surfactants come with an additional headgroup. Thus, many of methylene groups are close to a hydrophilic charged group and do not trigger micellization. There is, however, an interesting benefit to this apparent waste. The vertical dotted lines in Figure 15 correspond approximately to the maximum number of methylene groups a surfactant can contain to be soluble in water (meaning neither crystals nor mesophases) at room temperature. It is below 16

for monomers and above 32 for dimers, and reaches at least 36 for trimers. Hence the benefit of surfactant oligomers may not be as much to with reducing the cmc as compared to conventional surfactants. It is certainly to allow cmc values that could never be reached by increasing the length of a conventional surfactant, because this would have induced a phase separation [109].

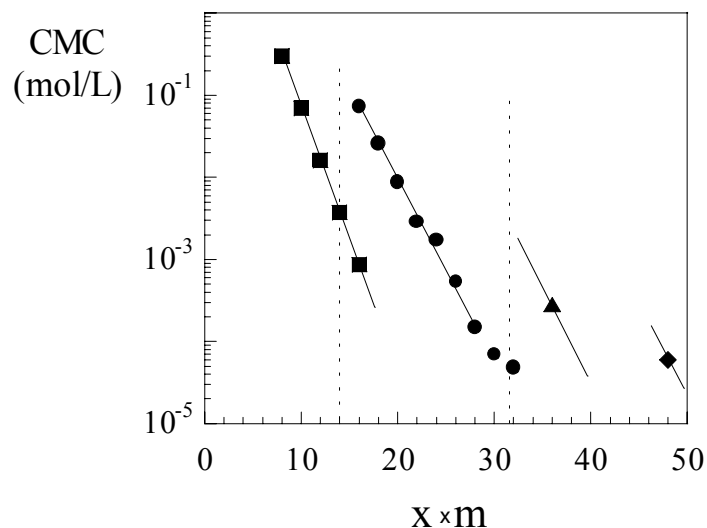


Figure 15: Cmc versus number of methylene groups per surfactant molecule for cationic monomers (□), dimers (○), trimer (σ) and tetramer (v).

In cationic surfactant heterodimers, $m-2-m'$, 2Br, the cmc does not depend on the difference ($m-m'$) but on the total number of methylene groups in the surfactant [87].

The m dependence of the cmc values sometimes deviates from the exponential behavior described above when the alkyl chain becomes longer than a certain length (Figure 16), and can sometime reverse (Table 16). This has been

observed when the spacer contains either aromatic rings or oxygen atoms (oxyethylene or hydroxypropylene spacers) [23, 39,46, 117, 118]. The onset length of this unusual behavior, decreases with increasing ionic strength [117, 118]. With the star shaped anionic trimer (Figure 8e), the cmc increases with m [111,112] (Figure 17).

This unusual behavior is necessarily related to hydrophobic interactions. The formation of premicellar aggregates has been proposed to explain it [39]. Equilibrium constants for the formation of premicellar aggregates have been calculated from the difference between the experimental γ -logC plots and virtual plots established by extrapolating to high m values results obtained at low m values [46, 117].

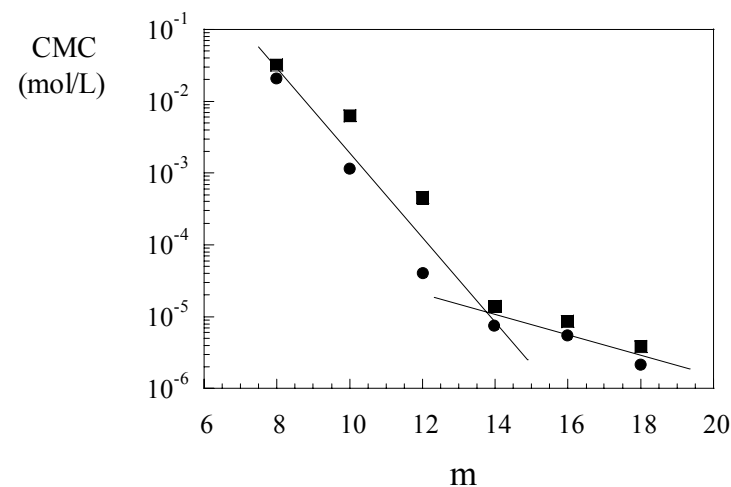


Figure 16: Deviation from the classical exponential m dependence of the cmc of cationic gemini surfactant of Figure 2c in 0.01 M NaCl (τ) and 0.1 NaCl (λ) at 50 °C [117].

Alternative hypotheses should be considered with more attention. An increase of the cmc means a decrease in the absolute value of the free energy of micellization. This can result either from a decrease of the chemical potential of the free (unmicellized) surfactant μ_s° , or from an increase of the chemical potential of the surfactant in the micelles μ_m° . In the same way, the unusual m dependence of the C_{20} mentioned above, can result either from a decrease of μ_s° , or from an increase of the chemical potential of the surfactant adsorbed at the air-water interface $\mu_{A/W}^\circ$. Premicellization indeed reduces the chemical potential in the bulk and explains lower surface activity and higher cmc. But an alternative, which would be less expensive in term of mixing entropy, would involve intramolecular association between the alkyl chains of a surfactant oligomer.

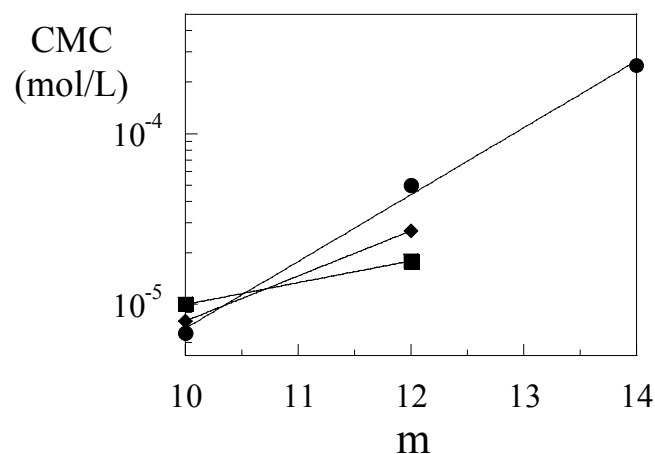


Figure 17: Inverted m dependence of the cmc in anionic trimers with hydrophilic star shaped-spacers (see structure Table 44) [111, 112].

This hypothesis has been suggested by experimental observations of the change in enthalpy and in volume upon micellization [119]. Intramolecular association would decrease the hydrophobic hydration shell and thus decrease μ_s° and increase the cmc as well as C_{20} . The other alternative corresponds to an increase of μ_m° , and could result for instance from the formation of micelles in which the hydrocarbon moieties would largely remain in contact with water. This would achieve Menger's initial goal [23] but would probably not lead to an increase in C_{20} . A convincing explanation for the unusual m dependence of the cmc is still to be found. NMR conformational studies on the long chain gemini such as the one carried out on $m = 8$ cationic surfactants with *o*-, *m*-, and *p*-phenylenedimethylene spacers [149] could be helpful. For this system, a recent neutron scattering study supports the formation of premicelles [150]. Also, an accurate determination of the Kraft temperature as done for 16-s-16, 2Br surfactants [151] would clarify the situation. Finally, Monte-Carlo simulations, where the cmc is defined as the surfactant concentration where half of the surfactants have at least one surfactant as nearest neighbor [128, 152], also yield an increase of the cmc as m increases.

2. Headgroup Nature Dependence of the Cmc.

As mentioned above, the cmc of gemini surfactants is essentially determined by the cmc of the corresponding monomer. Hence the influence of the headgroup, and the dependence of the cmc on the nature of the headgroup, is the same as in conventional surfactant. Figure 18 shows that for a given $s/3$, the cmc of anionic gemini surfactants varies with the headgroup nature as: $\text{COONa} > \text{OPO(OH)(ONa)} > \text{O(CH}_2)_3\text{SO}_3\text{Na} > \text{OSO}_3\text{Na}$ [59].

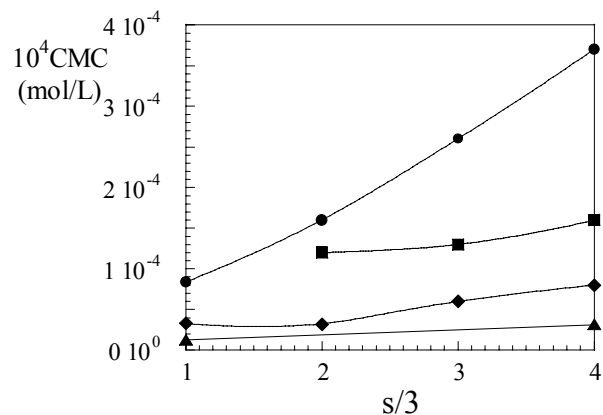


Figure 18: Cmc versus spacer chain length for carboxylate (Figure 3d), phosphate (Figure 3c) (∇), sulfonate (Figure 3a) (\diamond) and sulfate (Figure 3b) disodium gemini with $m = 10$ [59].

3. Spacer Chain Length Dependence of the Cmc

The cmc of cationic surfactants m-s-m, 2Br varies non-monotonically with s , when the spacer is hydrophobic (Figure 19) (Tables 3-7). It increases for short spacers up to 4-5 methylene groups, then decreases. This has been observed for $m = 8$ [149], 10 [162], 12[38] and 16 [41]. Note that the comparison is done on a linear scale. The same holds for anionic gemini surfactants (Table 35).

For the series $m = 12$, s has been varied up to high values [38, 153]. The decreasing part of the curve has been explained by the increasing hydrophobicity of the surfactant. For s larger or equal to 10, the cmc depends on s the same way it depends on m [38, 153]:

$$\ln \text{cmc} = A - B_s s. \quad (\text{Equation 6})$$

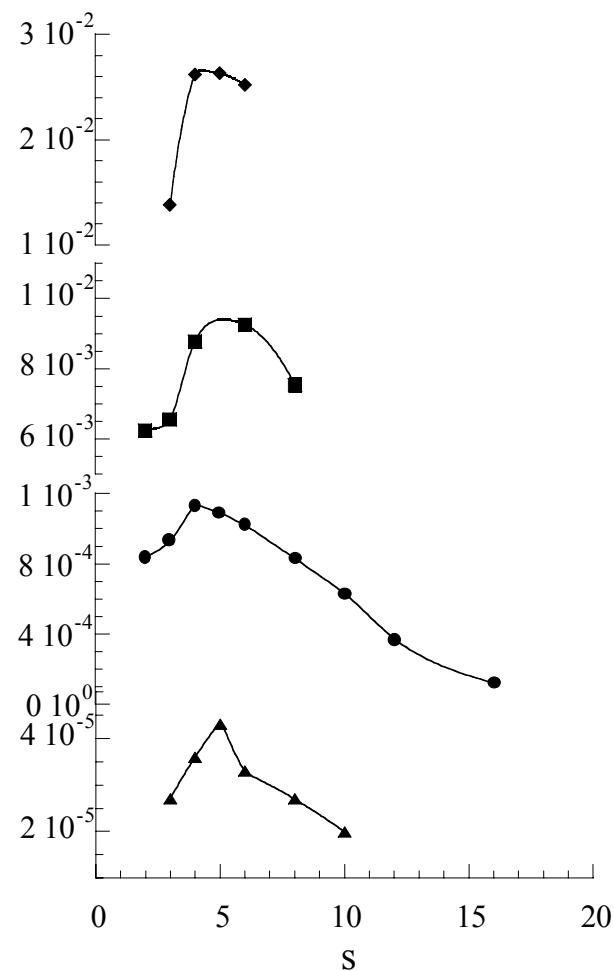


Figure 19: Spacer length dependence of the cmc for cationic gemini m-s-m, 2Br: $m = 8$ (∇) [149]; $m = 10$ (∇) [162]; $m = 12$ (λ) [38]; $m = 16$ (σ) [41].

The factor $B_s = 0.3$ is smaller than B_m . When long enough, the hydrophobic spacer group can buckle into the micelle core. However, this is apparently not so easy considering the low value obtained for B_s , which is even smaller than the one found for bolaform surfactants [154] (Figure 20). The data

of Figure 20 suggest that the impediment for the spacer to be inserted into the hydrophobic core of the micelle, results from the combined effect of electrostatic interaction, loss of conformational entropy (as in bolaform surfactant), and also steric hindrance (as in double chain surfactants).

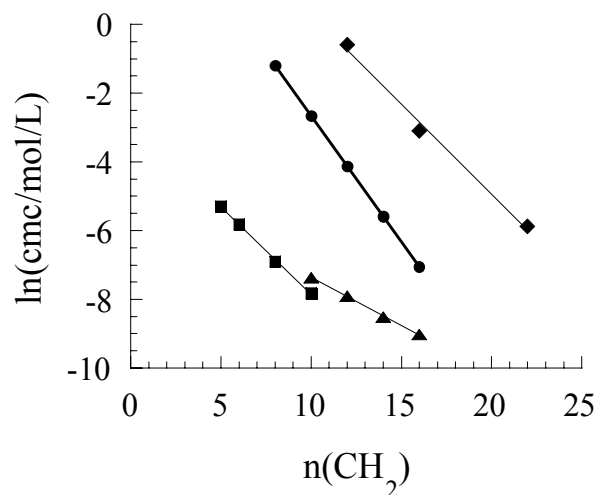


Figure 20: Influence on the cmc of increasing the number of methylene groups n in the hydrophobic tail of a conventional surfactant ($C_nH_{2n+1}N(CH_3)_3$, Br) (λ), in a bolaform surfactant ($(CH_3)_3NC_nH_{2n}N(CH_3)_3$, 2Br) (ν), in a double chain surfactant ($C_{12}H_{25}C_nH_{2n+1}N(CH_3)_2$, Br) (ν), and in the spacer of a gemini surfactant ($C_{12}H_{25}(CH_3)_2N(CH_2)_nN(CH_3)_2$ $C_{12}H_{25}$, 2Br) (σ).

The increase of the cmc with s when $s < 5$ (Figure 19), is probably related to electrostatic interactions between the headgroups. When the spacer is short, part of the work against electrostatic repulsion necessary to bring the surfactants together upon micellization, has already been done at the synthesis step as discussed in [99]. This hypothesis is supported by several arguments. First, the cmc increases with s up to $s = 4-5$, which corresponds to the length of

the spacer where the interfacial surface area per amphiphilic moiety is equal in gemini and in conventional surfactants. The second argument relies upon Monte Carlo simulations. With ionic gemini surfactants, non-monotonic variation of the cmc is observed, whereas the cmc of nonionic gemini surfactants increases monotonically with s [128].

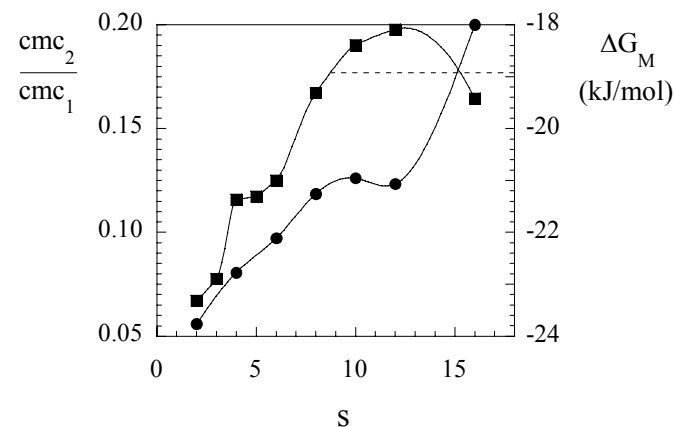


Figure 21: Ratio of cmc of the cationic geminis 12-s-12, 2Br (cmc2) over the cmc of the corresponding monomer $C_{12}H_{25}C_{s/2}H_{s+1}N(CH_3)_2$, Br (cmc1) (λ) and free energy of micellization per amphiphilic moiety ΔG_M (ν) versus spacer length s .

This small electrostatic effect is clearly pointed out by considering the free energy of micellization per amphiphilic moiety. ΔG_M is slightly more negative for short spacers than for long spacers [104, 162]. The differences in ΔG_M are not large but they are systematic and the trend is confirmed with

surfactant trimers and tetramers. ΔG_M decreases with the degree of oligomerization for $s = 3$, whereas it is constant for $s = 6$ (Figure 23).

To understand the s dependence of the cmc, it is useful to compare the cmc of geminis 12- s -12, 2 Br with the cmc of double chain surfactants $C_{12}H_{25}C_{s/2}H_{s+1}N(CH_3)_2$, Br [155, 156]. The latter correspond closely to the monomers in the sense that they have the same number of methylene groups per headgroup. Figure 21 shows that the reduction factor of the cmc, going from the monomer to the dimer, increases as the spacer increases. This increase is not regular and closely related the variation of ΔG_M . Note that only for $s = 10$ and 12 is ΔG_M less negative than ΔG_M of DTAB.

With hydrophilic oligo(oxyethylene) spacers, the cmc increases with s for cationic see (Table 10, 11) [47,48, 49] as well as for anionic surfactants (see Table 30 and Figure 18). A slightly lower cmc has been observed for cationic gemini of Figure 2b with very large oxyethylene spacers (Table 11) [47]. When hydrophilic spacers become very large, gemini surfactants look like telechelic hydrophobically modified polymers, which are known to micellize at fairly low concentrations to form flower-like micelles [157]. This has, however, not been observed with anionic gemini surfactants of Figure 3e with spacers consisting of up to 35 EO groups [62] (Table 30).

The chemical nature of the spacer influences the cmc value in a way, which is sometime difficult to rationalize. For intermediate spacer lengths, the cmc is lower when the spacer is hydrophilic than when the spacer is hydrophobic (see Tables 13, 16). The cationic surfactant trimer with hydroxypropylene spacer 12-3*-12-3*-12, 3Cl (Figure 8b) has a cmc of 9.6 mM while 12-3-12-3-12, 3Cl has a cmc of 160 mM. Devínsky *et al.* observed slight changes in the cmc of cationic gemini surfactants with different spacers of the type $-CH_2CH_2-X-CH_2CH_2-$, with $X = CH_2, NCH_3, O$ or S [120]. In this study, the lipophilicity of the spacer seems to be the determining parameter.

The ionization degree of the micelles is independent of s for $m = 8$ (Table 3), but increases with s for $m = 10$ and 12 (Table 4, 5).

4. Oligomerization degree

Figure 22 shows the decrease of the cmc as the degree of oligomerization x increases for an $m = 12, s = 3$ series of cationic surfactants [104]. The cmc appears to vary as a power law of the oligomerization degree for this series with $s = 3$, and the same is observed with $s = 2$ [108] and $s = 6$ [104] up to the trimer. The cmc of the cationic tetramer is 2.5 orders of magnitude lower than that of DTAB.

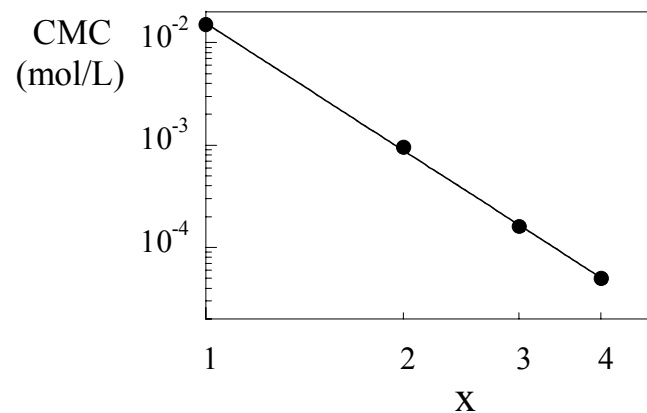


Figure 22: Cmc versus oligomerization degree for cationic surfactant oligomers [104].

The ionization degree of the micelle at the cmc, α , is independent of the x and is essentially determined by m and s (see Tables 3-5). With bromide counter-ions, and for $m = 12$, $\alpha = 0.2$ for $s = 3$ and $\alpha = 0.3$ for $s = 6$, independent

of x . The free energy of micellization decreases (becomes more negative) for short spacers but is constant for long spacer (Figure 23).

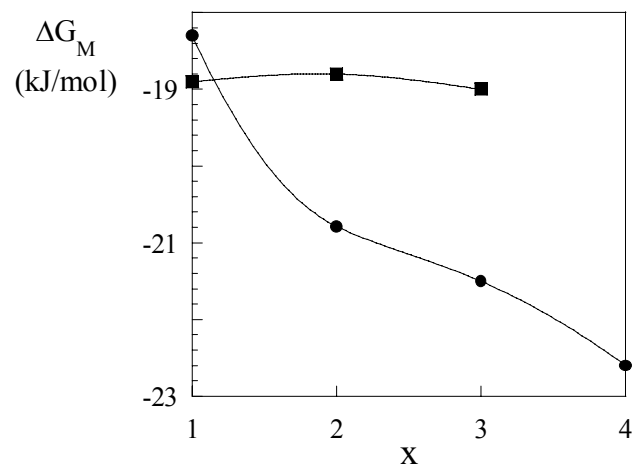


Figure 23: Free energy of micellization per cationic amphiphilic moiety versus degree of oligomerization x for $s = 3$ (λ), and $s = 6$ (ν) [104].

B. Micelle Properties

1. Micropolarity, Solubilization Capacity, and Emulsification

The micropolarity of cationic surfactant oligomers has been characterized by the value of the fluorescence intensity ratio I_1/I_3 of the first and third vibronic peaks in the emission spectra of micelle-solubilized pyrene [48, 92, 158]. It depends on the composition of the pyrene solubilization site, *i.e.* near the micelle/water interface. For cationic geminis with hydrophobic $-(CH_2)_s$ -spacers the micropolarity varies non-monotonically with the spacer chain length, going through a maximum at about $s = 6$ [158]. A similar behavior has been obtained for the corresponding monomer, $m-s/2$ [158]. Micropolarity does not change with spacer length in cationic gemini 16-(EO) $_{s/3}$ -16, 2Br [48]. The micropolarity of cationic surfactant oligomers does not depend on x [104, 158], but slightly decreases with x in nonionic surfactant oligomers of Figure 8g [115].

The solubilization capacity for transazobenzene, as expressed by the ratio of solubilize concentration over surfactant concentration, increases monotonically with m in cationic geminis as with conventional surfactants (see Table 14) [159]. It varies non-monotonically with s , going through a maximum at $s = 6$, where it is about twice that of $s = 2$ and five times that of $s = 12$ (Table 4).

The solubilization of toluene or *n*-hexane by cationic gemini surfactants is more efficient than by cationic surfactant monomers [40]. Cationic geminis have higher selectivity for toluene than for hexane [40]. Solubilization of β -naphthol in short spacer cationic surfactant dimers and trimers adsorbed onto silica [137, 138], titanium oxide [140], and laponite [139], increases with x . This is true when expressed as the molar ratio of β -naphthol adsolubilized to the adsorbed surfactants. However, as pointed out in [137] the solubilization

capacity decreases with x when expressed per dodecyl chain. This has been interpreted as a result of the increasing packing density as x increases.

The emulsification efficiency of cationic gemini was determined by comparing the rate of drop coalescence between heptane/water emulsions prepared from cationic geminis and their monomeric homologues. The drop coalescence was characterized by an exponential decay of the number of drops. The lifetime of the drops was found 1.7 times longer with the geminis [43]. The emulsification properties of non-ionic diol gemini has also been studied [57].

The phase behavior of ternary water/styrene/C12 cationic gemini surfactants with hydrophobic [160] and hydrophilic [123] spacers of different length has been reported. The extension of the single-phase region which lies in the water corner of the phase diagram triangle, depends strongly on the spacer chain length, for hydrophobic $-(\text{CH}_2)_s-$ spacers and more weakly for hydrophilic $-(\text{EO})_{s/3}-$ spacers. The extension of the single-phase region is strongly temperature dependent with $-(\text{EO})_{s/3}-$ spacer, but weakly with $-(\text{CH}_2)_s-$ spacers. At a fixed concentration of surfactant, between 5 and 20 weight percent, only the 12-2-12, 2Br surfactant had poorer solubilization capacity than DTAB (expressed as the molar ratio of solubilized styrene over surfactant). With hydrophobic spacers, the solubilization capacity increases with s and is maximum for $s = 12$, where it is six times higher than for DTAB. With hydrophilic spacers, it is maximum for spacers consisting of 1 or 2 EO groups. The influence of temperature, spacer rigidity and oil size on the oil-water-gemini ternary phase diagram has been studied by Monte Carlo simulation [161].

2. Microviscosity.

The microviscosity of gemini surfactants micelles decreases when the spacer goes from 2 to 12 in a 16-s-16, 2Br series when the spacer is hydrophilic [41] but not much when it is hydrophobic [48, 70, 115, 158].

The microviscosity depends, however, almost linearly on the degree of oligomerization x , and is about 6 to 10 times (depending on the temperature) higher for the cationic tetramer than for the monomer [104, 158]. This has also been observed for nonionic oligomers micelles, in which the dipyranylpropane excimer lifetime is three to four times larger [115]. Microviscosity of admicelles on silica determined from the order parameter of a paramagnetic probe, decreases with the oligomerization degree in the order dimer > trimer > monomer [137] and increases with added salt [138].

C. Morphology of the Aggregates

The size and the shape of surfactant oligomer micelles has been studied by small angle neutron scattering (SANS) [41, 48, 162, 163, 164, 168, 169] and directly observed by transmission electron microscopy at cryogenic temperature (cryo-TEM) [22, 165, 166]. Micellar shape can also be inferred from solubilization studies [159] or from the concentration dependence of the aggregation number measured by fluorescence quenching measurements [103, 166].

The spacer length, is a key parameter of the micelles morphology [22, 165, 165], as could have been deduced from the s -dependence of the surface area. Hydrophobic short spacers ($4 \geq s$) reduce the preferred curvature of the micelles as compared to conventional surfactants micelles. With cationic gemini, worm-like micelles are obtained when $m = 12$. Intermediate length spacers ($5 \geq s \geq 12$) favor the formation of spherical micelles. Interestingly the spherical shape is preserved up to very high concentrations for $s = 10$ and 12 [167]. Thus,

increasing s can be seen as releasing the spacer constraint for lower intermediate spacers, but actually corresponds to a strong constraint for upper intermediate spacers. For long spacers ($s \geq 16$) vesicles are obtained as in the corresponding surfactant monomer (double chain) [22, 165, 166]. The trend is confirmed by SANS of 16-s-16, 2Br surfactants [168] [169]. Due to electrostatic interactions the scattered intensity presents a maximum at a finite wave vector q^* , which is inversely proportional to the distance between the micelles. At low enough concentration, the distance between the micelles reflects the size of the micelles. At a fixed low concentration (between 10 and 50 mM) of 16-s-16, 2Br surfactants, q^* increases as s increases from 5 to 12, suggesting that the aggregation number of the micelles decreases as s becomes larger. The scattered intensity 16-3-16, 2Br varies like q^{-2} . This has been interpreted as the signature of the formation of disks, but cryo-TEM micrographs showed vesicles and bilayer membrane fragments coexisting with worm-like micelles [165] (and this is consistent with $I \propto q^{-2}$).

The same results have been obtained with $m = 16$ phosphate gemini of Figure 3f [70]. For $s = 2$, the scattered intensity varies like q^{-2} , which indicates zero curvature objects (disks or vesicles). For $s = 4$ worm-like micelles and for $s = 6$ or 10 prolate ellipsoids are formed.

With hydrophilic spacers (EO), the aggregation number of the micelles also depends on the length of the spacer. But even with the shortest spacer (1 EO) the growth of the micelle is limited, and the influence of the spacer length on the size of the micelles is less pronounced with hydrophilic spacers than with hydrophobic ones [41, 48]. Nonionic sugar-based geminis of Figure 5a, with $m = 14$, form cylindrical micelles when $s = 6$ and 8 and vesicles when $s = 10$ [84]. Nonionic sugar based gemini of Figure 5b form anisotropic micelles, cylindrical for $7 \geq m \geq 5$ and discoidal for $m = 8$ [164].

1. Worm-like micelles of cationic surfactant oligomers.

a) Micellar growth.

Cationic surfactant oligomers with short spacer are among the few systems where the transition from spherical to very long worm-like micelles occurs at low concentration (below 10 wt%), and does not require any addition of salt, cosurfactants or the presence of hydrophobic counter-ions. The formation of long worm-like micelles was directly observed by cryo-TEM on the 12-s-12, 2Br series [165, 166]. However, the micellar growth can be described more quantitatively by looking at the concentration dependence of the aggregation number $N(c)$, which is obtained from SANS [162, 163] or from fluorescence quenching measurements [103, 165]. The concentration dependence of the zero shear viscosity brings also information on the micellar growth [172, 175, 174].

$N(c)$ has been analyzed with the ladder model [170], which describes a prolate micelle as a cylinder capped at each end by hemispherical micelles. The concentration dependence of N is then expressed as:

$$N = N_0 + 2K^{1/2}(c - \text{cmc})^{1/2}, \quad (\text{Equation 7})$$

where N_0 is the aggregation number at the cmc and c and cmc are here mole fractions.

$$K = \exp(E_c/kT), \quad (\text{Equation 8})$$

where E_c is the end cap energy, *i.e.* the excess chemical potential of a surfactant being in the end caps as compared to the chemical potential of a surfactant residing in the central cylindrical portion. This equation describes well the SANS results obtained on 10-2-10, 2Br gemini [162, 163]. The parameters deduced from such an analysis are presented in Table 1. The end cap energy decreases as the spacer length increases.

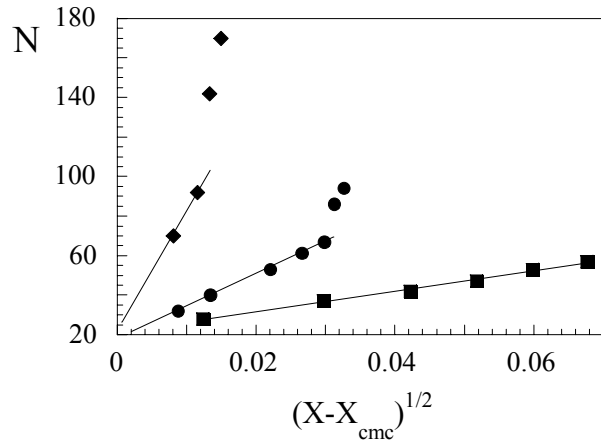


Figure 24: Aggregation number of cationic surfactant oligomers: 12-5-12, 2Br (ν); 12-3-12, 2Br (λ); 12-3-12-3-12, 3Br (ν) [103, 165] analyzed with the ladder model; c , the surfactant concentration and the cmc are expressed in mole fraction.

s	N_0	E_c/kT
2	25	15
3	23	12
4	24	10
6	22	7
8	17	5
10	18	5
12	13	6

Table 1: Characteristic parameters of the micellar growth of 10-s-10, 2Br geminis [162, 163]. N_0 is the aggregation number at the cmc. E_c is the end cap energy.

When applied to the data obtained by fluorescence quenching on the $m = 12$ series of cationic surfactant oligomers [103, 165], the ladder model yields an end cap energy of 11 kT for the 12-5-12, 2Br, 13 kT for the 12-3-12, 2Br and 17 kT for the trimer 12-3-12-3-12, 3Br. Data in Figure 24 show that when the tendency of the micelles to grow is strong, the ladder model however applies only for the lowest concentrations. Moreover, the differences in end cap energy it yields, are not pronounced in view of the large differences in viscosity observed at higher concentrations. Fluorescence quenching and SANS can provide information on the elongated micelle sizes only at low concentration. In this concentration range, the micelles are charged and not screened, and their growth is hindered by electrostatic repulsion [171]. Their growth rate does not only result from the end-cap energy but also from an electrostatic contribution that favors the breaking of the micelles. This contribution decreases with increasing concentration. Three growth regimes have been distinguished [171]: at low enough concentrations, such that the Debye screening length is larger than the micelle size, the concentration dependence of the size is weak and the micelles are nearly monodisperse. As the concentration increases, a sharp crossover to a rapid growth regime occurs (when the Debye length equals the micelle size). The crossover concentration coincides with the concentration, c^* , where the micelles begin to interact with each other (semi-dilute regime). As in the case of neutral micelles, the size distribution is large (exponential), but the characteristic size, N , grows faster than $c^{1/2}$ governing the growth of neutral micelles (Equation 7). Its concentration dependence reads:

$$N \approx 2c^{1/2} \exp\left[E / 2k_B T - l_B a v^2 / 2c\right] \quad (\text{Equation 9})$$

where l_B is the Bjerrum length, a is the diameter of the micelle and ν is an apparent charge density of the micelle. At higher concentration, the electrostatic contribution that tends to break the micelles, results essentially from the entropy of the counter-ions near the end caps, where they are less tightly bound. The growth may be characterized by an effective power law:

$$N \propto c^{(\Lambda+1)/2} \quad (\text{Equation 10})$$

where Λ is related to the net charge on an end cap and depends only logarithmically on c [171].

Surfactant	c^* (wt %)	$10/\sqrt{c^*}$
12-2-12	1	10
14-2-14	0.08	35
16-2-16	0.015	82
12-3-12	4	5
8-2-16	6	4
10-2-14	3	6
12-2-16	0.15	28
14-2-18	0.07	38
12-3-12-3-12	1	10
12-3-12-4-12-3-12	0.5	14

Table 2 : Crossover concentration from slow to fast micellar growth regime c^* for cationic surfactant oligomers. C^* is determined from viscosity measurements, as the concentration where the viscosity is twice the viscosity of the water. $100/\sqrt{c^*}$ is directly proportional to the end cap energy.

The crossover concentration c^* from the slow to the fast growth regime is observed in the concentration dependence of zero shear viscosity [172, 173]. For low concentration, the viscosity of surfactant oligomers solutions is not significantly higher than the viscosity of water. But at $c > c^*$, the viscosity increases very rapidly (Figure 25).

According to MacKintosh *et al.* [171], $c^* \propto E_c^{-1/2}$ and this allows a comparison of the end cap energy among various surfactant oligomers. In Table 2 we reported the values of c^* and $100/\sqrt{c^*}$ which is proportional to E_c , for various cationic surfactant oligomers. Decreasing s from 3 to 2 doubles the end cap energy. The same is obtained by going from the dimer to the trimer, keeping $s = 3$ constant [174]. The rheology of heterodimers m -2- m' , 2Br has been studied by Oda *et al.* [175]. Differences in alkyl chain length markedly affect the end-cap energy (see 12-2-12, 10-2-14, and 8-2-16 in Table 2).

End cap energy values can be estimated rather indirectly from the dynamical properties of the systems (rheology or diffusion coefficient). For instance, in the plateau region of the relaxation spectrum, the storage modulus $G' = G_0$ is nearly independent of the frequency and the loss modulus G'' goes through a minimum. The ratio G'/G''_{\min} is related to the ratio of the length of the micelles to the mesh size of the entanglement network. The latter depends essentially on the concentration while the temperature strongly determines the micelle length. The temperature dependence of the ratio G'/G''_{\min} gives an end cap energy of about 50 kT for 12-2-12, 2Br at 4%, but lower values as the concentration increases (down to 30 kT at 10%) [172]. For the trimer 12-3-12-3-12, 3Br, the same analysis leads also to a decrease of the end cap energy from 80kT to 10kT as the concentration increases from 4 to 10% [106]. The accuracy of such analysis is however questionable and would need a better understanding of the relaxation mechanism to be proven.

Diffusion coefficient measurements by fluorescence recovery after photobleaching (FRAP) [176] interpreted assuming Cates model [177] holds in the concentration range studied, yields about 30 kT for 12-2-12, 2Br, 12-3-12, 2Br, and 16-4-16, 2Br, inconsistently with the differences observed in c^* [176].

The end cap energy can also be estimated by fitting the concentration dependence of the zero shear viscosity in the fast growth regime [172]. This supposes to assume a relation between the viscosity, the length of the micelles L (proportional to N) and the concentration c , and introduce it in the growth law for charged micelles (Equation 9). This has been done for the 12-3-12, 2Br and 12-3-12-3-12, 3Br surfactants [174], assuming Fuoss Law:

$$\eta_0 = Lc^{1/2}, \quad (\text{Equation 11})$$

leading to $E_c = 40 \text{ kT}$ and 80 kT , respectively. Fuoss' law has been assumed, rather than the relations proposed in [172], because the micelles were probably not fully entangled in the concentration range where the viscosity increases rapidly (see next section) [174].

According to the values of $100/\sqrt{c^*}$ and the estimated values of E_c for $m=12$ surfactants, surfactants with longer chain length (16-2-16, 2Br, for example) would have very high end cap energies of several hundreds of kT. These are unreasonable values and shows that large m surfactant oligomers solutions have been most often studied in a metastable state [175, 200], and at equilibrium they exist as two-phase systems. (The Kraft temperature of 16-2-16, 2Br is $45 \text{ }^\circ\text{C}$ [151]). In those conditions, the increase in viscosity does probably not reflect the growth of worm-like micelles.

Addition of DTAB to 12-2-12, 2Br decreases the size of the micelles but DTAB does not concentrate in the end-cap [178].

b) Rheology.

Cationic surfactant oligomers provide systems of charged and unscreened worm-like micelles, and many aspects remain to be understood in the dynamics of these polyelectrolyte type of living polymers [179].

For instance, as the concentration increases, η_0 goes through a maximum at a concentration c^{**} and then decreases (Figure 25). The same is observed for relaxation time, as well as for the diffusion coefficient [176]. This decrease has been attributed to a shortening of the micelles due to a theoretically predicted increase in ionization degree [172]. However, a decrease in the relaxation time and in the viscosity is also observed upon addition of salt [172, 174], which is expected to increase the length of the micelles. (Upon further addition of salt, 12-2-12, 2Br solutions phase separate, and lead to the coexistence of a dilute micellar phase and a lamellar phase [180]. Addition of salt to 12-3-12, 2Br solutions yields phase separation, but in this case a hexagonal phase is formed [106]).

It has been proposed that, in the concentration range where the viscosity increases rapidly, the systems were not fully entangled [174]. This is suggested by the strong concentration dependence of the elasticity at low concentration (Figure 26). The cross over to a fully entangled regime seems to be reached at maximum viscosity concentration, c^{**} . For fully entangled systems, the elasticity is expected to vary like c^2 , as observed for the dimer 12-3-12, 2Br system at $c > 10 \text{ wt\%}$ (Figure 26).

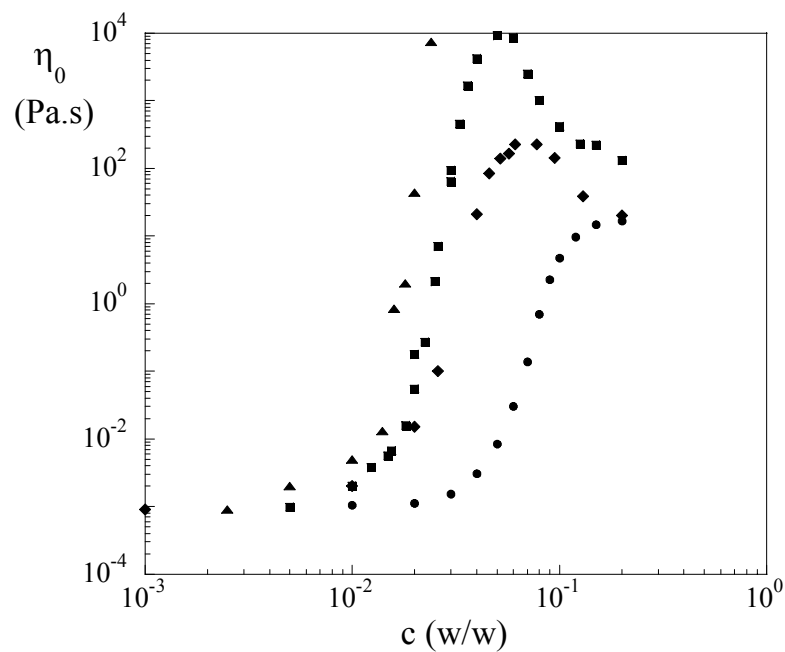


Figure 25: Concentration dependence of the zero shear viscosity of aqueous solutions of 12-2-12, 2Br (ν), 12-3-12, 2Br (λ), 12-3-12-3-12, 3Br (ν) and 12-3-12-4-12-3-12, 4Br (σ). Reprinted from ref [104]

The existence of a concentration regime of overlapping yet not fully entangled micelles, may be a clue to understand the non-monotonic behavior of the viscosity. It also provides a simple explanation for the increase of the elastic plateau modulus upon addition of salt observed on 12-2-12, 2Br [181] and 12-3-12, 2Br solutions [106]. It may also explain why the temperature dependence of viscosity for concentrations close the maximum in viscosity does not follow on Arrhenius law [172]. The extension of the concentration range where the micelles overlap and are yet not entangled (expressed as c^{**}/c^*), would reflect

the rate at which they grow [174] and could provide a more reliable method to estimate E_c .

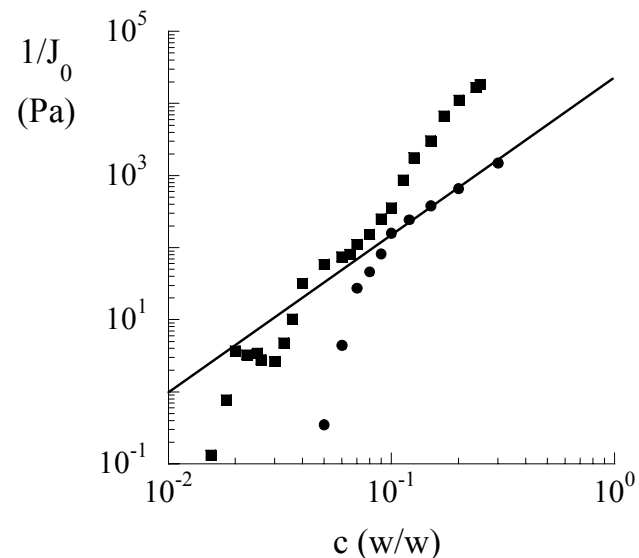


Figure 26: Concentration dependence of the elasticity (inverse of the recoverable compliance) of 12-3-12, 2Br (λ) and 12-3-12-3-12, 3Br (ν) aqueous solutions [174].

The non-linear rheology of 12-2-12, 2Br solutions has been subject to several studies. As in other worm-like micelle systems, shearing solutions of 12-2-12, 2Br close to c^* induces thickening [185, 182, 183]. The shear rate inducing thickening decreases with the concentration and increases with temperature [185]. Shear thickening is associated with anisotropy in neutron scattering [182] as well as in refractive index and conductivity [183]. Cryo-TEM micrographs on sheared samples [185] have shown that a phase separation occurs between surfactant rich and surfactant poor regions.

c) Branched and closed-looped worm-like micelles

In the trimer 12-3-12-3-12, 3Br solutions the extension of the overlap yet unentangled regime is as broad as in the 12-3-12, 2 Br system, although the c^* values suggests that the micelles are growing faster [174]. This could be good confirmation for the presence of branches which have been observed by cryo-TEM [184, 104]. In the fully entangled regime, the elasticity of 12-3-12-3-12, 3Br solutions is enhanced as compared to 12-3-12, Br solution (Figure 26). This may also result from branching [174]. The formation of branched worm-like micelles has also been observed by cryo-TEM in 12-2-12, 2Br solutions [185], and has been obtained in molecular dynamics simulations [186].

Figure 27: Cryo-TEM micrographs of a vitrified 1% aqueous solution of 12-3-12-4-12-3-12 showing many closed-loops coexisting with open worm-like micelles [188].

Formation of a dominant population of closed-loops in worm-like micellar systems, theoretically considered for a long time [32, 187], has recently been achieved with the cationic surfactant tetramer 12-3-12-4-12-3-12, 4Br [188] (Figure 27). The contour length distribution $N(L)$ of the closed-looped micelles has been determined from cryo-TEM micrographs (Figure 28). At large contour lengths, the distribution observed scales as $N(L) \propto L^{-5/2}$, as expected from ring-chain equilibrium polymerization theory [187]. At small contour lengths, the ring closure probability depends on the rigidity of the micelles, and the maximum of the distribution at $L = 150$ nm corresponds to twice the persistence length [188].

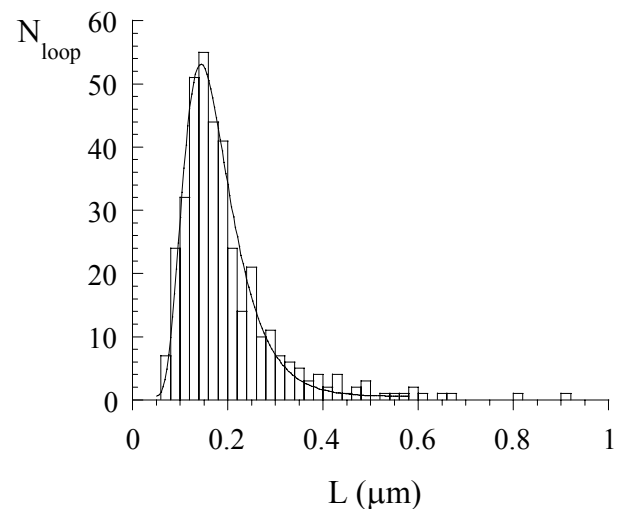


Figure 28: Loop size distribution in 1% aqueous solution of 12-3-12-4-12-3-12. The mode of the distribution corresponds to twice the persistence length ($l_p = 75$ nm). The decreasing part of the distribution scales as $L^{-5/2}$ as expected from the ring closure probability for gaussian polymers reprinted from ref. [188].

2. Vesicles and other low curvature aggregates of surfactant oligomers

The formation of vesicles from gemini surfactants has been specifically reviewed [189]. Vesicles are obtained with $m = 12$ and $s > 16$ but also for $m > 16$ and $s < 4$ gemini surfactants. This is true for diquatary ammonium [22, 165, 166] as well as diphosphates [67]. Vesicle formation has also been observed from nonionic sugar based gemini such as in Figure 5a (14-10-14) [84]. The cleavable heterodimer surfactant of Figure 6c [88] forms vesicles that can be destroyed by acid catalysis under milder conditions ($\text{pH} = 3$) than many other cleavable surfactants, a property that could find application in drug vectorization [88]. Other cleavable gemini surfactants have been shown to yield small unilamellar vesicles [96] having transition temperatures that are pH dependent.

An interesting result concerns the stereo dependence of the fusion of vesicles [91]. Upon addition of Ca^{2+} , vesicles formed from (S,S) and (R,R) stereoisomers of surfactants in Figure 7a undergo fusion whereas (R,S) isomer vesicles undergo fission. This observation has been correlated with the monolayer isotherms at the air-water interface. The surface area per headgroup is smaller for the meso compound than for the (S,S) isomer and decreases when Ca^{2+} ions are added while it increases for the (S,S) isomer [91].

Vesicles of diphosphate geminis 12-18-12, 2Na and 12-24-12, 2Na are characterized by a non-cooperative phase transition observed by DSC and fluorescence depolarization, the midpoint of the transition range being about 45 °C [67]. The transition is accompanied by a line broadening of the ^1H and ^{31}P NMR signal. X-ray diffraction suggests that the spacer hydrocarbon chain is membrane spanning in the 12-24-12, 2Na surfactant vesicles. This had been previously observed with glycerophosphate gemini surfactants of the type $n/2$ - $n/2$, 2Na [71]. The temperature transition is structure dependent and decreases as the pH increases. The authors pointed out that, for an equivalent thickness, the transition temperature was higher in membrane spanning spacer gemini vesicles than in classical phosphoglyceride bilayer lipid membranes [71]. This could explain, from the evolutionary standpoint, why such lipids have been found in bacteria living under extreme thermal conditions [71].

As with conventional surfactants, mixtures of cationic and anionic surfactants can yield vesicles [190, 191]. Bromide counter-ions of cationic geminis have been replaced by palmitate ions. The vesicles obtained have a higher transition temperature as expected with "catanionic" systems, but the interesting result is that this transition temperature decrease from 74 °C to 39 °C when the spacer goes from 2 to 12. Large spacer surfactants also form vesicles that are more permeable to hydroxyl anions. Other catanionic systems involving geminis have been studied. For instance, addition of an anionic gemini to CTAB

solutions induces a line broadening of the NMR signal of the methyl proton of CTAB which has been interpreted as the formation of a network of cross-linked micelles [192]. This interpretation has however been contradicted by a cryo-TEM study, which revealed the presence of vesicles and other large aggregates suggesting that the system was close to precipitation [193].

Vesicles have also been obtained from asymmetric phosphate gemini surfactants mixed with L-histidine based surfactants having two long alkyl chains [194]. The histidine surfactant is not soluble by itself. When mixed with (R,S) surfactant of Figure 7a, at pH = 6.5, large vesicles (150 to 750 nm diameter) are obtained. With the (R,R) surfactant ill-defined tubular structure are obtained. When added to the (S,S) isomer of the surfactant of Figure 7a, 40 nm width right-handed helical ribbons are obtained, with pitch of 90 nm rather independent of the composition. Similar helical ribbons are obtained with 16-2-16 having L-tartrate or D-tartrate as counter-ions [195]. But in that case, the width and the pitch of the ribbons can be tuned by adjusting the enantiomeric excess, $(c_L - c_D) / (c_L + c_D)$, or by adding an excess of chiral counter-ion. It is worth mentioning that this geminis with chiral counter-ion have the ability to gel halogenated organic solvents in the presence a small amount of water [196]. Several factors seem necessary to gel the organic solvent: the short spacer, the chirality of the counter-ion, and its ability to hydrogen-bond. Other cationic geminis ($m = 16$, and 2, 3 dimethoxybutane spacer) have shown the ability to self-assemble in chloroform in the presence a small amount of water [197].

The vesicle-micelle transition has been studied by adding spherical micelle forming surfactants like DTAB and 12-10-12, 2Br to a vesicle forming gemini surfactant 12-20-12, 2Br [198]. No worm-like micelle intermediate state has been observed. The vesicle-micelle transition can also be triggered by increasing the temperature of 16-3-16, 2Br solutions [199]. Addition of hexanol into solutions of 12-2-12, 2Br induces a transition from worm-like micelles to

vesicles [200]. This transition has been studied by rheology and cryo-TEM observation. When the molar ratio, r , of hexanol to gemini increases, the viscosity and the size of the micelles first increase up to $r = 1/8$. Increasing r further (up to $1/3$) leads to the formation of highly branched micelles coexisting with small vesicles of about 100 nm diameter. In this regime the viscosity decreases. Increasing r then induces the growth of the vesicles and eventually leads to phase separation [200]

D. Liquid Crystalline Phases

1. Lyotropic behavior

Cationic gemini surfactants 12- s -12, 2Br (with $16 \geq s \geq 4$) form lyotropic mesophases stable from room temperature up to temperature of 150-200 °C [167]. The concentration range of stability of the micellar solutions broadens on increasing s and spans almost the entire phase diagram (up to 90% where it start to coexist with crystals) when $s = 10$ and 12. This has been interpreted as being due to a maximum mismatch between the length of the spacer and the length of the alkyl chains. For long spacers the range of micellar phase narrows again, and with 12-16-12, 2Br surfactant, lyotropic mesophases are obtained at 30% [167]. The concentration range of stability of the lyotropic mesophases is widest for 12-8-12, 2Br. The mesomorphic behavior of 16- s -16, 2Br [201, 202] have been also studied with emphasis on short spacers ($s = 1, 2, 3$, and 6). The Kraft boundary of the mesophases decreases with increasing s , due to a disruption of the crystal packing. All these surfactants form a long rod nematic phase at the micellar (L_1)/hexagonal (H_1) boundary except for $s = 6$. For $s = 2$ and 3 the formation of an intermediate phase (Int) (non-cubic liquid crystals with curvature intermediate between hexagonal and lamellar) is observed but not for $s = 6$. Cubic bicontinuous (V_1) and lamellar (L_α) phases are obtained for all

surfactants but require high temperature (54 °C and 76 °C, respectively) for $s = 6$.

The succession of phases of cationic surfactant dimers and trimers, with $m = 12$, $s = 3$ and 6, and various counter-ions, has been surveyed using cross-polarized light microscopy and the water penetration technique [203]. Intermediate and bicontinuous cubic phases are confirmed for short spacers. More strongly binding counter-ions have a similar effect as a reduction in spacer length or an increase in oligomerization degree. This study illustrates the fine tuning one can achieve by varying parameters specific to surfactant oligomers, namely the spacer length and the degree of oligomerization.

Lyotropic behavior of cationic gemini surfactants with hydrophilic (EO) spacers (Figure 2b) has also been studied [49]. The concentration range of the L_1 phase broadens as $s/3$ increases as in hydrophobic spacer geminis.

The lyotropic behavior of the non-ionic gemin of Figure 5b with $m = 6$ was studied by polarized light microscopy, and deuterium NMR spectroscopy [81]. At 27°C, as the concentration decreases, the succession of phases reads : S- L_α (89%), L_α - V_1 (75%), V_1 - H_1 (71%), H_1 -VB(62%), VB- L_1 (50%), where S stands for solid phase, and VB for viscous birefringent phase. From ^2H NMR spectra it appears that L_α and H_1 phases always coexist with an isotropic phase (V_1 for L_α and L_1 for H_1). The VB phase has been identified later as a biphasic region [164]. This sugar-based surfactant does not exhibit any cloud point in the range of temperature studied (0-100°C). The study has been completed for other chain lengths [164]. For $m = 5$, the viscous birefringent phase does not appear any more. For $m = 7$ an upper critical solution temperature exists between 0.5 and 10%. The V_1 phase region is no longer seen but is supposed to exist in a very narrow range of concentration. For $m = 8$, the phase boundaries are less sensitive to temperature. The isotropic L_1 phase exists up to 0.8% and then coexists with an unidentified phase of optical texture resembling an L_α phase. A pure L_α phase

is formed at 48%. The surfactant of Figure 5b, with $m = 9$ is insoluble in water up to 100°C [164].

2. Thermotropic behavior

The thermotropic behavior of 16-s-16, 2Br surfactants has been reported [201, 202]. DSC experiments show a main transition around 100 °C, corresponding to a S→VN (viscous neat phase) transition, with further small transitions at higher temperature. Optical microscopy shows that, for short spacers ($s = 1$ and 2) the VN phase transforms into an isotropic phase at about 200°C (precise temperature transitions are difficult to get as a result of the progressive decomposition of the material). For longer spacers ($s = 3$ and 6), the system goes across to a smectic A phase at about 200-230°C. The transition at 100°C has an unexpectedly low enthalpy, which suggests that either the solid is not well ordered or that the VN phase has significant conformational restrictions. X-ray diffraction in the VN phase leads one to conclude a tilted bilayer structure with disordered alkyl chains filling the space between ordered headgroup layers including the spacer. The degree of order in the headgroup layer depends on the spacer length (higher with short spacer), and for longer spacers varies with the temperature. Thermotropic behavior was observed with cationic $m = 12$ gemini with $(EO)_{s/3}$ spacer [49] but not with their homologues with $(CH_2)_s$ - spacer [167].

V. CHEMISTRY WITH GEMINI SURFACTANTS

A. Analytical Chemistry

1. Micellar electrokinetic chromatography

Micellar electrokinetic chromatography (MEKC) allows the separation of neutral compounds by electrophoresis, based on their differential partition between micelles and the solution. The cmc and the hydrophobicity of the

micelles are critical parameters for the efficiency of this technique. Sulfonate gemini surfactant of Figure 3a ($Y = O$) were able to separate various substituted naphthalene and benzene derivatives at concentration as low as 7.5 mM [204]. Using SDS would have required 50 mM for the same resolution. The surfactant of Figure 3a and SDS were also shown to have remarkably different selectivity. The separation of chlorophenols has also been carried out with the same type of surfactants [205]. Cationic surfactants have been used to separate ergot alkaloids by MEKC [206]. With all types of gemini surfactants, the retention factor increases linearly with surfactant concentration as expected [205, 206]. Micellar-enhanced ultrafiltration could also take advantage of the various morphology observed in surfactant oligomer micelles, but as far as we know, no data have been reported in the literature.

2. Specific electrodes

Di- and triamide surfactant dimers and trimers of the type shown in Figure 29 have been synthesized in an attempt to prepare membrane systems having high selectivity for alkaline earth metal cations (Mg^{2+} and Ca^{2+}). Some of them have shown enough selectivity to allow measurements of Mg^{2+} activities in the millimolar range at physiological pH, without interference by H_3O^+ ions [28]. The selectivity of these ionophores for Mg^{2+} over monovalent cations have been studied in detail [207, 208] and the conditions for their use in membrane electrodes for application to human blood serum optimized [209].

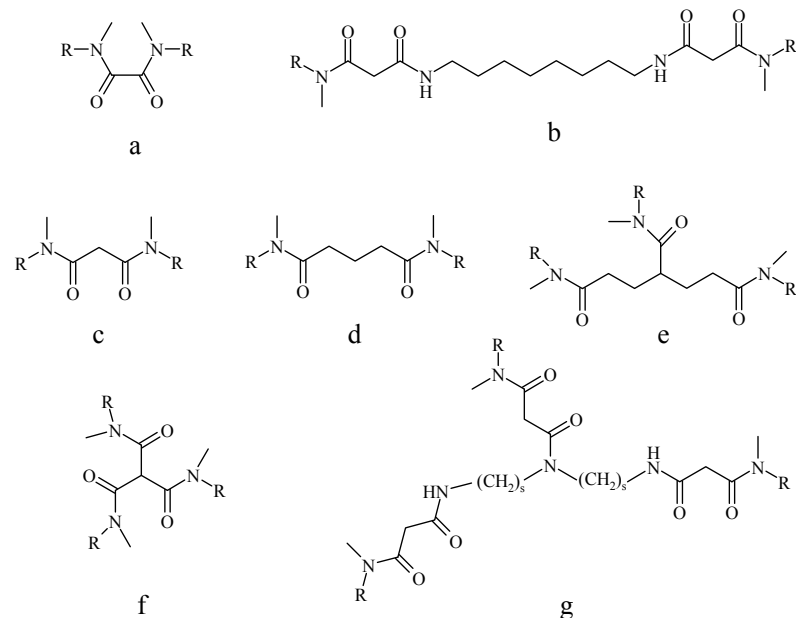


Figure 29: Surfactant dimers and trimers used as alkaline earth metal cation ionophores [28].

The synthesis of lipophilic receptors has been reported [210] and is still an active field of research. The synthesis of lipocyclopolymines as potential adenosine mono-, di-, and tri- phosphates has already been mentioned [29]. More recently, the interfacial behavior of a new amphiphilic cage molecule (tetra-(N-2-tetradecyl-carboxamideoethyl)-tetraazacyclotetradecane) showing selective complexation of copper ions, has been studied [211]. The use of this compound for liquid-liquid extraction has been demonstrated in the case of chlorinated solvents.

B. Micellar Catalysis

Bunton and co-workers, noticing the higher catalytic activity of polyelectrolytes compared to micelles, were interested in surfactants which would “combine some features of polyelectrolytes and detergents”. They studied the catalytic activity of gemini surfactants 16-s-16, 2Br ($s = 2, 4,$ and 6) for the reaction of hydroxide ion with chloro- and fluoro-2,4-dinitrobenzene and hydroxide and fluoride ion with *p*-nitrophenyl diphenyl phosphate [34]. Surfactants with $s = 4$ and 6 have shown much higher catalytic activity than CTAB for all the reactions studied. A short spacer ($s = 2$) or a rigid spacer (2,3 butinediyl) did not show any catalytic activity for reactions involving hydroxide ions. Cyclization of 2-(3-bromopropoxy) and 2-(3-bromododecyloxy)phenoxide ion in micelles of cationic gemini ($m = 16,$ spacer = butanediyyl or 2,3-dimethoxybutanediyyl) has been studied recently [197]. Intramolecular reactions are better suited to address the catalytic activity of micelles because they are independent of the reaction volume. The observed rate constant k_{obs} is 3 times higher with the butanediyyl spacer gemini than with the 2,3-dimethoxybutanediyyl spacer. The surfactant concentration dependence of k_{obs} showed a plateau, followed by an increase associated with the formation of larger aggregates. In preparative condition, i.e. with a large ratio of substrate to surfactant, only the product of intramolecular reaction was obtained.

C. Chemistry Hosted or Templated by Surfactant Oligomer Self-Assemblies.

1. Synthesis of colloidal metallic particles

A nonionic surfactant gemini known as Surfynol 465 has been used to synthesize gold [212, 213] and silver [214] colloidal particles. The amphiphilic moieties in this surfactant consist of a branched alkyl chain with an oxyethylene headgroup. They are linked by an acetylenic spacer. The physicochemical

properties of surfynol 465 have been studied in detail by tensiometry, densitometry, osmometry, calorimetry and UV and NMR spectroscopy [215, 216, 217]. The main properties are the following : cmc ranges between 10 to 16 mol/g, $\gamma_{cmc} = 26\text{mN/m}$, $A_{a/w} = 0.64\text{ nm}^2$ per molecule, cloud point at about 40 °C, $N_0 = 13$. Mixing Surfynol 465 with chloroauric acid (HAuCl_4) or silver perchlorate (AgClO_4) leads to the formation of metallic particles in a higher yield than with other synthesis methods. The mechanism has been studied by UV-VIS and Raman scattering [214, 218, 219]. The particles form by successive first order reduction reactions, where the acetylenic group of the surfactant acts as the reducing agent. The surfactant then adsorbs at the particles interface and stabilizes the colloidal solution. Anisotropic colloidal gold particles have been obtained by UV photolysis of HAuCl_4 in solutions of 12-2-12, 2Cl cationic gemini surfactant [220]. The concentration necessary to produce these particles was 15 times lower than with CTAC. An excess of surfactant is necessary to disperse the insoluble complex 12-2-12, 2AuCl_4 and allow efficient UV radiation, but if the surfactant/Au ratio is too high, polyhedral isotropic particles are obtained.

2. Emulsion polymerization

The γ -radiation polymerization of styrene microemulsions described in section IV.B.1 led to spherical latex particles, whose size range could be controlled by the monomer/surfactant ratio but also depends on the spacer length of the gemini surfactant involved [123, 160]. With $-(\text{CH}_2)_s-$ spacers and in the absence of cross-linker, the latex particle size goes through a maximum at $s = 10$, but goes through a minimum at $s = 6$ in the presence of cross-linker. The optimum microemulsion formulations leading to both small particle and high molecular weight are obtained with $s = 6$ gemini [160]. In such conditions, the molecular weight is 4 times the one obtained in CTAB microemulsions. With -

$(\text{EO})_{s/3}$ - hydrophilic spacers, the same type of behavior is observed. The spacer length leading to the maximum molecular weight (which in this case corresponds to the maximum particles size) is $s/3 = 3$ [123]. These observations led the authors to conclude that the polymerization behavior of ternary microemulsions with cationic geminis is rather independent of the chemical nature of the spacer provided that the flexibility of the interface is sufficient [123].

3. Gemini Surfactants as Templating Agent for Mesoporous material

Tailoring the porosity of inorganic material is an issue for applications such as molecular sieving or selective catalysis. It has become a very active field of research since the pioneering work of scientists at Mobil Oil Research and Development, who used the cooperative self-assembling of silicate polyanions and cationic surfactant micelles to produce mesoporous silica [221], see the chapter by Stein and Melde in this volume]. A large variety of surfactants have now been used, including cationic gemini surfactants [217-219]. The greatest advantage of using gemini surfactants for templating the formation of mesoporous material, may be that they provide a new parameter, s , to control the structure, independently of, m , which is the determining variable for the average pore size. However, the quality of the material obtained is also sensitive to s [224].

Typical syntheses proceed by mixing m - s - m , 2Br surfactants, with tetraethyl orthosilicate (TEOS) in water (in molar proportions 0.06/1/150) under basic or acidic conditions, at room temperature or/and under hydrothermal conditions for one or several days [223]. The crystallinity of the precipitate obtained is improved by subsequent hydrothermal treatment in fresh water. Most often, the structure of the ordered organic/inorganic composite material obtained is determined by the lyotropic behavior of the surfactant. Hence, short spacers

favor lamellar phases (MCM-50) while intermediate spacers favor hexagonal phases (MCM-41) for $s < 10$. 12-12-12, 2Br yields MCM-41 at room temperature [223], and cubic structure (MCM-48) is obtained with 16-12-16, 2Br under hydrothermal conditions [224]. The use of gemini surfactants has been shown to reduce the synthesis time of high quality (in terms of crystallinity and pore size distribution) cubic mesoporous silica [224].

VI. CONCLUSIONS

The large variety of surfactant oligomer structures of interest nowadays has been demonstrated. Their synthesis is sometime involved, but does not necessarily require new chemistry and can often rely upon well-known procedures. Surfactant oligomers have been shown to exhibit good surface activity. Their efficiency to lower surface tension relies upon an adsorption triggered by several hydrophobic chains and interfacial interactions that take place at lower concentration because of their larger size. The cmc depend strongly on the degree of oligomerization and slightly on the spacer length. These two parameters, specific to surfactant oligomers, also determine the optimum area per head group and hence the morphology of the micelles as well as the mesoscopic behavior. Original structures, as compared to conventional monomeric surfactant, are obtained essentially for short spacers. Surfactant solutions behaving as polymers can be obtained and their viscosity controlled by the structure of the surfactant and not only through formulation. The stability of vesicles can also be controlled by varying the spacer characteristics.

The answer to the question : “Is it worth going to higher oligomerization degree?”, varies depending of the point of view. From the point of view of general applications, the answer is probably negative. The biggest gain is made from the monomer to the dimer, and the benefits of having higher degrees of oligomerization may not be worth the synthesis effort. For specialized

surfactant application and fundamental properties, it is the hope of the author that the reader will answer by the positive.

Acknowledgements : I would like to take this opportunity to thank Vesna Vukov and Sharon Krauss, whose help in gathering the references, and sometime in translating them, has been invaluable. I am also thankful to Corine Gérardin and Amit Kulkarni for their comments on the manuscript. Last, many thanks are also extended to Dave Tracy and Raoul Zana for sharing their immense knowledge in the field of surfactant oligomers.

VII. APPENDIX

Notation

Cmc: critical micelle concentration;

α : ionization degree of the micelles at the cmc;

γ_{cmc} : Surface tension at the cmc

pC₂₀: Logarithm of the inverse of the surfactant concentration necessary to decrease the surface tension by 20 mN/m.

A_m is the surface area per molecule at the air/water interface. In the absence of swamping electrolyte, the value reported in the following tables are obtained by taking $n=x+1$ in the Gibbs equation (Equation 9);

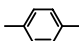
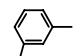
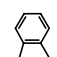
k: number of solubilized dye molecule per surfactant molecule above the cmc;

KT: Kraft temperature

A. Cationic gemini surfactants

1. Variable spacer

a) Hydrophobic

8-s-8, 2 Br		
s	cmc (M)	α
3	1.4×10^{-2}	0.70
4	2.6×10^{-2}	0.67
5	2.6×10^{-2}	0.69
6	2.5×10^{-2}	0.67
	2.3×10^{-2}	0.62
	2.3×10^{-2}	0.62
	2.5×10^{-2}	0.58

^a Conductimetry at 25 °C [149].

10-s-10, 2Br

s	cmc ^a (M)	k ^a	cmc ^b (M)	α^b
2 ^c	6.0×10^{-3}	99	6.2×10^{-3}	0.15
3	6.4×10^{-3}	105	6.5×10^{-3}	0.22
4	9.0×10^{-3}	121	8.7×10^{-3}	0.28
5	9.2×10^{-3}	147	-	-
6	8.7×10^{-3}	212	9.2×10^{-3}	0.29
8	6.8×10^{-3}	186	7.5×10^{-3}	0.32
10	4.7×10^{-3}	160	4.2×10^{-3}	0.37
12	3.7×10^{-3}	43	2.2×10^{-3}	0.39

^a Dye solubilization (trans-azobenzene) at 20 °C [159].

^b Conductimetry at 25 °C [162, 163].

^c Surface tension measurement by the maximum bubble pressure at 25 °C gives cmc= 6.5×10^{-3} M and $\gamma_{\text{cmc}} = 32$ mN/m [40].

12-s-12, 2Br

s	cmc ^a (M)	α^a	cmc ^b (M)	γ_{cmc}^b (mN/m)	A ^b (Å ²)
2	8.4×10^{-4} (1.5×10^{-2})	0.22	8.1×10^{-4c}	30 ^c	69 ^c
3	9.6×10^{-4}	0.22	9.1×10^{-4}	35.0	105
4	1.2×10^{-3} (1.4×10^{-2})	0.28	1.0×10^{-3}	39.8	116
5	1.1×10^{-3}	0.29	-	-	-
6	1.0×10^{-3} (1.1×10^{-2})	0.32	1.1×10^{-3}	42.5	143
8	8.3×10^{-4} (7.0×10^{-3})	0.45	8.9×10^{-4}	42.8	176
10	6.3×10^{-4}	0.54	3.2×10^{-4}	43.0	220
12	3.7×10^{-4}	0.62	2.8×10^{-4}	41.5	226
14	2.0×10^{-4}	-	1.8×10^{-4}	39.5	200
16	1.2×10^{-4} (1.0×10^{-3})	0.67	1.4×10^{-4}	39.4	154

^a conductimetry at 25 °C [38]. Values in parenthesis are for the corresponding monomer surfactant m-s/2, Br [155].

^b Surface tension (ring method) at 25 °C [122], unless otherwise specified.

^c Surface tension (wilhelmy plate open frame version) at 22 °C [132].

12-s-12, 2Cl

s cmc (M)

2 1.3×10^{-3} 3^a 1.8×10^{-3} 4 1.3×10^{-3} 6 1.3×10^{-3} 10 6.0×10^{-4} 20 7.0×10^{-5}

From ref. [153].

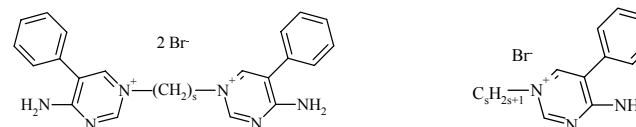
16-s-16, 2Br

s	cmc ^a (M)	cmc ^b (M)	α^b	cmc ^c (M)	KT ^d (°C)	cmc ^e (M)
2	1.4×10^{-5}	2.1×10^{-5}	0.60		45	3.4×10^{-5}
3	-	2.6×10^{-5}	0.35	2.5×10^{-5}		
4	3.2×10^{-5}	2.7×10^{-5}	0.56	2.7×10^{-5}	34	4.4×10^{-5}
5	-	-	-	3.6×10^{-5}		
6	6.5×10^{-5}	4.3×10^{-5}	0.43	4.3×10^{-5}	41	4.7×10^{-5}
8	-	3.3×10^{-5}	0.60	3.3×10^{-5}		
10	-	-		2.7×10^{-5}		
12	-	-		2.0×10^{-5}		

^a Surface tension (ring method) at 25 °C [34].^b Conductimetry at 25 °C [38].^c Fluorescence spectroscopy at 30 °C [41].^d Conductimetry [151].^e Conductimetry at 46.5 °C [151].

m	2	4	6	8	10	12
cmc (M)	3.2×10^{-3}	3.2×10^{-3}	3.1×10^{-3}	2.6×10^{-3}	2.3×10^{-3}	1.6×10^{-3}

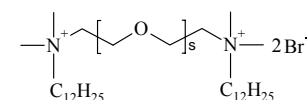
Dye solubilization [146].



s	cmc ^b (M)	γ_{cmc}^b (mN/m)	A ^b (Å ²)	cmc ^b (M)	γ_{cmc}^b (mN/m)	A ^b (Å ²)
8	4.0×10^{-4}	45.0	314	1.0×10^{-2}	42	208
9	6.3×10^{-5}	43	444	8.3×10^{-4}	50	150
10	1.6×10^{-4}	44	381	9.1×10^{-3}	37	178
11	3.0×10^{-4}	50	335	5.0×10^{-4}	47	153
12	3.0×10^{-5}	34	189	7.9×10^{-3}	37	113

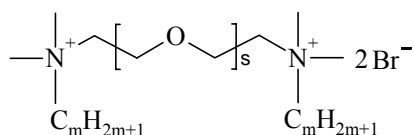
Surface tension (Du Nouy ring) at 25°C [43].

b) Hydrophilic spacer



s	cmc (M)	γ_{cmc} (mN/m)
1	8.0×10^{-4}	38.2
2	9.2×10^{-4}	41.0
3	8.6×10^{-4}	40.8
4	9.0×10^{-4}	42.1
5	1.2×10^{-3}	42.0

Surface tension (Wilhelmy plate) at 25 °C [123].



s-m	cmc1 ^a (M)	cmc2 ^a (M)	cmc ^b (M)	KT ^c (°C)	cmc ^d (M)
1-12	-	-	4.8 x 10 ⁻⁴	-	-
1-14	5.0 x 10 ⁻⁵	2.5 x 10 ⁻⁴	-	-	-
1-16	3.4 x 10 ⁻⁵	1.5 x 10 ⁻⁴	3.8 x 10 ⁻⁵	28.8	1.9 x 10 ⁻⁵
2-16					1.7 x 10 ⁻⁵
3-16	6.0 x 10 ⁻⁵	7.0 x 10 ⁻⁵	6.5 x 10 ⁻⁵	12.4	2.0 x 10 ⁻⁵
7-16	1.6 x 10 ⁻⁴	1.4 x 10 ⁻³	1.6 x 10 ⁻⁴	0.0	-
1-18	1.2 x 10 ⁻⁵	8.7 x 10 ⁻⁵		40.5	-
3-18	3.8 x 10 ⁻⁵	3.7 x 10 ⁻⁵	3.3 x 10 ⁻⁴	23.0	-
7-18	8.2 x 10 ⁻⁵	6.6 x 10 ⁻⁴	8.4 x 10 ⁻⁵	4.00	-
1-22	7.0 x 10 ⁻⁶	3.4 x 10 ⁻⁵	-	53.2	-
3-22	1.4 x 10 ⁻⁵	8.0 x 10 ⁻⁵	-	40.6	-
7-22	2.4 x 10 ⁻⁵	2.3 x 10 ⁻⁴	2.3 x 10 ⁻⁴	24.8	
20-22	1.5 x 10 ⁻⁵	1.4 x 10 ⁻⁴			

^a Conductimetry at 25 °C, cmc1 and cmc2 correspond respectively to the first and second break in the slope of the plot of the conductivity versus concentration [47].

^b Surface tension (du Nouy ring method) 23 °C [47].

^c Conductimetry [47].

^d Fluorescence spectroscopy (I1/I3 pyrene) at 30 °C [48].

2. Variable hydrophobic Chain

m-2-m, 2Br		
m	cmc ^a (mM)	KT ^b
12	1.4 x 10 ⁻³	14
14	2.0 x 10 ⁻⁴	33
16	3.4 x 10 ⁻⁵	45

^a Conductimetry 46.5 °C [151].

^b Conductimetry [151].

m-5-m, 2Br					
m	cmc ^a (M)	cmc ^b (M)	γ _{cmc} ^b (mN/m)	A ^c (Å ²)	
6	1.6 x 10 ⁻¹	4.2 x 10 ⁻¹	42.4	120	
8	4.8 x 10 ⁻²	4.9 x 10 ⁻²	40.3	117	
9	2.5 x 10 ⁻²	1.5 x 10 ⁻²	39.7	130	
10	8.9 x 10 ⁻³	7.7 x 10 ⁻³	39.5	128	
11	3.0 x 10 ⁻³	2.3 x 10 ⁻³	40.1	100	
12	1.1 x 10 ⁻³	1.0 x 10 ⁻³	40.0	115	
13	4.1 x 10 ⁻⁴	4.9 x 10 ⁻⁴	39.7	123	
14	1.8 x 10 ⁻⁴	2.0 x 10 ⁻⁴	39.6	120	
16	3.2 x 10 ⁻⁵	9.3 x 10 ⁻⁵	36.6	105	

From ref. [120].

^a Conductimetry at 20 °C.

^b Surface tension (ring method) at 20 °C.

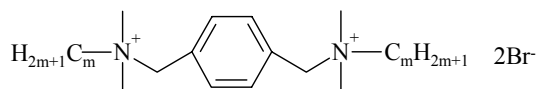
^c assuming n=2 in Gibbs equation (equation 1).

m-6-m, 2Br

m	cmc ^a (M)	cmc ^b (M)	k ^b (μmol/mol)
8	2.5 x 10 ⁻²	7.26 x 10 ⁻²	69
9	2.2 x 10 ⁻²	2.59 x 10 ⁻²	123
10	8.2 x 10 ⁻³	8.65 x 10 ⁻³	212
11	2.7 x 10 ⁻³	2.89 x 10 ⁻³	229
12	1.2 x 10 ⁻³	1.71 x 10 ⁻³	228
13	4.6 x 10 ⁻⁴	5.40 x 10 ⁻⁴	282
14	1.50 x 10 ⁻⁴	-	415
15	7.00 x 10 ⁻⁵	-	432
16	4.80 x 10 ⁻⁵	-	555

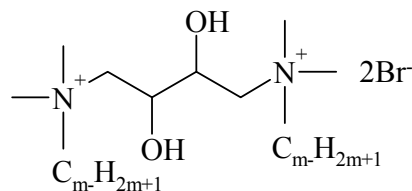
^a Conductimetry at 20 °C [146]

^b Dye solubilization (trans-azobenzene) at 20 °C [159].



m	cmc (M)	γ _{cmc} (mN/m)
8	1.0 x 10 ⁻²	38
12	1.0 x 10 ⁻³	39
16	6.7 x 10 ⁻⁵	41
18	3.7 x 10 ⁻⁴	38

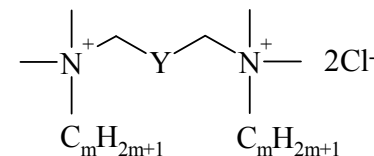
Surface tension (ring method) at 50 °C [39].



m	cmc ^a (M)	γ _{cmc} ^a mN/m	pC ₂₀ ^a	cmc ^b (M)	γ _{cmc} ^b mN/m	pC ₂₀ ^b	A _{min} ^b (Å ²)
8	-	-	-	1.1 x 10 ⁻²	38.3	3.1	79.0
10	3.7 x 10 ⁻³	35.5	3.24	3.3 x 10 ⁻⁴	33.8	5.17	75.0
12	7.0 x 10 ⁻⁴	35.4	3.89	6.0 x 10 ⁻⁶	31.8	6.47	64.0
14	8.5 x 10 ⁻⁵	36.0	5.50	1.0 x 10 ⁻⁶	29.7	6.9	42.0
16	5.0 x 10 ⁻⁵	41.4	5.50	-	-	-	-

^a (Wilhelmy plate) at 25 °C [46].

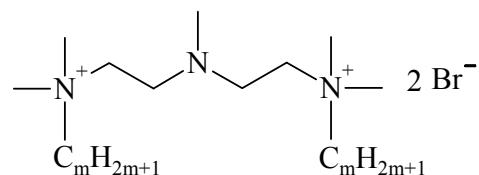
^b Surface tension (Wilhelmy plate) at 25 °C, in 0.1MNaBr [46].



Y	m	cmc ^a (M)	γ _{cmc} ^a (mN/m)	pC ₂₀ ^a	cmc ^b (M)
-CH ₂ -	12	9.8 x 10 ⁻⁴	37	3.2	
-CHOH-	12	7.8 x 10 ⁻⁴	39.2	3.3	
-CHOHCH ₂ -	12	6.5 x 10 ⁻⁴	40.9	3.5	
-CH ₂ -O-CH ₂ -	12	5.0 x 10 ⁻⁴	39.2	3.6	
-CHOH-	8				4.5 x 10 ⁻²
	9				1.4 x 10 ⁻²
	10	3.2 x 10 ⁻³	36.5	2.9	6.5 x 10 ⁻³
	11				2.9 x 10 ⁻³
	12	7.8 x 10 ⁻⁴	37.0	3.2	2.1 x 10 ⁻³
	13				1.5 x 10 ⁻³
	14	1.4 x 10 ⁻⁴	39.0	4.4	
	16	1.9 x 10 ⁻⁵	42.2	5.3	
-CH ₂ -	12	9.8 x 10 ⁻⁴	39.2	3.3	
	14	1.1 x 10 ⁻⁴	41.8	4.5	
	16	1.5 x 10 ⁻⁵	42.0	5.4	

^a Wilhelmy plate at 20 °C. All surfactant have a point kraft below 0 °C [45].

^b Dye solubilization by UV spectroscopy [146].

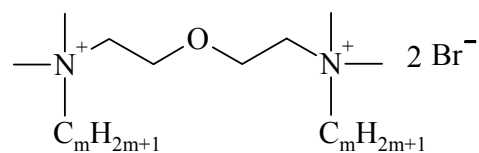


m	cmc ^a (M)	cmc ^b (M)	γ _{cmc} ^b (mN/m)	A ^b (Å ²)
8	3.1 x 10 ⁻²	3.7 x 10 ⁻²	37.1	98
9	1.8 x 10 ⁻²	1.5 x 10 ⁻²	38.0	100
10	8.4 x 10 ⁻³	4.7 x 10 ⁻³	35.5	98
11	3.0 x 10 ⁻³	2.1 x 10 ⁻³	37.5	103
12	1.1 x 10 ⁻³	1.2 x 10 ⁻³	36.1	108
13	3.3 x 10 ⁻⁴	4.1 x 10 ⁻⁴	38.0	111
14	1.2 x 10 ⁻⁴	1.2 x 10 ⁻⁴	38.0	102
15	4.3 x 10 ⁻⁵	4.2 x 10 ⁻⁵	40.1	112
16	1.2 x 10 ⁻⁵	1.4 x 10 ⁻⁵	42.9	119

From ref. [120].

^a Conductimetry at 20 °C.

^b Surface tension (ring method) at 20 °C.

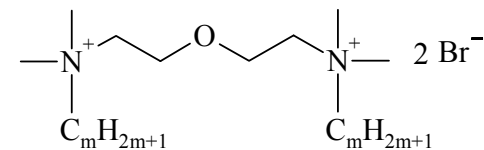


m	cmc ^a (M)	cmc ^b (M)	γ _{cmc} ^b (mN/m)	A _m ^b (Å ²)
8	4.4 x 10 ⁻²	4.2 x 10 ⁻²	41.7	128
9	2.2 x 10 ⁻²	1.7 x 10 ⁻²	40.4	133
10	7.7 x 10 ⁻³	7.7 x 10 ⁻³	40.8	135
11	2.6 x 10 ⁻³	2.1 x 10 ⁻³	39.1	127
12	1.0 x 10 ⁻³	1.1 x 10 ⁻³	38.2	129
13	3.8 x 10 ⁻⁴	3.1 x 10 ⁻⁴	39.7	126
14	1.9 x 10 ⁻⁴	1.0 x 10 ⁻⁴	40.1	138
16	6.4 x 10 ⁻⁶	6.4 x 10 ⁻⁶	47.2	141

From ref. [120].

^a Conductimetry at 20 °C.

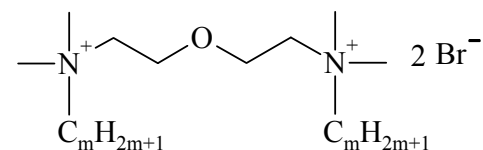
^b Surface tension (ring method) at 20 °C.



m	cmc ^a (M)	γ _{cmc} ^a (mN/m)	pC ₂₀ ^a	A ^a (Å ²)	cmc ^b (M)
10	5.6 x 10 ⁻³				6 x 10 ⁻³
12	5.2 x 10 ⁻⁴	40	4.0	170	6 x 10 ⁻⁴
14	5.8 x 10 ⁻⁵	39	4.9	156	6 x 10 ⁻⁵
16	6.6 x 10 ⁻⁶	< 40		102	6 x 10 ⁻⁶
18	1.4 x 10 ⁻⁶	40	6.3	84	6 x 10 ⁻⁶
20	4.0 x 10 ⁻⁶	55			2 x 10 ⁻⁵

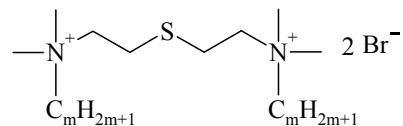
^a Surface tension (Wilhelmy plate) at 25 °C [118]

^b Fluorescence spectroscopy of pyrenecarboxaldehyde at 25 °C [118]



m	cmc ^a (M)	γ _{cmc} ^a (mN/m)	pC ₂₀ ^a	A ^a (Å ²)
12	3.0 x 10 ⁻⁵	39	6.0	95
14	1.2 x 10 ⁻⁶	36	7.3	79
16	9.5 x 10 ⁻⁷	34	6.5	24
18	7.1 x 10 ⁻⁷	30	6.4	14

^a Surface tension (Wilhelmy plate) at 25 °C, in 0.1M NaCl [118].

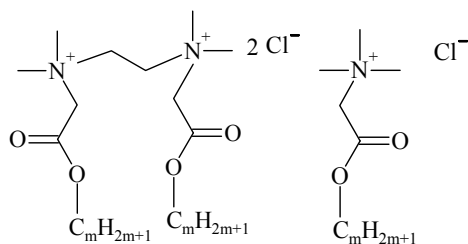


m	cmc ^a (M)	cmc ^b (M)	γ _{cmc} ^b (mN/m)	A _m ^b (Å ²)
6	1.3 x 10 ⁻¹	6.1 x 10 ⁻²	28.7	79
8	3.7 x 10 ⁻²	2.1 x 10 ⁻²	33.1	88
10	6.2 x 10 ⁻³	8.8 x 10 ⁻³	35.0	85
12	9.6 x 10 ⁻⁴	8.4 x 10 ⁻⁴	34.5	84
14	1.0 x 10 ⁻⁴	1.5 x 10 ⁻⁴	33.9	114
16	9.7 x 10 ⁻⁶	1.7 x 10 ⁻⁵	41.9	121
18	1.0 x 10 ⁻⁶	5.2 x 10 ⁻⁶	40.9	120

From ref. [120].

^a Conductimetry at 20 °C.

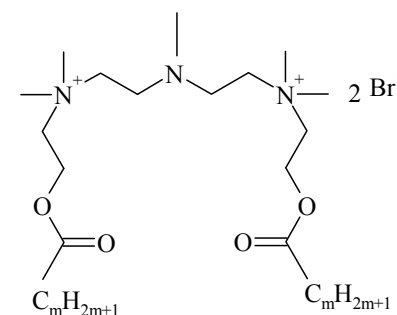
^b Surface tension (ring method) at 20 °C.



m	cmc _{dimer} ^a (M)	cmc _{dimer} ^b (M)	cmc _{monomer} ^b (M)
8	8.7 x 10 ⁻³	8.1 x 10 ⁻³	
9	5.2 x 10 ⁻³		
10	4.0 x 10 ⁻³	1.3 x 10 ⁻³	
11	3.2 x 10 ⁻³		
12	2.2 x 10 ⁻³	3.0 x 10 ⁻⁴	5.5 x 10 ⁻³
14	1.2 x 10 ⁻³	1.2 x 10 ⁻⁴	1.9 x 10 ⁻³
16	7.5 x 10 ⁻⁴	4.0 x 10 ⁻⁵	3.3 x 10 ⁻⁴

^a conductimetry [124]

^b calorimetric at 25 °C [42]



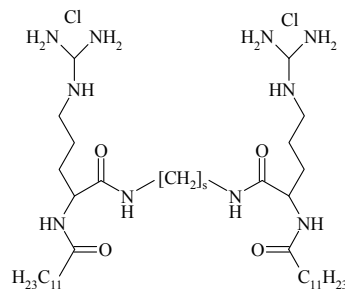
m	cmc ^a (M)	cmc ^b (M)	γ _{cmc} ^b (mN/m)	A _{min} ^b (Å ²)
6		4.8 x 10 ⁻²		
7	4.7 x 10 ⁻²	4.2 x 10 ⁻²	38.8	101
8	9.1 x 10 ⁻³	1.3 x 10 ⁻²	31.1	119
9	6.2 x 10 ⁻³	5.1 x 10 ⁻³	36.3	109
10	2.2 x 10 ⁻³	1.9 x 10 ⁻³	34.2	110
11	7.8 x 10 ⁻⁴	5.9 x 10 ⁻⁴	37.1	118
11'	1.9 x 10 ⁻³	2.0 x 10 ⁻³	37.3	129
12	2.2 x 10 ⁻⁴	3.0 x 10 ⁻⁴	34.3	101
14	9.6 x 10 ⁻⁶	1.7 x 10 ⁻⁵	40.0	87
18''	9.9 x 10 ⁻⁶	4.0 x 10 ⁻⁵	52.6	155

From ref. [121].

^a Conductimetry at 20 °C.

^b Surface tension (ring method) at 20 °C.

3. Miscellaneous

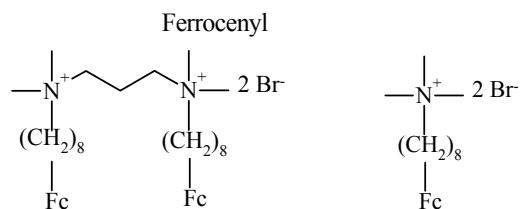


s	cmc ^a (M)	cmc ^b (M)	cmc ^c (M)	γ_{cmc}^c (mN/m)	pC ₂₀ ^c	A ^c (Å ²)
2			9.5 x 10 ⁻⁶	30	5.7	91
3	4 x 10 ⁻⁴	4 x 10 ⁻⁴	4.4 x 10 ⁻⁶	35	5.9	86
4			2.8 x 10 ⁻⁶	30	6.5	130
6	6 x 10 ⁻⁴	4 x 10 ⁻⁴	1.3 x 10 ⁻⁶	30	6.7	113
9	3 x 10 ⁻⁴	3 x 10 ⁻⁴	2.8 x 10 ⁻⁶	34	6.0	77
10			1.9 x 10 ⁻⁶	34	6.2	74
Mono.	6 x 10 ⁻³	5 x 10 ⁻³	6.0 x 10 ⁻³	33	3.2	67

^a Conductimetry (chloride selective electrode) at 25 °C [78].

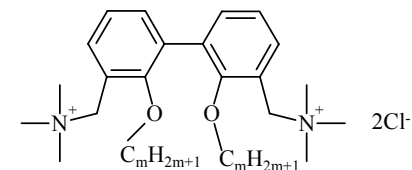
^b Fluorescence spectroscopy of pyrene [78]

^c Surface tension (Wilhelmy plate) at 25 °C (aged 24-48hours) [77]



	cmc (M)	γ_{cmc} (mN/m)	A _m (Å ²)	cmc (M)	γ_{cmc} (mN/m)	A (Å ²)
Fc	1-2 x 10 ⁻⁵	50	39	2 x 10 ⁻³	53	55
Fc ⁺	>2 x 10 ⁻³	<60	50	>10 ⁻²	<60	65

Surface tension (Wilhelmy plate) in 0.1 M Li₂SO₄ at pH=2 and T=25 °C [99].

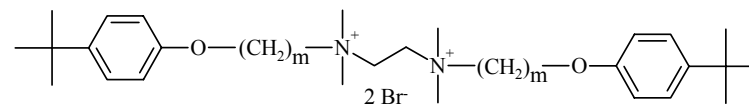


m	cmc ^a (M)	γ_{cmc}^a (mN/m)	A ^a (Å ²)	α^b
1	7.23 x 10 ⁻²	46.1	345	
6	9.4 x 10 ⁻³	43.6	325	.73
12	1.9 x 10 ⁻⁴	41.1	329	.56

From ref. [92].

^a Surface tension (Wilhelmy plate) at 25 °C.

^b Conductimetry at 25 °C.

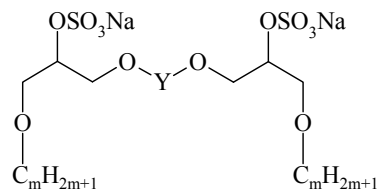


m	2	3	4	5	6	10
cmc (M)	7.0 x 10 ⁻³	5.9 x 10 ⁻³	4.2 x 10 ⁻³	3.1 x 10 ⁻³	2.1 x 10 ⁻³	1.1 x 10 ⁻³

Conductimetry at 20 °C [146]

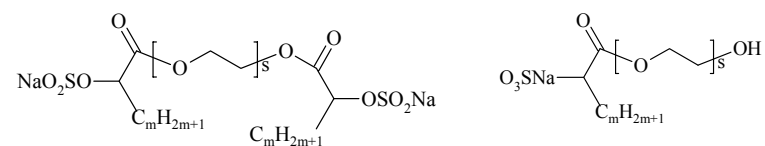
B. Anionic gemini surfactants

1. Sulfates



-Y-	m=8		m=10	
	cmc (M)	γ_{cmc} (mN/m)	cmc (M)	γ_{cmc} (mN/m)
CH ₂ CH ₂	6.0×10^{-4}	29.2	1.3×10^{-5}	27.0
CH ₂ CH ₂ CH ₂ CH ₂	1.5×10^{-3}	32.0	6.0×10^{-4}	32.5
CH ₂ [CH ₂ OCH ₂] ₂ CH ₂	1.8×10^{-4}	32.5	3.2×10^{-5}	32.0
	3.0×10^{-4}	41.8	3.5×10^{-5}	38.8
	1.7×10^{-4}	42.0	3.5×10^{-5}	39.5

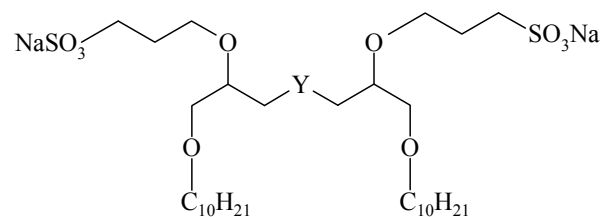
Surface tension (Wilhelmy plate) at 20 °C [52]



s	cmc (M)							
	m=10	m=12	m=14	m=16	m=10	m=12	m=14	m=16
1	9.9×10^{-4}	2.5×10^{-4}	7.2×10^{-5}	1.7×10^{-5}	5.5×10^{-3}	1.0×10^{-3}	3.0×10^{-4}	7×10^{-5}
2	1.1×10^{-3}	2.7×10^{-4}	7.5×10^{-5}	1.8×10^{-5}	6.5×10^{-3}	1.3×10^{-3}	3.2×10^{-4}	8×10^{-5}
3	1.1×10^{-3}	2.9×10^{-4}	7.8×10^{-5}	1.9×10^{-5}	7.0×10^{-3}	1.7×10^{-3}	3.5×10^{-4}	9×10^{-5}
5	1.2×10^{-3}	3.2×10^{-4}	8.5×10^{-5}	2.1×10^{-5}	7.6×10^{-3}	1.9×10^{-3}	3.7×10^{-4}	1.0×10^{-4}
9	1.3×10^{-3}	3.4×10^{-4}	8.5×10^{-5}	2.2×10^{-5}	9.0×10^{-3}	2.1×10^{-3}	4.5×10^{-4}	1.1×10^{-4}
14	1.4×10^{-3}	3.6×10^{-4}	9.0×10^{-5}	2.3×10^{-5}	1.0×10^{-2}	2.2×10^{-3}	4.7×10^{-4}	1.2×10^{-4}
23	1.5×10^{-3}	3.7×10^{-4}	9.6×10^{-5}	2.5×10^{-5}	1.0×10^{-2}	2.4×10^{-3}	4.8×10^{-4}	1.3×10^{-4}
35	1.5×10^{-3}	3.8×10^{-4}	9.8×10^{-5}	2.6×10^{-5}	1.0×10^{-2}	2.4×10^{-3}	5.0×10^{-4}	1.3×10^{-4}

Fluorescence spectroscopy of pinacyanol chloride at 25 °C [62]

2. Sulfonates

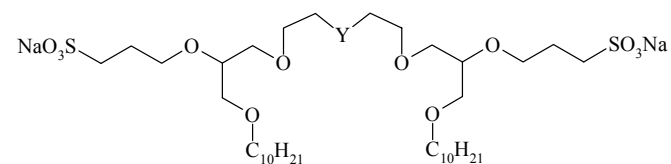


Y	m	cmc (M)	γ_{cmc} (mN/m)
-O-	10	3.3×10^{-5}	28.0
	12	1.4×10^{-5}	30.0
	14	2.5×10^{-5}	37.5
-OCH ₂ CH ₂ O-	8 ^b	7.0×10^{-4}	29.2
	10	3.2×10^{-5}	30.0
-O[CH ₂ CH ₂ O] ₂ -	10	6.0×10^{-5}	36.0
-O[CH ₂ CH ₂ O] ₃ -	10	8.0×10^{-5}	35.0
-O[CH ₂] ₄ O-	10	1.0×10^{-4}	36.0
-OCH ₂ CH=CHCH ₂ O- ^c	10	2.5×10^{-5}	33.0

^a Surface tension (Wilhelmy plate) at 20 °C from ref [54] unless otherwise specified.

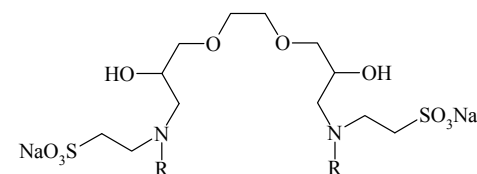
^b from ref [51].

^c from ref [97].



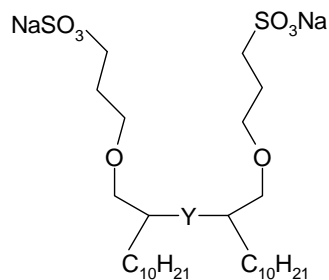
Y	In deionized water			In 0.1M NaCl		
	cmc (M)	γ_{cmc} (mN/m)	pC ₂₀	cmc (M)	γ_{cmc} (mN/m)	A (Å ²)
O	6.0×10^{-5}	36	5.7	2.4×10^{-5}	40	115
S	4.4×10^{-5}	34	4.8	2.0×10^{-5}	35	112
SO	1.1×10^{-4}	36	4.4	5.6×10^{-5}	41	116
SO ₂	2.0×10^{-4}	39	4.9	6.0×10^{-5}	39	132

Surface tension (Wilhelmy plate) at 20 °C [57].



m	cmc (M)	γ_{cmc} (mN/m)	pC ₂₀
8	1.9×10^{-3}	37.5	3.7
10	8.0×10^{-5}	37.0	5.2
12	6.1×10^{-6}	33.0	5.9
Mono.	1.0×10^{-2}	35.5	2.8

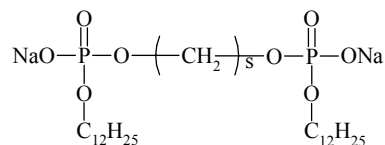
Surface tension (Wilhelmy plate) at 20 °C [56].



Y	cmc (M)	γ_{cmc} (mN/m)	pC ₂₀
-O-	9.3×10^{-5}	31.4	8.6
-(OCH ₂ CH ₂) ₃ O-	4.8×10^{-5}	35.5	6.5

Surface tension (Wilhelmy plate) at 23°C [65].

3. Phosphates



s	cmc ^a (M)	α^a	cmc ^b (M)	cmc ^c (M)	cmc ^d (M)
6	3.5×10^{-4}	.84		1.9×10^{-4}	$[2 \times 10^{-4}, 5 \times 10^{-4}]$
8	4.8×10^{-4}	.62	1.5×10^{-4}	1.0×10^{-4}	$[8 \times 10^{-5}, 3 \times 10^{-4}]$
12	6.0×10^{-5}	.88	4.4×10^{-5}	3.5×10^{-5}	$[2 \times 10^{-5}, 5 \times 10^{-5}]$

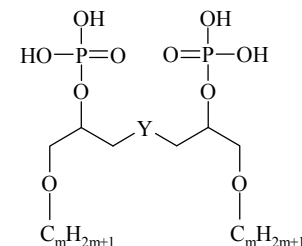
From ref [67]

^a Conductimetry

^b fluorescence pyrene

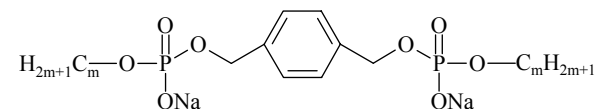
^c UV spectroscopy (pinacyanol chloride).

^d range of concentration from titration microcalorimetry at 30 °C.



Y	m=8		m=10		
	cmc (M)	γ_{cmc} (mN/m)	cmc (M)	γ_{cmc} (mN/m)	
Disodium	-OCH ₂ CH ₂ O-	7.2×10^{-4}	32.0	1.2×10^{-4}	30.0
	-O[CH ₂ CH ₂ O] ₂ -	5.2×10^{-4}	30.5	1.3×10^{-4}	31.5
	-O[CH ₂ CH ₂ O] ₃ -	1.8×10^{-3}	32.0	1.6×10^{-4}	33.0
Tetrasodium	-O-	4.0×10^{-3}	36.0	8.5×10^{-4}	30.0
	-OCH ₂ CH ₂ O-	3.3×10^{-3}	41.0	3.6×10^{-4}	32.5
	-O[CH ₂ CH ₂ O] ₂ -	1.8×10^{-3}	42.0	3.1×10^{-4}	33.5
	-O[CH ₂ CH ₂ O] ₃ -	4.3×10^{-3}	38.5	3.6×10^{-4}	33.5

Surface tension (Wilhelmy plate) at 20 °C [53].



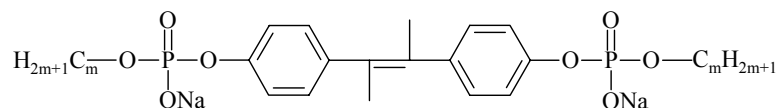
m	cmc ^a (M)	γ_{cmc}^a (mN/m)	cmc ^b (M)	cmc ^c (M)	γ_{cmc}^c (mN/m)
8	5.5×10^{-3}	42	1.6×10^{-2}	4.1×10^{-3}	42
12	1.7×10^{-4}	43	2.5×10^{-4}	1.1×10^{-4}	41
16	-	-	3.3×10^{-4}	2.6×10^{-3}	38

From ref. [39]

^a Surface tension (ring method) at 23°C.

^b ²³Na NMR at 23 °C.

^c Surface tension (ring method) at 50 °C.

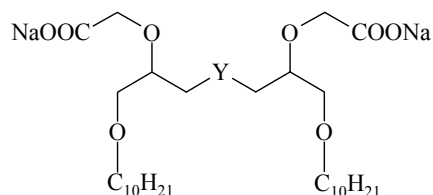


m	cmc ^a (M)	γ_{cmc}^a (mN/m)	cmc ^b (M)	cmc ^c (M)	γ_{cmc}^c (mN/m)
12	2.7×10^{-4}	46	4.8×10^{-4}	1.2×10^{-4}	45
16	1.6×10^{-3}	54	1.9×10^{-4}	7.1×10^{-4}	37
20	1.8×10^{-3}	60	2.5×10^{-4}	9.2×10^{-4}	40

[39]

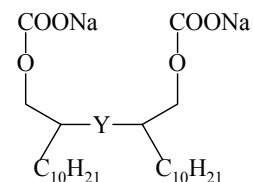
^a Surface tension (ring method) at 23 °C.^b ²³Na NMR at 23 °C.^c Surface tension (ring method) at 50 °C.

4. Carboxylates



-Y-	In deionized water			In 0.1M NaCl		
	cmc (M)	γ_{cmc} (mN/m)	pC ₂₀	cmc (M)	γ_{cmc} (mN/m)	A (Å ²)
-O-	8.4×10^{-5}	30	5.4	9.8×10^{-6}	30	82
-OCH ₂ CH ₂ O-	1.6×10^{-4}	33	5.0	1.4×10^{-5}	35	94
-O[CH ₂ CH ₂ O] ₂ -	2.6×10^{-4}	39	4.4	2.5×10^{-5}	37	106
-O[CH ₂ CH ₂ O] ₃ -	3.7×10^{-4}	43	4.1	3.0×10^{-5}	39	110
-O[CH ₂] ₄ O-	1.0×10^{-3}	36	4.1			

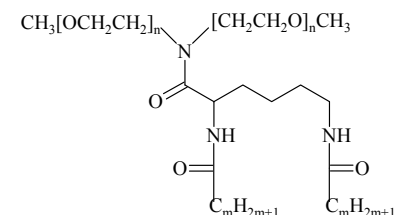
Surface tension (Wilhelmy plate) at 20 °C [59].



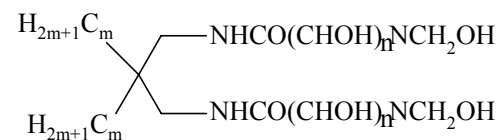
Y	cmc (M)	γ_{cmc} (mN/m)	pC ₂₀
-O-	1.3×10^{-5}	26.4	5.4
-(OCH ₂ CH ₂) ₃ O-	8.0×10^{-6}	38.7	4.4

Surface tension (Wilhelmy plate) at 23°C [65].

C. Non-ionic gemini surfactants



n-m	cmc (M)	γ_{cmc} (mN/m)	A (Å ²)
2-5	5.7×10^{-2a}	35.5	103
2-7	5.8×10^{-3a}	32.3	96
2-9	8.8×10^{-4b}	32.9	79
3-7	7.2×10^{-3b}	34.8	103
3-9	9.7×10^{-4b}	30.8	85
	6.6×10^{-5a}		

Surface tension at ^a25 °C and ^b6 °C [73].

m-n	cmc (M)	cmc (wt %)	γ_{cmc} (mN/m)	pC ₂₀	A (Å ²)	KT
5-3		0.29	-			66
5-4	1.1 x 10 ⁻²	0.709	36.8			81
6-3		0.08	-	4.5		
6-4	1.4 x 10 ⁻³	0.159	32.6	4.3	76	
7-4	1.6 x 10 ⁻⁴	0.013	28.6		68	35
7-5		0.018	-	5.4	76	29
8-4	4.2 x 10 ⁻⁵	0.0012	26.2		72	

Surface tension (du Nouy ring) at 35 °C [82, 83, 164].

D. Surfactant Oligomers

1. Cationic trimers

	cmc (M)	α	γ_{cmc} mN/m	A (Å ²)	pC ₂₀
12-2-12-2-12, 3Br ^a	8.0 x 10 ⁻⁵	0.93	25.2	128	
12-3-12-3-12, 3Br ^b	1.4 x 10 ⁻⁴	0.24	32	148	
12-3-12-3-12, 3Cl ^c	3.3 x 10 ⁻⁴	0.34			
12-6-12-6-12, 3Br ^b	2.8 x 10 ⁻⁴	0.30	44	248	
12-3-12-4-12-3-12, 4Br ^b	6.0 x 10 ⁻⁵	0.20			
12-3*-12-3*-12, 3Cl ^d	9.6 x 10 ⁻⁶		32		5.36
12-3*-1-3*-12, 3Cl ^d	4.6 x 10 ⁻⁴		39		3.68
12-3*-12°-3*-12, 2Cl ^d	6.2 x 10 ⁻⁶		35		5.60
12-3*-1°-3*-12, 2Cl ^d	9.9 x 10 ⁻⁴		42		3.34

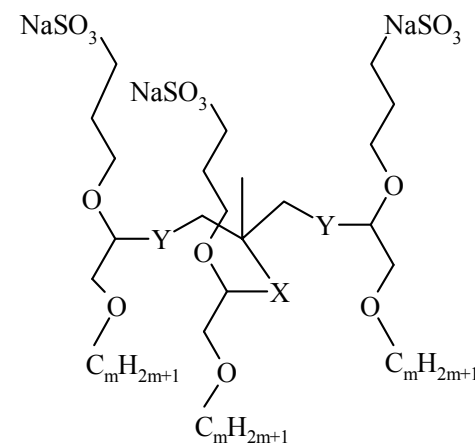
^a Surface tension (wilhelmy plate) at 25 °C [108].

^b Cmc by conductimetry at 25 °C; surface tension measured by pendant drop method at 25 °C [104].

^c Conductimetry at 25 °C [103].

^d Surface tension (wilhelmy plate) at 20 °C [109]; 3*: hydroxypropylene spacer; m°: tertiary amine head group.

2. Anionic trimers

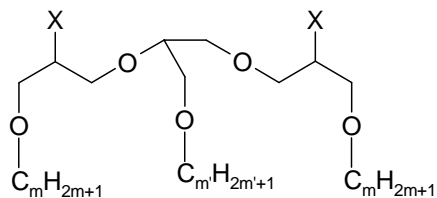


Y	X	m	cmc (M)	γ_{cmc} (mN/m)	pC ₂₀
-O-	-CH ₂ O ^{-a}	10	6.8 x 10 ⁻⁶	31.5	7.4
-O-	-CH ₂ O ^{-a}	12	5.0 x 10 ⁻⁵	33.0	5.8
-O-	-CH ₂ O ^{-a}	14	2.5 x 10 ⁻⁴	34.0	4.8
-OCH ₂ CH ₂ O-	-CH ₂ OCH ₂ CH ₂ O ^{-b}	10	8.0 x 10 ⁻⁶	33.5	7.1
-OCH ₂ CH ₂ O-	-CH ₂ OCH ₂ CH ₂ O ^{-b}	12	2.7 x 10 ⁻⁵	34.0	6.4
-OCH ₂ CH ₂ O-	-OCH ₂ CH ₂ O ^{-b}	10	1.0 x 10 ⁻⁵	31.0	6.5
-OCH ₂ CH ₂ O-	-OCH ₂ CH ₂ O ^{-b}	12	1.8 x 10 ⁻⁵	32.5	7.5

^a Surface tension (Wilhelmy plate) at 20 °C. m=16 compound is insoluble even in hot water [111].

^b Surface tension (Wilhelmy plate) at 20 °C [112].

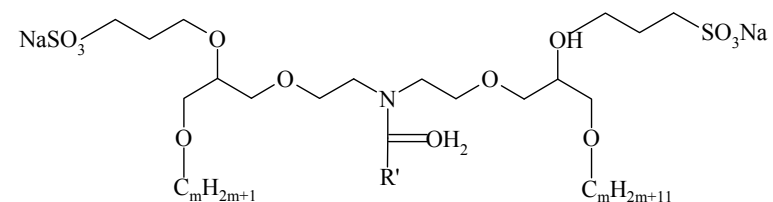
3. Unequal number of ionic head groups and alkyl chains



X	m	m'	cmc	γ_{cmc} mN/m	pC ₂₀
CH ₂ COONa	10	10	4.0×10^{-5}	29	5.7 ^a
OSO ₃ Na	10	10	9.0×10^{-6}	27	6.7 ^a
OCH ₂ CH ₂ CH ₂ SO ₃ Na	8	1	8.5×10^{-4}	36.5	3.9
	10	1	8.1×10^{-5}	36	5.0
	8	8	4.6×10^{-5}	29	5.6
	10	8	1.6×10^{-5}	28	6.3 ^a
	8	10	1.9×10^{-5}	28	6.4 ^a
10	10	1.4×10^{-5}	28	6.6 ^a	

Surface tension (Wilhelmy plate) at 20 °C [113].

^a extrapolated values



R'	m=8			m=10		
	Cmc (M)	γ_{cmc} (mN/m)	pC ₂₀	Cmc (M)	γ_{cmc} (mN/m)	pC ₂₀
CH ₃	5.2×10^{-4}	33.5	4.2	4.3×10^{-5}	32.5	5.3
C ₉ H ₁₉	3.5×10^{-5}	31.0	5.6	8.0×10^{-6}	28.0	6.7 ^a
C ₁₁ H ₂₃	1.2×10^{-5}	30.5	6.5 ^a	7.2×10^{-6}	27.5	6.9 ^a

Surface tension (wilhelmy plate) at 20 °C [55].

^a extrapolated values

VIII. REFERENCES

-
1. R. Zana, in *Novel Surfactants. Preparation, Applications and Biodegradability* C. Holmberg, Ed.; M. Dekker Inc.: New York 1998, Chapter 8, p. 241-277.
 2. P. Alexandridis, *Curr. Opin. Colloid Interface Sci.* 1: 490-501 (1996); Th. F. Tadros, *Annu. Surfactants Rev.* 1: 179-204 (1998).
 - 3 Patents before 1990:
Cationic: R. B. McConnell, US Patent 3,855,235 (1974); R. B. McConnell, US Patent 3,887,476 (1975); R. B. Login, US Patent 4,764,306 (1988); R. B. Login, US Patent 4,734,277 (1988); R. B. Login, US Patent 4,812,263 (1989); R.K. Chauhuri, D.J. Tracy, and R.B. Login, US Patent 4,886,890 (1989);
Anionic : French patent 1,055,420 (1954); French patent 1,464,243 (1966); G. Reitz, and G. Boehmke, Great Britain Patent 1,503,280 (1978);
Non-ionic: F. Bersworth, US Patent 2,524,218 (1950); F. Bersworth, US Patent 2,530,147 (1950); F. Bersworth, US Patent 2,532,391 (1950); Schmitz, G.B. Patent 1,149,140 (1967);
 4. M. J. Rosen, *Chemtech.* 23: 30-33 (1993).
 5. R. Zana, *Curr. Opin. Colloid Interface Sci.* 1: 566-571 (1996).
 6. Y. Nakatsuji and I. Ikeda, *Chimica Oggi/Chemistry today*: 40-43 (1997).
 7. R. Zana, in *Specialty Surfactants*, I.D. Robb Ed., Blackie: London 1997, p. 81-103.
 8. E. Fiscaro, *Cell. & Mol. Bio. Lett.* 2, supp.1: 45-63 (1997).
 9. E. Fiscaro, B. Różycka-Roszack, G. Viscardi, and P.L. Quagliotto, *Curr. Top. Colloid Interface Sci.* 2: 53-68 (1997).
 10. Zana, R. In *Structure-Performance Relationships in Surfactants*, K. Esumi and M. Ueno, Eds.; M. Dekker Inc.: New York 1997, Chapter 6, p. 255-283.
 11. M. J. Rosen, *Cosmetics & Toiletries* 113: 49-55 (1998).
 12. M. J. Rosen and D. J. Tracy, *J. Surfact. and Deterg.* 1: 547-554 (1998).
 13. E. N. Vulfson, *Lipid Technol.* 11: 31-36 (1999).
 14. A. J. Wysocki and D. Taber in *Cationic Surfactants* Jungermann, E., Ed.; M. Dekker Inc.: New York 1970 Chapter 3 p. 71-146.
 15. M. Katzman, US Patent 2,217,683 (1940).
 16. H.-J. Engelbert, US patent 2,445, 319 (1948).
 17. M.A.T. Rogers, U.S. Patent 2,386,141 (1945).
 18. M.A.T. Rogers, U.S. Patent 2,386,143 (1945).
 19. K. Thomae, German patent 914387 (1963) ; US Patent 3,121,088.
 20. D. Jerchel and K. Thomas, US Patent 3,121,088 (1964).
 21. T. Imam, F. Devínsky, I. Lacko, D. Mlynarčík, and L. Krasnec, *Pharmazie* 38: 308-310 (1983).
 22. R. Zana, and Y. Talmon, *Nature* 362: 228-231 (1993).
 23. F. M. Menger and C. A. Littau, *J. Am. Chem. Soc.* 113: 1451-1452 (1991).
 - 24 Patents after 1989:
Cationic: J. Li, M. Dahanayake, R.L. Reiersen and D.J. Tracy, US Patent 5,643,498 (1997).
Anionic: Behler, R. Piorr, and M. Schaefer, US Patent 4,936,551 (1990); M. Okahara, and A. Masuyama, US Patent 5,160,450 (1992); B. Gruber, Ger. Offen. DE 4,232,414 A1 (1994); F. Wangemann, Ger. Offen. DE 4,321,022 A1 (1995); H.C. Rath, and W.E. Noack, Ger. Offen. DE 4,401,565 (1995); R.J. Kaiser, US Patent 5,487,778 (1996); R.J. Kaiser, US Patent 5,507,863 (1996); R.J. Kaiser, US Patent 5,599,933 (1997); R. Varadaraj, and S. Zushma, US Patent 5,493,050 (1996); R. Varadaraj, and S. Zushma, US Patent 5,585,516 (1996); T. Okano, M. Fukuda, J. Tanabe, M. Ono, Y. Akabane, H. Takahashi, N. Egawa, T. Sakatoni, H. Kanao, and Y. Yoneyanna US Patent 5,681,803 (1997); H.C. Rath, Ger. Offen. DE 19,622,612 (1997); D.J. Tracy, J. Li, and J.M. Ricca US Patent 5,710,121 (1998); T. Kitsubi, M. Uno, K. Kita, Y. Fujikura, A. Nakano, M. Tosaka, K. Yahagi, S. Tamura, and K. Maruta, US Patent 5,714,457 (1998).
Non-ionic: C.B.A. Briggs and A.R. Pitt US Patent 4,892,806 (1990); R. Corelli-Calvet, F. Brisset, J. Rivo, A. Lattes, and L. Godefroy, US Patent 5,403,922 (1995); K. Adams, Eur. Pat. Appl. EPO 688781 (1995); J. Scheibel, D.S. Connor, and E.Y Fu, US Patent 5,534,197 (1996); D.S. Connor, E.Y Fu and J. Scheibel, US Patent 5,512,699 (1996); K. Tsubone, H. Nishio, M. Kusumaru, Jpn. Kokai Tokkyo Koho JP 08,291,040 (1996); K. Tsubone, H. Nishio, M. Kusumaru, Jpn. Kokai Tokkyo Koho JP 08,319,262 (1996); S. Wong, US Patent 5,622,938 (1997).

-
- Zwitterionic: J. Li, M. Dahanayake, R.L. Reiersen and D.J. Tracy, US Patent 5,643,498 (1997); Nakamo, T. Kitsuki, K. Kita, M. Asuga, International Patent PCT WO 96 / 01800 (1996); K. Kwetkat, International Patent PCT WO 97 / 31890 (1997).
- 25 A. Haces and V. C. Ciccarone International Patent PCT WO 95 / 17373 (1995)
 - 26 E. Unger, D. Shen, and G. Wu, International Patent PCT WO 96 / 26179 (1996)
 27. R. K. Scheule and S. H. Cheng, in *Artificial Self-Assembling Systems for Gene Delivery*, P. L. Felgner, M. J. Heller, P. Lehn, J. P. Behr, and F. C. Szocka Eds, Acs Conference Proceedings Series, ACS: Washington 1995, chapter 17, p.177-190.
 28. D. Erne, N. Stojanac, D. Ammann, P. Hofstetter, E. Pretsch, and W. Simon, *Helv. Chim. Acta* 63: 2271-2279 (1980). F. Lanter, D. Erne, D. Ammann, and W. Simon, *Anal. Chem.* 52: 2400-2402 (1980).
 29. G. Brand, M. W. Hosseini, and R. Ruppert, *Helv. Chim. Acta* 75:721-728 (1992).
 30. A. Laschewsky, *Adv. Polym Sci.* 124: 1-86 (1995).
 31. C. Tanford, *The hydrophobic Effect: Formation of Micelles and Biological Membranes*, John Wiley & Sons, New York 1973.
 32. J. Israelachvili, D. J. Mitchell, and B. W. Ninham, *J. Chem Soc. Faraday Trans 2*: 1525-1568 (1976).
 33. J. C. H. Hwa, US patent 2,933,529 (1960).
 34. C. A. Bunton, L. Robinson, J. Schaak, and M. F. Stam, *J. Org. Chem.* 36: 2346-2350 (1971).
 35. I. Lacko, F. Devínsky, D. Mlynarčík and Ľ. Krasnec, *Acta Fac. Pharm. Univ. Comeniana* 30: 109 (1977).
 36. T. Imam, F. Devínsky, I. Lacko, D. Mlynarčík, and Ľ. Krasnec, *Pharmazie* H.5, 38:308 (1983).
 37. F. Devínsky, L. Masárová, I. Lacko and D. Mlynarčík, *Collect. Czech. Chem Commun.* 49: 2819-2827 (1984).
 38. R. Zana, M. Benrraou, and R. Rueff, *Langmuir* 7: 1072-1075 (1991).
 39. F. M. Menger and C. A. Littau, *J. Am. Chem. Soc.* 115:10083-10090 (1993).
 40. Th. Dam, J.B.F.N. Engberts, J. Karthäuser, S. Karaborni, and N.M. van Os, *Colloid Surfaces A* 118: 41-49 (1996).
 41. S. De, V. K. Aswal, P. S. Goyal, and S. Bhattacharya, *J. Phys. Chem.* 100: 11664-11671 (1996).
 42. B. Rozycka-Roszak, S. Witek, and S. Przystalski, *J. Colloid Interface Sci.* 131: 181-185 (1989).
 43. S. Pegiadou-Koemtzopoulou, V. Papazoglou, and A. H. Kehayoglou, *J. Surfact. Deterg.* 1: 73-76 (2000).
 44. T.-S. Kim T. Hirao, and I. Ikeda, *J. Am. Oil Chem. Soc.* 73: 67-71 (1996).
 45. T.-S. Kim, T. Kida, Y. Nakatsuji, T. Hirao, and I. Ikeda, *J. Am. Oil Chem. Soc.* 73: 907-911 (1996).
 46. M.J. Rosen, and L. Liu, *J. Am. Oil Chem. Soc.* 73: 885-890 (1996).
 47. H. C. Parreira, E. R. Lukenbach, and M. K. Lindemann, *J. Am. Oil Chem. Soc.* 56: 1015-1021 (1979).
 48. S. De, V. K. Aswal, P.S. Goyal, and S. Bhattacharya, *J. Phys. Chem B* 102: 6152-6160 (1998).
 49. Dreja, S. Gramberg, and B. Tieke, *Chem. Commun.* : 1371-1372 (1998).
 50. E. Girod, US Patent 2,759,020 (1956).
 51. M. Okahara, A. Masuyama, Y. Sumida, and Y.-P. Zhu, *J. Jpn. Oil Chem. Soc.* 37: 746-748 (1988).
 52. Y.-P. Zhu, A. Masuyama, and M. Okahara, *J. Am. Oil Chem. Soc.* 67: 459-463 (1990).
 53. Y.-P. Zhu, A. Masuyama, and M. Okahara, *J. Am. Oil Chem. Soc.* 68: 268-271 (1991).
 54. Y.-P. Zhu, A. Masuyama, T. Nagata and M. Okahara, *J. Jpn. Oil Chem. Soc.* 40: 473-477 (1991).
 55. Y.-P. Zhu, A. Masuyama, A. Kirito, and M. Okahara, *J. Am. Oil Chem. Soc.* 68: 539-543 (1991).
 56. A. Masuyama, T. Hirono, Y.-P. Zhu, M. Okahara, and M. J. Rosen, *J. Jpn. Oil Chem. Soc.* 41: 301-305 (1992).
 57. Y.-P. Zhu, A. Masuyama, Y. Nakatsuji, and M. Okahara, *J. Jpn. Oil Chem. Soc.* 42: 86-94 (1993).

-
58. Y.-P. Zhu, K. Ishahara, A. Masuyama, Y. Nakatsuji, and M. Okahara, *Jpn. Oil Chem. Soc.* 42:161 (1993).
 59. Y.-P. Zhu, A. Masuyama, Y. Kobata, Y. Nakatsuji, M. Okahara, and M. J. Rosen, *J. Colloid Interface Sci.* 158: 40-45 (1993).
 60. X. P. Gu, I. Ikeda and M. Okahara, *Synthesis*: 649-651 (1985).
 61. Y. Sumida, A. Masuyama, T. Oki, T. Kida, Y. Nakatsuji, I. Ikeda, and M. Nojima, *Langmuir* 12: 3986-(1996).
 62. T. Okano, N. Egawa, M. Fujiwara and M. Fukuda, *J. Am. Oil Chem. Soc.* 73: 31-37 (1996).
 63. T. Okano, J. Tanabe, M. Fukuda, and M. Tanaka, *J. Am. Oil Chem. Soc.* 69: 44-46 (1992).
 64. A. van Zon, J.T. Bouman, H.H. Deuling, S. Karaborni, J. Karthaeuser, H.T.G.A. Mensen, and N.M. van Os, *Tenside Surf. Det.* 36: 84-86 (1999).
 65. P. Renouf, D. Hebrault, J.-R. Desmurs, J.-M. Mercier, C. Mioskowski, and L. Lebeau, *Chem. Phys. Lipids* 99: 21-32 (1999).
 66. K. Aratani, T. Oida, T. Shimizu, Y. Hayashi, *Comun. Jorn. Com. Esp. Deterg.* 28: 45-56 (1998).
 67. F. L. Duivenvoorde, M. C. Feiters, S. J. van der Gaast, and J. B. F. N. Engberts, *Langmuir* 13: 3737-3743 (1997)
 68. R. A. Bauman, *Synthesis*: 870-872 (1974)
 69. H. Eibl, J. O. McIntyre, E. A. M. Fleer, and S. Fleischer, *Methods Enzymol.* 98: 623-632 (1983).
 70. V. K. Aswal, S. De, P. S. Goyal, and S. Bhattacharya, and R. K. Heenan, *Phys. Rev. E.* 59: 3116-3122 (1999).
 71. J.-M. Kim, and D. H. Thompson, *Langmuir* 8: 637-644 (1992).
 72. C. Helbig, H. Baldauf, T. Lange, R. Neumann, R. Pollex, and E. Weber, *Tenside Surf. Det.* 36: 58-62 (1999).
 73. J. Seguer, C. Selve, M. Allouch, and M. R. Infante, *J. Am. Oil Chem. Soc.* 73: 79-86 (1996).
 74. M. R. Infante, j. Seguer, A. Pinazo, and M.P. Vinardell, *J. Dispersion Sci. Technol.* 20: 621-642 (1999).
 75. M. R. Infante, J. J. Garcia Dominguez, P. Erra, M. R. Juliá, and M. Prats, *Int. J. Cosmet. Sci.* 6:275 (1984).
 76. L. Pérez, J. L. Torres, A. Manresa, C. Solans, and M. R. Infante, *Langmuir* 12: 5296-5301 (1996).
 77. L. Pérez, A. Pinazo, M. J. Rosen, and M. R. Infante, *Langmuir* 14: 2307-2315 (1998).
 78. A. Pinazo, X. Wen, L. Pérez, M. R. Infante, and E. I. Franses, *Langmuir* 15: 3134-3142 (1999).
 79. K. Jennings, I. Marshall, H. Birrell, A. Edwards, N. Haskins, O. Sodermann, A. J. Kirby, and P. Camilleri, *J. Chem. Soc., Chem. Commun.*: 1951-1952 (1998).
 80. R. Valivety, I. S. Gill, and E. N. Vulfson, *J. Surfact. Deterg.* 1: 177-185 (1998).
 81. J. Eastoe, P. Rogueda, B. J. Harrison, A. M. Howe, and A. R. Pitt, *Langmuir* 10: 4429-4433 (1994).
 82. C. B. A. Briggs and A. R. Pitt US Patent 4,892,806 (1990)
 83. C. B. A. Briggs, I. M. Newington and A. R. Pitt, *J. Chem. Soc., Chem. Commun.*: 379-380 (1995).
 84. J. M. Pestman, K. R. Terpstra, M. C. A. Stuart, H. A. Van Doren, A. Brisson, R. M. Kellog, and J. B. F. N. Engberts, *Langmuir* 13: 6857-6860 (1997).
 85. M. J. L. Castro, J. Kovensky, and A. Fernandez Cirelli, *Tetrahedron Lett.* 38: 3995-3998 (1997).
 86. C. Gao, A. Millqvist-Fureby, M. J. Whitcombe, and E. N. Vulfson, *J. Surfactants Deterg.* 2: 293-302 (1999).
 87. R. Oda, I. Huc, and S. J. Candau, *J. Chem. Soc., Chem. Commun.*: 2105-2106 (1997).
 88. D. A. Jaeger, B. Li, and T. Clark, Jr., *Langmuir* 12: 4314-4316 (1996).
 89. P. Renouf, C. Mioskowski, L. Lebeau, D. Hebrault, and J.-R. Desmurs, *Tetrahedron Lett.* 39: 1357-1360 (1998).
 - 90 I. Huc and R. Oda, *Chem. Commun.*: 2025-2026 (1999).
 91. N. A. J. M. Sommerdijk, T. H. L. Hoeks, M. Synak, M. C. Feiters, R. J. M. Nolte and B. Zwanenburg, *J. Am. Chem. Soc.* 119: 4338-4344 (1997).
 92. T. Takemura, N. Shiina, M. Izumi, K. Nakamura, M. Miyazaki, K. Torigoe, and K. Esumi, *Langmuir* 15: 646-648 (1999).
 93. A. Pinazo, M. Diz, C. Solans, M. A. Pés, P. Era, and M. R. Infante, *J. Am. Oil Chem. Soc.* 70: 37-42 (1993).
 94. D. Ono, T. Tanaka, A. Masuyama, Y. Nakatsuji and M. Okahara, *J. Jpn. Oil Chem. Soc.* 42: 10-16 (1993).

-
95. D. A. Jaeger, S. G. C. Russell and H. Shinozaki, *J. Org. Chem.* 59: 7544-7548 (1994).
 96. D. A. Jaeger, and E. L. Brown, *Langmuir* 12: 1976-1980 (1995).
 97. A. Masuyama, C. Endo, S. Takeda, M. Nojima, *Chem. Commun.*: 2023-2024 (1998).
 98. S.M. Krisovitch and S.L. Regen, *J. Am. Chem. Soc.* 114: 9828- (1992); S. M. K. Davidson and S. L. Regen, *Chem. Rev.* 97: 1269-1279 (1997).
 99. B. S. Gallardo, and N. L. Abbott, *Langmuir* 13: 203-208 (1997).
 100. T. Saji, K. Hoshino, Y. Ishii, and M. Goto, *J. Am. Chem. Soc.* 113: 450 (1991)
 101. A. Guyot, in *Novel Surfactants. Preparation, Applications and Biodegradability*, C. Holmberg Ed.; M. Dekker Inc.: New York 1998, Chapter 10, p. 301-322.
 102. K. Goldann and A. Kirstahler, German Patent 1 086 709 (1958).
 103. R. Zana, H. Lévy, D. Papoutsi, and G. Beinert, *Langmuir* 11: 3694-3698 (1995).
 104. M In, V. Bec, O. Aguerre-Chariol and R. Zana, *Langmuir* 16: 141-148 (2000).
 105. A. G. Giumanini, G. Chiavari and F. L. Scarponi, *Z. Naturforsch.* 30b: 820-821 (1975).
 106. Unpublished results
 - 107 R.W. Alder, D. Colclough, and R.W. Mowlam, *Tetrahedron letters* 32: 7755-7758 (1991).
 108. K. Esumi, K. Taguma, and Y. Koide, *Langmuir* 12: 4039-4041 (1996).
 109. T.-S. Kim, T. Kida, Y. Nakatsuji, and I. Ikeda, *Langmuir* 12: 6304-6308 (1996).
 110. T. Kida, M. Yokota, A. Masuyama, Y. Nakatsuji, and M. Okahara, *Synthesis*: 487-489 (1993).
 111. A. Masuyama, M. Yokota, Y.-P. Zhu, T. Kida, and Y. Nakatsuji, *Chem. Comm.*: 1435-1436 (1994).
 112. Y. Sumida, T. Oki, A. Masuyama, H. Maekawa, M. Nishiura, T. Kida, Y. Nakatsuji, I. Ikeda, and M. Nojima, *Langmuir* 14: 7450-7455 (1998).
 113. Y. Zhu, A. Masuyama, Y.-I. Kirito, M. Okahara, and M. J. Rosen, *J. Am. Oil Chem. Soc.* 69: 626-632 (1993).
 114. D. J. Tracy, R. Li, and J. Yiang, US Patent 5,846,926(1998).
 115. O. Regev and R. Zana, *J. Colloid Interface Sci.* 210: 8-17 (1999)
 116. M. J. Rosen, *Surfactant and Interfacial Phenomena*, Wiley & Sons: New York 1989.
 117. L. D. Song and M. J. Rosen, *Langmuir* 12: 1149-1153 (1996)
 118. M. J. Rosen, J. H. Mathias, and L. Davenport, *Langmuir* 15: 7340-7346 (1999).
 119. B. Róøycka-Roszack, E. Fisicaro, and A. Ghiozzi, *J. Colloid Interface Sci.* 184: 209-215 (1996).
 120. F. Devínsky, I. Lacko, F. Bittererová, and L. Tomečková, *J. Colloid Interface Sci.* 114: 314-322 (1986).
 121. F. Devínsky, L. Masárová, and I. Lacko, *J. Colloid Interface Sci.* 105: 235-239 (1985).
 122. E. Alami, G. Beinert, P. Marie, and R. Zana, *Langmuir* 9:1465-1467 (1993).
 123. M. Dreja, W. Pyckhout-Hintzen, H. Mays, and B. Tieke, *Langmuir* 15: 391-399 (1999).
 - 124 Y. F. Deinega, Z. R. Ul'berg, L. G. Marochko, V. P. Rudi, and V. P. Denisenko, *Kolloidn. Zh.* 36: 649-653 (1974).
 125. Z. X. Li, C. C Dong, and R. K. Thomas, *Langmuir* 15: 4392-4396 (1999).
 126. H. Diamant, and D. Andelman, *Langmuir* 10: 2910-2916 (1994).
 127. H. Diamant, and D. Andelman, *Langmuir* 11: 3605-3606 (1995).
 128. P. K. Maiti, and D. Chowdhury, *J. Chem. Phys.* 109: 5126-5133 (1998).
 - 129 A. Tomlinson, T. N. Danks, D.M. Heyes, S. E. Taylor, and D. J. Moreton, *Langmuir* 13: 5881-5893 (1997).
 130. E. J. Osburn, L.-K. Chau, S.-Y. Chen, N. Collins, D. F. O'Brien, and N. R. Armstrong, *Langmuir* 12: 4784-4796 (1996).
 131. D. J. Cooke, J. R. Lu, E. M. Lee, R. K. Thomas, A. R. Pitt, E. A. Simister, J. Penfold, *J. Phys. Chem.* 100: 10298-10303 (1996).
 132. A. Espert, R. v. Klitzing, P. Poulin, A. Colin, R. Zana, and D. Langevin, *Langmuir* 14:4251-4260 (1998).
 133. V. Bergeron, *Langmuir* 13: 3474-3482 (1997).

-
134. C. Chorro, M. Chorro, O. Dolladille, S. Partyka, and R. Zana, *J. Colloid Interface Sci.* 199:169-176 (1998).
135. C. Chorro, M. Chorro, O. Dolladille, S. Partyka, and R. Zana, *J. Colloid Interface Sci.* 210:134-143 (1999).
136. M.L. Fielden, P.M. Claesson, R.E. Verrall, *Langmuir* 15: 3924-3934 (1999).
137. K. Esumi, M. Goino, and Y. Koide, *J. Colloid Interface Sci.* 183: 539-545 (1996).
138. K. Esumi, M. Goino, and Y. Koide, *Colloids Surfaces A* 118: 161-166 (1996).
139. K. Esumi, Y. Takeda, M. Goino, K. Ishiduki, and Y. Koide, *Langmuir* 13: 2585-2587 (1997)
140. K. Esumi, S. Uda, M. Goino, K. Ishiduki, T. Suhara, H. Fukui, and Y. Koide, *Langmuir* 13: 2803-2807 (1997)
141. K. Esumi, M. Matoba, and Y. Yamanaka, *Langmuir* 12: 2130-2135 (1996).
142. S. Manne, J. P. Cleveland, H. E. Gaub, G. D. Stucky, and P. K. Hansma, *Langmuir* 10: 4409-4413 (1994).
143. S. Manne, and H. E. Gaub, *Science* 270: 1480-1482 (1995).
144. S. Manne, T. E. Schäffer, Q. Huo, P. K. Hansma, D. E. Morse, G. D. Stucky, and I. A. Aksay, *Langmuir* 13: 6382-6387 (1997).
145. M. Frindi, B. Michels, and R. Zana, *Langmuir* 10: 1140-1145 (1994).
146. F. Devínsky, I. Lacko, D. Mlynarčík, V. Račanský, and L. Krasnec, *Tenside Surf. Det.* 22: 10-15 (1985).
147. R. Zana and H. Lévy, *Colloids and Surfaces A* 127: 229-232 (1997).
148. R. Zana, *Langmuir* 12:1208 (1996).
149. N. Hattori, A. Yoshino, H. Okabayashi, and C. J. O'Connor, *J. Phys. Chem.* 102: 8965-8973 (1998).
150. N. Hattori, H. Hirata, H. Okabayashi, C. J. O'Connor, *Colloid Polym. Sci.* 277: 361-371 (1999).
151. J. Zhao, S. D. Christian, and B. M. Fung, *J. Phys. Chem. B* 102: 7613-7618 (1998).
152. P. K. Maiti, and D. Chowdhury, *Europhys. Lett.* 41: 183-188 (1998).
153. Z. R. Ul'berg, and V. I. Podol'skaya, *Kolloidn. Zh.* 40: 292-296 (1978).
154. R. Zana, S. Yiv, and K. Kale, *J. Colloid Interface Sci.* 77: 456-465 (1980).
155. R. Zana, *J. Colloid Interface Sci.* 78: 330-337 (1980).
156. R. Zana, in *Cationic Surfactants*, Ed.; M. Dekker Inc.: New York 1985, Chapter 2, p. 41-85.
157. M. A. Winnik, and A. Yekta, *Curr. Opin. Colloid Interface Sci.* 2: 424-436 (1997) and references therein.
158. R. Zana, M. In, H. Lévy, and G. Duportail, *Langmuir* 13: 5552-5557 (1997).
159. F. Devínsky, I. Lacko, and T. Imam, *J. Colloid Interface Sci.* 143: 336-342 (1991).
160. M. Dreja, and B. Tieke, *Langmuir* 14: 800-807 (1998).
161. K. M. Layn, P. G. Debenedetti, and R. K. Prud'homme, *J. Chem. Phys.*
162. H. Hirata, N. Hattori, M. Ishida, H. Okabayashi, M. Frusaka, and R. Zana, *J. Phys. Chem.* 99: 17778-17784 (1995).
163. N. Hattori, H. Hirata, H. Okabayashi, M. Furusaka, C. J. O'Connor, and R. Zana, *Colloid. Polym. Sci.* 277: 95-100 (1999)
164. J. Estaoe, P. Rogueda, A.M. Howe, A.R. Pitt, and R.K. Heenan, *Langmuir* 12: 2710-2705 (1996).
165. D. Danino, Y. Talmon, and R. Zana, *Langmuir* 11: 1448-1456 (1995).
166. D. Danino, A. Kaplun, Y. Talmon, and R. Zana, in *Structure and Flow in Surfactant Solutions*, ACS Symp. Ser. 578, (C. A. Herb and R. K. Prud'Homme, Eds.), American Chemical Society, 1994.
167. E. Alami, H. Lévy, R. Zana, and A. Skoulios, *Langmuir* 9: 940-944 (1993).
168. V. K. Aswal, S. De, P. S. Goyal, S. Bhattacharya, and R. K. Heenan, *Phys. Rev E* 57: 776-783 (1998).
169. V. K. Aswal, S. De, P. S. Goyal, S. Bhattacharya, and R. K. Heenan, *Phys. Rev E* 59: 3116-3122 (1999).
170. P. J. Missel, N. A. Mazer, G. B. Benedek, C. Y. Young, and M. C. Carey, *J. Phys. Chem* 84: 1044- (1980).

-
171. F. C. Mackintosh, S. Safran, and P. Pincus, *Europhys. Lett.* 12: 697-702 (1990); S. Safran, P. Pincus, M. Cates, and F. C. Mackintosh, *J. Phys. France* 51: 503-510 (1992).
172. F. Kern, F. Lequeux, R. Zana, and S. J. Candau, *Langmuir* 10: 1714-1723 (1994).
173. S. J. Candau, P. Hebraud, V. Schmitt, F. Lequeux, F. Kern, and R. Zana, *Nuovo Cimento* 16D: 1401 (1994).
174. M. In M, G. G. Warr, R. Zana, *Phys. Rev. Lett.* 83: 2278-2281 (1999).
175. R. Oda, I. Huc, J.-C. Homo, B. Heinrich, M. Schmutz, and S. Candau, *Langmuir* 15: 2384-2390 (1999).
176. J. Narayanan, W. Urbach, D. Langevin, C. Manohar, and R. Zana, *Phys. Rev. Lett.* 81: 228-231 (1998).
177. M.E. Cates, *Macromolecules* 20: 2289-2296 (1987); M.E. Cates, *J. Phys. (France)* 49: 1593-1600 (1988); M.S. Turner and M.E. Cates, *Langmuir* 7: 1590-1594 (1991); R. Granek and M.E. Cates, *J. Chem. Phys.* 96: 4758-4767 (1992).
178. F. Schosseler, O. Anthony, G. Beinert, and R. Zana, *Langmuir* 11: 3347-3350 (1995).
179. L. J. Magid, *J. Phys. Chem. B* 102: 4064- (1998).
180. E. Buhler, E. Mendes, P. Boltenhagen, J. P. Munch, R. Zana, and S. J. Candau, *Langmuir* 13: 3096-3102 (1997).
181. V. Schmitt and F. Lequeux, *J. Phys II France* 5: 193-197 (1995).
182. V. Schmitt, F. Schosseler, and F. Lequeux, *Europhys. Lett.* 30: 31-36 (1995).
183. R. Oda, F. Lequeux, and E. Mendes, *J. Phys. France* 6: 1-19 (1996).
184. D. Danino, Y. Talmon, H. Lévy, G. Beinert, and R. Zana, *Science* 269: 1420-1421 (1995).
185. R. Oda, P. Panizza, M. Schmutz, and F. Lequeux, *Langmuir* 13: 6407-6412 (1997).
186. S. Karaborni, K. Esselink, P. A. J. Hilbers, B. Smit, J. Karthäuser, N. M. van Os, and R. Zana, *Nature* 266: 254-256 (1994).
187. Porte G. *J. Phys. Chem.* 87: 3541-3550 (1983).
188. M. In, O. Aguerre-Chariol, R. Zana, *J Phys. Chem. B* 103: 7747-7750 (1999).
189. J. B. F. N. Engberts and J. Kevelam, *Curr. Opin. Colloid Interface Sci.* 1: 779-789 (1996).
190. S. Bhattacharya and S. De, *Chem. Commun.*: 651-652 (1995).
191. S. Bhattacharya and S. De, *Langmuir* 15: 3400-3410 (1999).
192. F. M. Menger and A. V. Eliseev, *Langmuir* 11: 1855-1857 (1995).
193. R. Zana, H. Lévy, D. Danino, Y. Talmon, and K. Kwetkat, *Langmuir* 13: 402-408 (1997).
194. N. A. J. M. Sommerdijk, M. H. L. Lambermon, M. C. Feiters, R. J. M. Nolte, and B. Zwanenburg, *Chem. Commun.*: 1423-1424 (1997).
195. R. Oda, I. Huc, and S. J. Candau, *Angew. Chem. Int. Edn* 37: 2689-2691 (1998).
196. R. Oda, I. Huc, M. Schmutz, S. J. Candau and F. C. MacKintosh, *Nature* 399: 566-569 (1999).
197. G. Cerichelli, L. Luchetti, G. Mancini, and G. Savelli, *Langmuir* 15: 2631-2634 (1999).
198. D. Danino, Y. Talmon, and R. Zana, *J. Colloid Interface Sci.* 185: 84-93 (1997).
199. V. K. Aswal, S. De, P. S. Goyal, S. Bhattacharya, and R. K. Heenan, *J. Chem. Soc., Faraday Trans.* 94: 2965-2967 (1998).
200. R. Oda, L. Bourdieu, M. Schmutz, *J. Phys. Chem. B* 101: 5913-5916 (1997).
201. S. Fuller, N. Shinde, G. J. Tiddy, G. S. Attard, and O. Howell, *Langmuir* 12: 1117-1123 (1996).
202. S. Fuller, J. Hopwood, A. Rahman, N. Shinde, G. J. Tiddy, G. S. Attard, O. Howell, and S. Sproston, *Liq. Cryst.* 12: 521 (1992).
203. M. In and G. G. Warr, in preparation.
204. M. Tanaka, T. Ishida, T. Araki, A. Masuyama, Y. Nakatsuji, and M. Okahara, *J. Chromatogr.* 648: 469-473 (1993).
205. H. Harino, S. Tsunoi, J. Yoshioka, T. Araki, A. Masuyama, Y. Nakatsuji, I. Ikeda, M. Tanaka, *Anal. Sci.* 14: 719-724 (1998).
206. K. Chen, D. C. Locke, T. Maldacker, J.-L. Lin, S. Aawassiripong, and U. Schurrath, *J. Chromatogr. A* 822: 281-290 (1998).
207. Z. Hu, T. Bühner, M. Müller, B. Rusterholz, M. Rouilly, and W. Simon, *Anal. Chem.* 61: 574-576 (1989).

-
208. M. Maj-Zurawska, M. Rouilly, W. E. Morse, and W. Simon, *Analytica Chimica Acta* 218: 47-59 (1989).
209. U. E. Spichiger, R. Eugster, E. Haase, G. Rumpf, P. Gehrig, B. Rusterholz, and W. Simon, *Fresenius J. Anal. Chem.* 341: 727-731 (1991).
210. A. E. Martell and S. Charberek, *J. Am. Chem. Soc.* 72: 5357-5361 (1950).
211. L. Galet, I. Pezron, W. Kunz, C. Larpent, J. Zhu, and C. Lheveder, *Colloids Surf. A* 151: 85-96 (1999).
212. S. Sato and H. Kishimoto, *J. Surface Sci. Technol.* 8: 209-216 (1992).
213. S. Sato, H. Sezaki, and H. Kishimoto, *Prog. Colloid. Poly. Sci.* 93: 277-278 (1993).
214. S. Sato, N. Asai, and M. Yonese, *Colloid. Polym. Sci.* 274: 889-893 (1996).
215. S. Sato and H. Kishimoto, *J. Colloid Interface Sci.* 123: 216-223 (1988).
216. S. Sato and H. Kishimoto, *J. Colloid Interface Sci.* 126: 108-113 (1988).
217. S. Sato and H. Kishimoto in *Novel Surfactants in Solution* 7. K. L. Mittal Ed.; Plenum: New York 1989, p. 341-357.
218. S. Sato, *Colloid. Polym. Sci.* 274: 1161-1169 (1996).
219. S. Sato, K. Toda, and S. Oniki, *J. Colloid Interface Sci.* 218: 504-510 (1999).
220. K. Esumi, J. Hara, N. Aihara, K. Usui, and K. Torigoe, *J. Colloid Interface Sci.* 208: 578-581 (1998).
221. C.T. Kresge, M.E. Leonowicz, W.J. Roth, J.C. Vartuli, and J.S. Beck, *Nature* 359: 710-712 (1992); C.T. Kresge, M.E. Leonowicz, W.J. Roth, and J.C. Vartuli, US Patent 5098684 (1992); J. S. Beck et al., *J. Am. Chem. Soc.* 114: 10834-10843 (1992).
222. Q. Huo, D. I. Margolese, U. Ciesia, P. Feng, T. E. Gier, P. Sieger, R. Leon, P. M. Petroff, F. Schuth, and G. D. Stucky, *Nature*, 368: 317-323 (1994).
223. Q. Huo, R. Leon, P. M. Petroff, and G. D. Stucky, *Nature* 268: 1324-1327 (1995).
-
224. P. Van der Voort, M. Mathieu, F. Mees, and E. F. Vansant, *J. Phys. Chem. B* 102: 8847-8851 (1998).